



THE HONG KONG
POLYTECHNIC UNIVERSITY

香港理工大學

Pao Yue-kong Library

包玉剛圖書館

Copyright Undertaking

This thesis is protected by copyright, with all rights reserved.

By reading and using the thesis, the reader understands and agrees to the following terms:

1. The reader will abide by the rules and legal ordinances governing copyright regarding the use of the thesis.
2. The reader will use the thesis for the purpose of research or private study only and not for distribution or further reproduction or any other purpose.
3. The reader agrees to indemnify and hold the University harmless from and against any loss, damage, cost, liability or expenses arising from copyright infringement or unauthorized usage.

IMPORTANT

If you have reasons to believe that any materials in this thesis are deemed not suitable to be distributed in this form, or a copyright owner having difficulty with the material being included in our database, please contact lbsys@polyu.edu.hk providing details. The Library will look into your claim and consider taking remedial action upon receipt of the written requests.

**INVESTIGATION ON THERMAL PERFORMANCE
ENHANCEMENT OF SELF-ROTATING TWISTED
TAPES IN A DOUBLE-PIPE HEAT EXCHANGER**

ZHANG SHAOJIE

PhD

The Hong Kong Polytechnic University

2019

The Hong Kong Polytechnic University

Department of Building Service Engineering

**Investigation on Thermal Performance Enhancement of
Self-rotating Twisted Tapes in a Double-pipe Heat
Exchanger**

Zhang Shaojie

**A thesis submitted in partial fulfillment of the requirements
for the Degree of Doctor of Philosophy**

July 2019

CERTIFICATE OF ORIGINALITY

I hereby declare that this thesis is my own work and that, to the best of my knowledge and belief, it reproduces no material previously published or written, nor material that has been accepted for the award of any other degree or diploma, except where due acknowledgement has been made in the text.

(Signed)

Zhang Shaojie (Name of student)

Abstract

With the rapid population increase and industrial development, global energy demand is rising significantly in recent decades. In order to achieve energy-saving benefit, heat transfer enhancement techniques become crucial to promote the thermal efficiency of heat exchanger system. Among various heat transfer techniques of passive method, twisted tape have been considered as a promising alternative for convective heat transfer due to the caused extra swirl flow. Nowadays, a novel type of twisted tapes, namely self-rotating twisted tapes (SRTTs), has been widely commercialized in many practical applications. It is defined as the device that can rotate automatically when fluids flow through the tube with high water velocity. Considering the existence of rotating behavior, SRTTs appear to perform greater performance in terms of inducing stronger turbulence and reducing pressure drop. However, limited studies are found to comprehensively investigate the thermal characteristic of the heat exchanger tube fitted with SRTTs. Hence, this study aims to investigate and compare the thermal performance enhancements of SRTTs and stationary twisted tapes (STTs) in a double-pipe heat exchanger, and also to examine as the effect of various fabrications (e.g. twist ratios, perforated ratio and length ratio) for different Nusselt numbers, friction factors and thermal performance factors. In addition, experiments on measuring the rotational speed of SRTTs at given Reynolds number were conducted to explore the effect of rotational speed on thermal performance.

Firstly, STTs and SRTTs were prepared with the same geometry (e.g. twist ratio, thickness and tapes width). The experiment was carried out in the turbulence flow from 12000-45000. The experimental results reported that STTs performed similar thermal

performance as SRTTs when SRTTs keep stationary. Also, it is found that the tube fitted with SRTTs could increase the average heat transfer rate by 18.8% and reduce the average friction factor by 12.1% in rotating condition. Interesting findings were observed that the thermal performance factor of SRTTs increases considerably when SRTTs switch from stationary to rotating conditions.

Then, SRTTs with different twist ratios ($Y=2.2, 3, 4$ and 6) were fabricated to study the influences of twist ratios on rotational speed and thermal performance. The results indicated that twist ratio has less effects on the start of rotating behavior and lower twist ratios were found to have considerably increased the rotational speed as compared with higher twist ratios. In addition, the tube fitted SRTTs yield higher Nusselt number by 22.2%, 16.2%, 12% and 7.4% and friction factor of 101%, 116%, 126% and 137% for twist ratio of 2.2, 3, 4 and 6, respectively. It was observed that the maximum thermal performance factor of 1.03, 0.944, 0.924 and 0.898 could be obtained at the start of rotating behavior for twist ratios of 2.2, 3, 4 and 6, respectively. The valuable findings from the experiment could be further recommended for proper application of SRTTs. Also, some correlations varying with twist ratios were proposed to predict the Nusselt number and friction factor within 10% deviation.

Afterwards, the influences of perforated SRTTs with different perforated ratios ($PR=0, 1.61, 3.63, 6.46$ and 10.1%) on thermal behavior were studied experimentally. Perforated ratio is defined as the ratio of perforated area to twisted tapes area. Smaller perforated ratio was found to function in rising rotational speed and start to rotate at relatively lower Reynolds number. Our results revealed that the increase of perforated ratio could play positive role in enhancing heat transfer rate, friction factor and thermal performance factor.

Interestingly, the thermal performance factor increases obviously from 0.862 to 0.924, 0.987 to 1.025, 1.04 to 1.078, 1.084 to 1.101 and 1.042 to 1.055 for PR=0, 1.61, 3.63, 6.46 and 10.1%, respectively. Comparison of perforated twisted tapes and perforated SRTTs was conducted based on thermal performance factor. In addition, some correlations associated with perforated ratios were established to estimate the heat transfer and friction factor characteristics of the perforated SRTTs in double-pipe heat exchangers.

According to the previous researches, fabrication of short length to twisted tapes was proposed for mitigating the pressure drop. Therefore, in this project, an experiment was carried out to explore the effects of length ratio (LR) on the thermal characteristics. The definition of length ratio is the length of SRTTs to the tube length. The experimental results reported that SRTTs with larger length ratio seem to rotate faster than those with smaller length ratio. Heat transfer rate can be increased by 57-66%, 61-114%, 62-127% and 95-160% for LR=0.3, 0.45, 0.6 and 1 respectively. The tube equipped with full-length SRTTs (LR=1) gave higher heat transfer performance, pressure drop and thermal performance factor as compared with those equipped with lower length ratio (LR=0.3, 0.45 and 0.6). Therefore, full-length SRTTs were suggested as alternatives to be employed in the heat exchanger system. Finally, two correlations regarding length ratio were formulated to evaluate the thermal performance in form of Nusselt number and friction factor.

To conclude, this thesis introduced a novel type of twisted tapes, namely self-rotating twisted tapes (SRTTs), into heat exchanger system, and experimentally investigated the thermal performance of SRTTs in a double-pipe heat exchanger with various configurations (e.g. twist ratio, perforated ratio and length ratio). Accordingly, the findings and results gave that the optimal configurations for proper use of SRTTs are lower twist

ratio ($Y=2.2$), large perforated ratio ($PR=10.1\%$) and full length ($LR=1$). Additionally, some correlations associated with these fabricated parameters were suggested for the prediction of Nusselt number and friction factor. The experimental correlations were validated by experimental values within acceptable level and could be widely and easily used for thermal performance evaluation of heat exchanger systems with SRTTs.

Publications during PhD study

Journal papers

- [1] **Zhang, S.J.**, Lu, L, Dong, C.S, and Cha, S.Y, Performance evaluation of a double-pipe heat exchanger fitted with self-rotating twisted tapes, *Applied Thermal Engineering*, 158(2019): 113770. 2019.
- [2] **Zhang, S.J.**, Lu, L, Dong, C.S, and Cha, S.Y, Thermal characteristics of perforated self-rotating twisted tapes in a double-pipe heat exchanger, *Applied Thermal Engineering*, under review, 2019.
- [3] **Zhang S.J.**, Lu L., Wang Q.W, Thermal-hydraulic characteristic of short-length self-rotating twisted tapes in a circular tube, *International Communications in Heat and Mass Transfer*, under review, 2019.
- [4] **Zhang, S.J**, Pilot study on ascension-pipe heat exchanger used for waste heat recovery of coke oven gas, *Energy Procedia*, 158 (2019) 26-31.
- [5] Koo C.W, Li W.Z, Cha S.Y, **Zhang S.J**, A novel estimation approach for the solar radiation potential with its complex spatial pattern via machine-learning techniques, *Renewable Energy*, 133 (2019), 575-592.

Conference papers

- [1] **Zhang, S.J**, Pilot study on ascension-pipe heat exchanger used for waste heat recovery of coke oven gas, 10th International Conference on Applied Energy (ICAE2018), 22-25 August 2018, Hong Kong.

- [2] **Zhang, S.J**, Kim J.H, Shih S.Y, Koo C.W, Cha S.Y, Immersive Virtual Environment (IVE) as a potential tool for interior colour study in office environments, 34th International Symposium on Automation and Robotics in Construction, 28 June-1 July, Taipei, Taiwan.

Acknowledgement

First of all, I would like to express my special appreciation and thanks to my supervisor Prof Lu Lin for all support and encouragement. Thanks to her constructive advices, patient guidance and useful help, I could have a chance to complete my PhD study within normal period. Her attitude towards academic research helps me learn the way to be a qualified researcher. During the period in her group, I also realize the importance of teamwork to conduct successful research.

I also would like to thank Dr. Cha Seunghyun for providing an opportunity for me to do my PhD study at The Hong Kong Polytechnic University.

In addition, I greatly appreciate all the member in the Renewable Energy Research Group for their help and encouragement during my Ph.D study. Especially, I would like to express deepest thanks to Dr. Dong Chuanshuai for his guidance and comments at beginning of my research. Without his help, it is impossible for me to go through all the difficulties of my Ph.D. study.

I am indebted to all my friends in Hong Kong and my family who always help me in numerous ways. Thanks for their advices and encouragement to help me choose a correct way to make my dream comes true.

My deep appreciation goes to Teaching Postgraduate Studentship of Hong Kong Polytechnic University for financially supporting my Ph.D. study.

At the end, I would like keep my sincere thanks for my girlfriend, Ms. Xing Lufei. Because of her accompany last year, I am able to be optimistic to face all the difficulties of my study.

Table of Content

Certificate of Originality	i
Abstract.....	ii
Publications during PhD study.....	vi
Acknowledgement.....	viii
Table of Content.....	ix
List of Figures.....	xv
List of Tables.....	xx
Nomenclature	xxi
CHAPTER 1	
INTRODUCTION	1
1.1 Introduction.....	1
1.2 Research objectives.....	5
1.3 Organization of this thesis.....	6

CHAPTER 2

LITERATURE REVIEW AND RESEARCH METHOD	9
2.1 Background	9
2.2 Classification of heat transfer enhancement techniques.....	11
2.2.1 Categories of heat transfer enhancement techniques	11
2.2.2 Some passive methods in heat exchanger	12
2.3 Introduction of twisted tapes	17
2.3.1 Enhancement mechanism and performance criteria	17
2.3.2 Various configuration of twisted tapes.....	18
2.3.3 Application of twisted tapes.....	22
2.4 Twisted tapes and other heat transfer enhancement methods.....	24
2.4.1 Twisted tapes and surface modification	24
2.4.2 Twisted tapes and nanofluids.....	28
2.5 Research methodology on twisted tapes	30
2.5.1 Experimental study.....	31
2.5.2 Numerical study	35
2.5.3 Optimization of twisted tapes based on different algorithms	38

2.6 Research gaps and research methodology.....41

CHAPTER 3

**COMPARISON OF THERMAL PERFORMANCE OF SELF-
ROTATING AND STATIONARY TWISTED TAPES IN A
CIRCULAR TUBE46**

3.1 Introduction.....47

3.2. Experimental methodology53

3.2.1 Experimental facilities53

3.2.2 Experimental procedure.....56

3.3 Data reduction.....57

3.4 Results and Discussion.....61

3.4.1 Validation test of plain tube..... 61

3.4.2 Effects of twist ratio on rotational speed 63

3.4.3 Comparison between SRTTs and STTs..... 64

3.4.4 Effect of twist ratios (Y) on thermal performance 68

3.4.5 Comparison between SRTTs and previous work 75

3.5 Summary.....77

CHAPTER 4

THERMAL CHARACTERISTIC OF PERFORATED SELF-

RPTATING TWISTED TAPES..... 78

4.1 Introduction..... 79

4.2 Experimental methodology 85

4.2.1 Experimental facilities 85

4.3 Data processing 89

4.3.1 Heat transfer characteristic 89

4.3.2 Friction factor characteristics 90

4.3.3 Thermal performance factor 90

4.3.4 Uncertainty analysis 91

4.4 Results and Discussion..... 91

4.4.1 Verification test: plain tube 91

4.4.2 Effect of the PR on the rotation speed 94

4.4.3 Effect of the PR on the heat transfer characteristic 95

4.4.4 Effect of the PRs on the friction factor characteristic..... 97

4.4.5 Effect of the PR on the thermal performance factor 99

4.4.6 Proposed correlations..... 100

4.4.7 Comparison of perforated SRTTs and perforated twisted tapes..... 102

4.5 Summary..... 103

CHAPTER 5

**THERMO-HYDRAULICS CHARACTERISTIC OF THE TUBE
FITTED WITH SHORT-LENGTH SELF-ROTATING TWISTED
TAPES..... 104**

5.1 Introduction..... 105

5.2 Experimental strategy 110

5.3 Data processing 113

5.4 Results and Discussion..... 116

5.4.1 Verification results for the plain tube..... 116

5.4.2 Influences of length ratio on the rotational speed 119

5.4.3 Effect of the length ratio on the thermal characteristics 120

5.4.4 Proposed correlations..... 125

5.4.5 Comparison of short-length SRTTs and previous work..... 126

5.5 Summary..... 127

CHAPTER 6

CONCLUSION AND FUTURE WORK..... 129

6.1 Conclusion 130

6.2 Limitations and recommendation for future work 132

References..... 134

List of Figures

Chapter 2

Figure 2.1 Total energy consumption and composition in China (2016)	10
Figure 2.2 Introduction of heat transfer enhancement techniques	11
Figure 2.3 Typical coiled tube in heat exchangers.....	12
Figure 2.4 (a) Helically corrugated tube; (b) Spirally corrugated tube.....	13
Figure 2.5 (a) louvered fin; (b) typical offset strip fin	14
Figure 2.6 (a) V shape type ribs; (b) Parallel type rib.....	15
Figure 2.7 TEM micrographs: (a) CuO/water nanofluids with 5 vol%; (b) CuO/water nanofluids with 7.5 vol%.	16
Figure 2.8 Flow pattern in (a) plain tube and (b) the tube with twisted tapes	18
Figure 2.9 Corrugated tube: (a) Schematic diagram; (b) Picture diagram.....	25
Figure 2.10 (a): Helical-ribbed tube and double twisted tape; (b) corrugated tube with loose-fit twisted tape	26
Figure 2.11 Micro-fin tube and twisted tapes	28
Figure 2.12 SEM or TEM images of various nanoparticles to be combined with twisted tapes: (a) CuO/water; (b) Al ₂ O ₃ /water; (c) TiO ₂ /water.....	30
Figure 2.13 Schematic view of twisted tapes with different thickness	31
Figure 2.14 Photograph of twisted centre wings and alternate-axes.....	32
Figure 2.15 Sketch map of cross hollow twisted tape with different hollow width	33

Figure 2.16 Photograph of tapered twisted tapes different with taper angle	33
Figure 2.17 Serrated twisted tapes: (a) serration width ratio, (b) serration depth ratio ...	34
Figure 2.18 Contour plots of flow structure at different clearance ratios	35
Figure 2.19 Contour plots of tangential velocity for the tube fitted with center-cleared twisted tapes at different central clearance ratios	36
Figure 2.20 Velocity streamline distribution in the cross hollow twisted tapes	37
Figure 2.21 Velocity distribution in triple twisted tapes with different clearance ratios.	38
Figure 2.22 Flowchart of ANN method].....	39
Figure 2.22 Flowchart of optimal design of multi-channel twisted tapes.....	40
Figure 2.23 Research flowchart of this thesis	43

Chapter 3

Figure 3.1 (a) SRTTs and STTs with the same geometry; (b) Pictorial view of SRTTs with different twist ratios	54
Figure 3.2 (a) Test tube with observational section; (b) Digital Tachometer RPM Meter with contactless mode; (c) Schematic of test rig used	55
Figure 3.3 Validation of experimental Nu in plain tube	62
Figure 3.4 Validation of experimental f in plain tube	62
Figure 3.5 Variation of rotational speed (RPM) with Reynolds number.....	63
Figure 3.6 Variation of (a) Nu and (b) Nu_t/Nu_p at given Reynolds for STTs and SRTTs65	

Figure 3.7 Variation of (a) f and (b) f_t/f_p at given Reynolds number for STTs and SRTTs	67
Figure 3.8 Variation of thermal performance factor at given Reynolds number for STTs and SRTTs	68
Figure 3.9 Variation of (a) Nu and (b) Nu_t/Nu_p at given Reynolds number	69
Figure 3.10 Variation of (a) f and (b) f_t/f_p at given Reynolds number.....	71
Figure 3.11 Variation of thermal performance factor at given Reynolds number	73
Figure 3.12 Experimental value versus prediction of Nusselt number	74
Figure 3.13 Experimental value versus prediction of friction factor	74
Figure 3.14 SRTTs versus plain twisted tapes at the Reynolds number of 12000-45000: (a) Nusselt number and (b) Friction factor	76

Chapter 4

Figure 4.1 (a) Structure of SRTTs; (b) Perforated SRTTs, for different PRs.....	86
Figure 4.2 (a) Fabricated tube with an observational section; (b) Digital tachometer RPM meter in the contactless mode	88
Figure 4.3 Diagrammatic sketch of the test bed.....	88
Figure 4.4 Experimental results versus empirical correlations results: Nu.....	93
Figure 4.5 Experimental results versus empirical correlation results: f	93

Figure 4.6 Relationship between the rotation speed (RPM) and the Reynolds number (The red circles denote the initial phase of rotation behavior) 94

Figure 4.7 Variation of (a) the Nu and (b) the Nu_t/Nu_p ratio with Re for the SRTTs with different PRs 96

Figure 4.8 Variation of (a) the f and (b) the f_t/f_p ratio with Re for the SRTTs with different PRs 98

Figure 4.9 Variation of the η with the Re for SRTTs with different PRs (Red arrow denotes the change of the SRTTs from the stationary to rotation condition) 100

Figure 4.10 Comparison of the experimental and predicted Nusselt numbers for the SRTTs with different PRs 101

Figure 4.11 Comparison of the experimental and predicted friction factors for the SRTTs with different PRs 101

Figure 4.12 Comparison of f of perforated SRTTs and those of perforated PTTs..... 102

Chapter 5

Figure 5.1 Schematic diagram of the test bed.....111

Figure 5.2 (a) The circular tube designed with observational section; (b) Rotational speed measurement: Digital tachometer RPM meter with contactless mode 112

Figure 5.3 (a) The structures of the SRTTs; (b) short-length SRTTs with different length ratios..... 113

Figure 5.4 Validation test for the plain tube: Nu 118

Figure 5.5 Validation test for the plain tube: f	118
Figure 5.6 Variation in the rotational speed (RPM) as a function of the Re number	119
Figure 5.7 Variation of heat transfer performance with Reynolds number: (a) Nu and (b) Nu_t/Nu_p	121
Figure 5.8 Variation of friction factor with Reynolds number: (a) f ; (b) f_t/f_p	123
Figure 5.9 η vs Re for SRTTs at different length ratios (Colored arrow means that SRTTs changed from stationary to rotating conditions)	124
Figure 5.10 Experimental results versus predicted results for the SRTTs with different length ratios: Nu.....	125
Figure 5.11 Experimental results vs predicted results for the SRTTs with different length ratios: f	126
Figure 5.12 Comparisons of the thermal performance factor between short-length SRTTs and short-length twisted tapes (TT)	127

List of Tables

Table 3.1: Various Configurations of twisted tapes.....	51
Table 3.2: Details of experimental setup	57
Table 4.1: Previous studies on the correlations of twisted tape	82
Table 5.1: Previous research on application of various twisted tape	107
Table 5.2: Uncertainties of experimental parameters	116

Nomenclature

A	Surface area	m^2
c_p	Specific heat of water	$\text{Jkg}^{-1}\text{K}^{-1}$
D	Tube diameter	m
f	Friction factor	[-]
h	Heat transfer coefficient	$\text{W/m}^2\text{K}$
I	Current	A
L	Length of test tube	m
LR	Length ratio	[-]
m	Mass flow rate	kg/s
Nu	Nusselt number	[-]
ΔP	Pressure drop	Pa
Pr	Prandtl number	[-]
PR	Perforated ratio	[-]
Q	Heat transfer rate	W
Re	Reynolds number	[-]
T	Temperature	K
\bar{T}	Mean temperature	K
V	Voltage	V
\bar{V}	Volume	m^3
v	Fluids velocity	m/s
W	Twisted tapes width	m

Y	Twist ratio	[-]
-----	-------------	-----

Greek symbols

λ	Thermal conductivity	W/m ² K
-----------	----------------------	--------------------

μ	Dynamic viscosity	Pa·s
-------	-------------------	------

ρ	Density	kg/m ³
--------	---------	-------------------

η	Thermal performance factor	[-]
--------	----------------------------	-----

ε	Thickness of tube	m
---------------	-------------------	---

Subscript

b	Bulk
-----	------

$conv$	Convective
--------	------------

c	Cold water
-----	------------

h	Hot water
-----	-----------

i	Inner
-----	-------

in	Inlet
------	-------

o	Outer
-----	-------

out	Outlet
-------	--------

p	Plain tube
-----	------------

pp	Pumping power
------	---------------

s	Surface
-----	---------

t	Tube with twisted tapes
-----	-------------------------

w	Water
-----	-------

CHAPTER 1

INTRODUCTION

1.1 Introduction

Accompanying with industrial development, overpopulation and overconsumption, global energy demands has been on a rise in the past decades. Most of energy generation comes from power plants which are mainly relying on various fossil fuels, such as coal, oil and natural gas. Heat transfer devices (e.g. heat exchangers) play significant role in extracting primary energy from these fossil fuels for energy supply. In order to maximize the thermal efficiency of heat exchangers, much efforts were made on investigating various techniques of heat transfer enhancements. Heat transfer enhancement techniques can be broadly classified into three types, including active method, passive method and compound method. Without external energy being involved, passive method of heat transfer enhancement is preferred over the two other methods which is widely utilized in many practical applications. Generally, passive method of heat transfer enhancement techniques is to modify the surface property and geometry of flow channel or to introduce inserts and additives. Among these passive techniques, twisted tapes are often adopted by engineers due to their simple structure and easy installation. The twisted tapes have been considered

as swirl flow generator to induce stronger turbulence intensity that could disrupt thermal boundary layer and promote fluids mixing.

Efforts have been made by previous researches to investigate various configurations and fabrications of twisted tapes in heat exchanger tube. S. Eiamsa-ard et al. [1] have investigated oblique delta-winglet twisted tape and straight delta-winglet twisted tape with different depth wing cut ratios ($DR=0.11, 0.21$ and 0.32) and twist ratios ($Y=3, 4$ and 5). Their results concluded that oblique delta-winglet twisted tapes performed better efficient thermal performance than straight delta-winglet twisted tape. Hong et al. [2] studied overlapped multiple twisted tapes with different overlapped twisted ratios from 0.74 to 2.97 . They reported that the maximal thermal performance factor could be obtained with value of 1.08 for overlapped twisted ratio of 0.74 . In addition, the thermal characteristic of cross hollow twisted tape inserts in the tube has been explored by previous researchers. Their experimental results showed that the increase of hollow width could result in the decrease of Nusselt number and friction factor [3]. Piriyaarungrad et al. [4] attempted experimentally to investigate the thermal behavior of multiple twisted tapes in heat exchanger tube at Reynolds number of 6000 to 20000 . It was found that increasing the number of twisted tapes could give augmentation of heat transfer rate as compared with lowering the number of twisted tapes. A numerically study have demonstrated that the use of center-cleared twisted tapes could improve the thermal performance factor by $7-20\%$ relatively compared with the conventional twisted tapes [5].

Additionally, great efforts have been made on various fabrication to twisted tapes for further improvement of heat transfer. Several conventional twisted tapes with different types of cut were fabricated, such as V-cut [6], U-cut [7], square-cut [8] and peripherally-

cut twisted tapes [9]. Their results showed that these fabrications with proper designs (e.g. depth ratio and width ratio) could improve heat transfer performance with an acceptable rise in pressure drop, thus resulting in an apparent increase in the thermal performance factor. Moreover, a large number of researchers attempted to perforate the twisted tapes with proposed parameters (e.g. porosities [10], perforation diameter and perforation pitch [11,12]). They sought out to find the optimal design of perforation fabrication based on the evaluation of thermal performance. In addition, short-length fabrication has been considered to be applied in various twisted tapes (e.g. conventional twisted tape [13], a new twisted tape [14], helical tapes [15]) for increasing heat transfer with less pressure drop. However, most of them revealed that full-length fabrication should be an alternative solution for enhancing thermal performance of heat exchangers maximally.

In order to achieve higher thermal efficiency, many researchers paid much attention on combining different twisted tapes with other methods of heat transfer. Considering high capacity of thermal conductivity, some researchers explored the combined effects of different nanofluids and diverse twisted tapes on enhancement of heat transfer, like dimpled twisted tapes and $\text{Al}_2\text{O}_3/\text{water}$ [16], twisted tapes and $\text{Al}_2\text{O}_3/\text{water}$ [17], twisted tapes and CuO/water [18]. Mostly, the combination of nanofluids with the maximum volume concentration and twisted tapes were found to offer greater performance in form of Nusselt number and thermal performance factor as compared with those with those with lower volume concentration. Besides, various twisted tapes and other passive methods of heat transfer have been extensively studied as well. For example, twisted tapes and corrugated tube [19], helical rib roughness and centre-cleared twisted tape [20] as well as

groove tube and twisted tapes [21]. The studies have proven that such combination could play positive role in improving the thermal performance of heat exchanger system.

Most relevant studies mainly adopted experimental-based method or numerical analysis to evaluate thermal-hydraulic performance of various twisted tapes. The optimal configuration related to non-dimensional and dimensional parameters could be offered due to numerical and experimental results of thermal performance, such as perforated twisted tapes [10], center-cleared twisted tapes [5] and hollow twisted tapes [22]. Rarely, some researchers have attempted to optimize design parameters of different twisted tapes by utilizing Imperialist Competitive Algorithm (ICA) [23] and Artificial Neural Network (ANN) [24].

In general, twisted tapes have been adopted in many practical projects because of their low cost, convenient installation and simple manufacturing. They can function in improving thermal efficiency by generating extra swirl flow and turbulence for excellent fluids mixing. Extensive researches have been done to optimize the twisted tapes by evaluating various configurations, fabrications and combining with other methods. Nowadays, a novel type of twisted tapes, namely self-rotating twisted tapes (SRTTs) have been commercialized for many heat transfer devices. SRTTs is defined as a device that can rotate automatically when working fluids flow through the tube with high velocity. Unlike other previous twisted tapes, there is existence of rotating behavior for SRTTs at the operation condition with larger Reynolds number. SRTTs have been widely adopted due to their ability for solving fouling problem, and fouling can be generated through five stages (e.g. generation, deliver, adhesion, aging, and denudation). The existence of rotation behavior can mitigate the fouling problem during the three stages, i.e. adhesion, denudation

and generation. In addition, it may strengthen the turbulence intensity for greater convective heat transfer. However, limited studies were carried out to comprehensively investigate such twisted tapes. In addition, design parameters and feasible fabrications also have not been explored to optimize the design of SRTTs.

Therefore, this thesis aims to investigate the thermal performance enhancement of a double-pipe heat exchanger fitted with SRTTs experimentally and to examine the effect of various configurations (e.g. twist ratios, perforated ratio and length ratio) on the thermal performance in form of Nusselt numbers, friction factors and thermal performance factors.

1.2 Research objectives

The purpose of this thesis is to evaluate the thermal performance of various SRTTs in form of Nusselt number, friction factor and thermal performance factor in a double-pipe heat exchanger. The main objectives of this thesis are listed as below:

- To compare the thermal performance of SRTTs and STTs in a double-pipe heat exchanger under stationary and rotating conditions. SRTTs and STTs with the same geometry were fabricated to experimentally investigate their discrepancies of thermal performance;
- To explore the effects of twisted ratio and rotational speed of SRTTs on heat transfer and pressure drop characteristics. The rotational speed of all SRTTs with different twisted ratios needed to be measured for analyzing its influences on enhancement of heat transfer. Some correlations varying with twisted ratios are

- proposed to predict Nusselt number and friction factor. Moreover, SRTTs are also compared with plain twisted tapes according to the empirical correlations;
- To explore the influences of perforation ratios and rotational speed of SRTTs on the thermal characteristics. The effects of perforation ratios from 0% to 10.1% on Nusselt number, friction factor and thermal performance factor have been comprehensively studied in turbulence flow. Some correlations associated with perforation ratios can be established for further prediction of thermal performance. In addition, perforated SRTTs will be compared with perforated twisted tapes in terms of thermal performance factor;
 - To study the effects of length ratio and rotational speed of SRTTs on the thermo-hydraulic characteristics. The influences of length ratio on the initial stage of rotating behavior and rotational speed were explored. Besides, the effects of length ratio ranging from 0.3 to 1 are analyzed at the Reynolds number of 12000-45000. Two correlations regarding length ratio were derived to accurately estimate Nusselt number and friction factor. Comparison of short-length SRTTs and short-length twisted tapes are conducted based on experimental results.

1.3 Organization of this thesis

The thesis is divided into six chapters, and details of each chapter are describes as below:

Chapter 1 describes the importance of heat transfer enhancement to improve the thermal efficiency of heat transfer devices for solving energy crisis. Twisted tape as a popular strategy has been widely utilized in many industrial projects. Therefore, this thesis introduces a new type of self-rotating twisted tapes, and the research objectives of this thesis also are concluded in this chapter accordingly.

Chapter 2 extensively reviews previous literatures regarding heat transfer enhancement techniques and twisted tapes. Some statistical results of energy demand and use of fossil fuels are presented, which implies the significance of heat transfer devices. Then, categories of heat transfer enhancement techniques are listed out. Afterwards, some passive methods of heat transfer enhancement are summarized, such as coiled tube, corrugated tube and ribbed tube. A large number of research on various twisted tapes, application of twisted tapes and as well as twisted tapes and other methods are extensively reviewed. At the end, some research gaps of conventional twisted tapes and research methods used in this study are displayed as well.

In Chapter 3, an experiment was conducted to compare the thermal performance of SRTTs and STTs in a double-pipe heat exchanger in turbulence flow. SRTTs and STTs with same geometry (e.g. twisted ratio, thickness and width) are fabricated. Heat transfer rate, Nusselt number and thermal performance factor under stationary and rotating condition are investigated, respectively. Then, the effects of twist ratio and rotational speed on the enhancement of heat transfer are explored experimentally. Rotational speed of SRTTs with different twisted ratios are recorded at steady state. The relationship between thermal performance and rotational speed of rotating behavior is analyzed. Heat transfer and pressure drop characteristics in the tube fitted with SRTTs at different twisted ratios

are identified. According to the measured experimental data, some correlations regarding twist ratio are proposed to further calculate the thermal performance in form of Nusselt number and friction factor.

Chapter 4 implements perforation fabrication to SRTTs for strengthening the thermal efficiency of heat exchangers. SRTTs with four perforation ratios (PR=0%, 1.16%, 3.63%, 6.46%, and 10.1%) are prepared to study the effects of perforation ratio on thermal behavior. The role of perforation ratio in affecting rotational speed is investigated experimentally. The combined influences of perforation ratio and rotational speed are analyzed based on the experimental results. Similarly to Chapter 3, some correlations of perforation ratio are provided for the prediction of Nusselt number and friction factor.

In Chapter 5, SRTTs with different length ratios are successfully fabricated for enhancing the tube heat transfer with less increase of pressure drop. The experiment is carried out with four length ratios (LR=0.3, 0.4, 0.6 and 1) and Reynolds number of 12000-45000. In the experiment, the rotational speeds of SRTTs with different length ratios were measured. The relationships of length ratio and rotational speed for heat transfer enhancement are discussed. Then, some correlations varying with length ratios are also established according to the experimental data.

Finally, Chapter 6 summarizes major outcomes of this thesis, and gives some useful recommendation for future work to investigate SRTTs.

CHAPTER 2

LITERATURE REVIEW AND RESEARCH METHOD

2.1 Background

In recent decades, population explosion, increase of energy demand and depletion of fossil fuels have been the major roots of energy crisis in developing countries. According to Chinese energy statistical yearbook, the total population increased from 0.912 billion to 1.379 billion and per-capita electricity raised from 306 kWh to 4446 kWh during 1980-2016 [25]. As presented in Figure 2.1, in China, over 80% of energy sources for power generation are still fossil fuels, such as coal, natural gas and petroleum. For the power plants, primary heat of these fossil fuels should be extracted by transferring to heat transfer medium. During the heat transfer process, various heat exchangers can play an important role in making full use of fossil fuels. Therefore, heat exchangers are widely used in power industry and energy recovery systems.

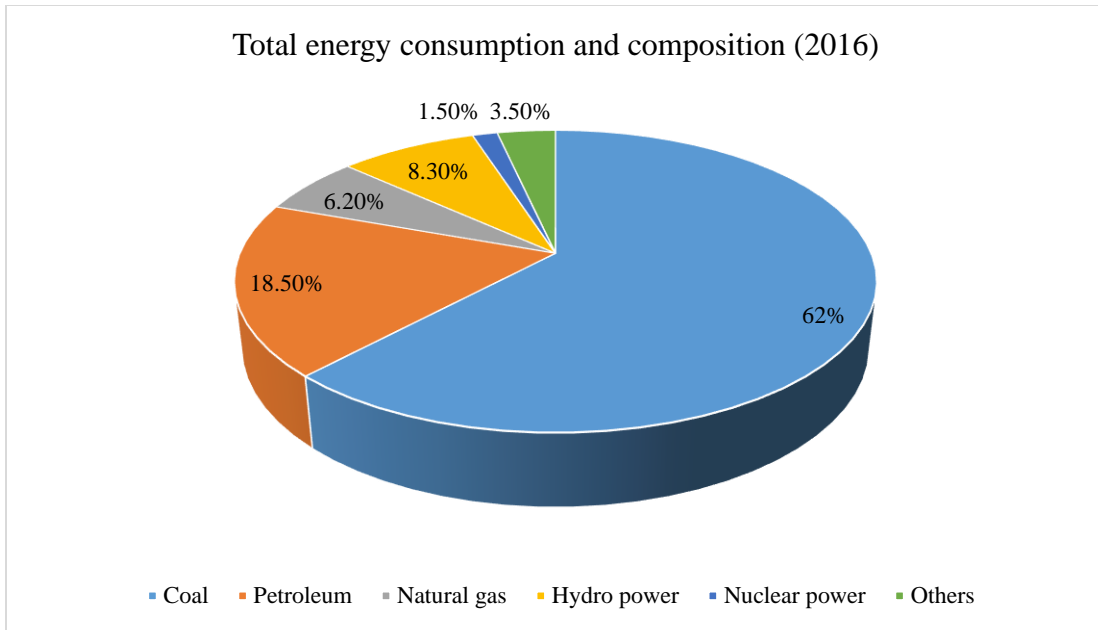


Figure 2.1 Total energy consumption and composition in China (2016) [25]

Heat exchangers are designed to transfer sensible heat between two fluids with temperature differences. Nowadays, different types of heat exchangers have been widely adopted in oil refiners and chemical processing units. For example, shell-and-tube heat exchanger, consisting of a set of tubes in shell side, is applicable to most industrial projects. Plate heat exchangers have turned out to be more efficient with more plates in pairs. In addition, spiral heat exchanger is attractive due to the utilization of weld-seams and head arrangements for solving fouling problems. Among all of them, double-pipe heat exchanger as the simplest one is usually applicable for most industrial projects because of convenience of modifying fluids pattern and structure. Heat transfer enhancement is of great importance to maximize the efficiency of double-pipe heat exchangers. There are a large number of researches conducted to investigate the various techniques of heat transfer enhancement.

2.2 Classification of heat transfer enhancement techniques

2.2.1 Categories of heat transfer enhancement techniques

Extensive techniques of heat transfer enhancement have been invented and studied by previous researchers. They can be broadly categorized into three types: active method, passive method and compound method. Some details of classification of heat transfer enhancement techniques are summarized as Figure 2.2. Active method is defined as the method requiring external energy to maintain intensification mechanism. The combination of active method and passive method for heat transfer enhancement is named compound method. Compared with active method, passive method commonly performed geometrical fabrication and additives to increase thermal performance without any external energy involved. Many passive methods of heat transfer enhancements are reviewed in the following section.

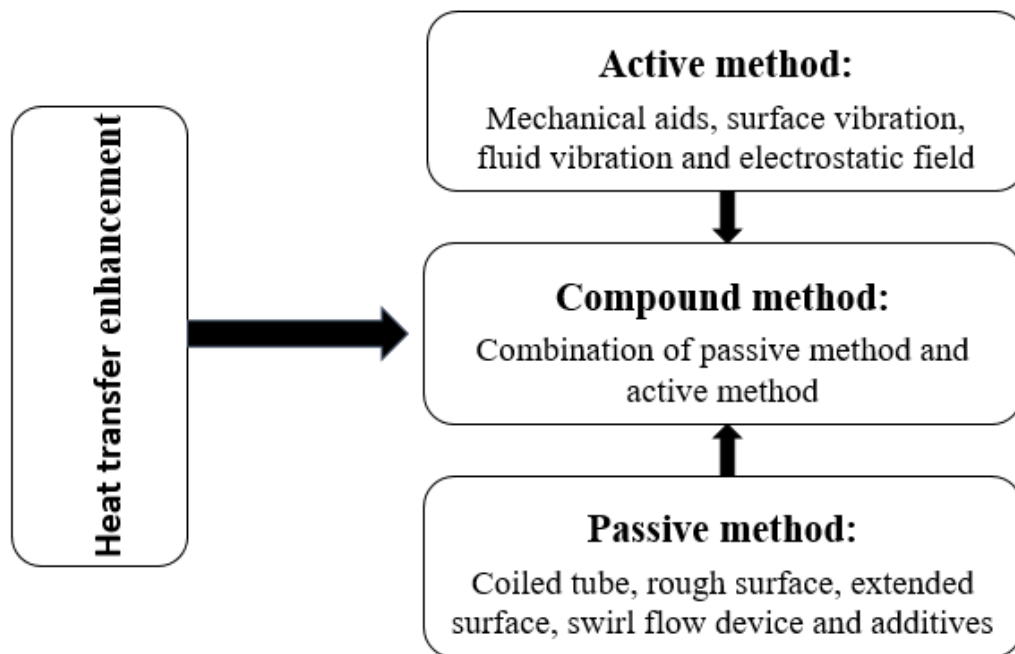


Figure 2.2 Introduction of heat transfer enhancement techniques

2.2.2 Some passive methods in heat exchanger

Coiled tube or shell and coil heat exchanger are often adopted as small unit in energy recovery devices. Many attempts have been made to optimize the design of coiled tube. Salimpour [26] studied helically coiled tube in shell-and-tube heat exchanger with different coil pitches and flow pattern, as shown in Figure 2.3. Their results reported that the decrease of coiled pitch and counter-flow configuration could significantly improve heat transfer rate in tube side. In addition, Zhao et al. [27] have investigated H-type finned oval tube with longitudinal vortex generators and dimples in terms of heat transfer and erosion characteristics. They pointed out that such arrangements could raise the overall thermal efficiency and the anti-wear performance. Ghorbani et al. [28] have explored different arrangements of coil pitch and tube diameters coil-in-shell heat exchanger. Some correlations were established to find the most optimal operation condition in coiled tube based on thermal characteristic.

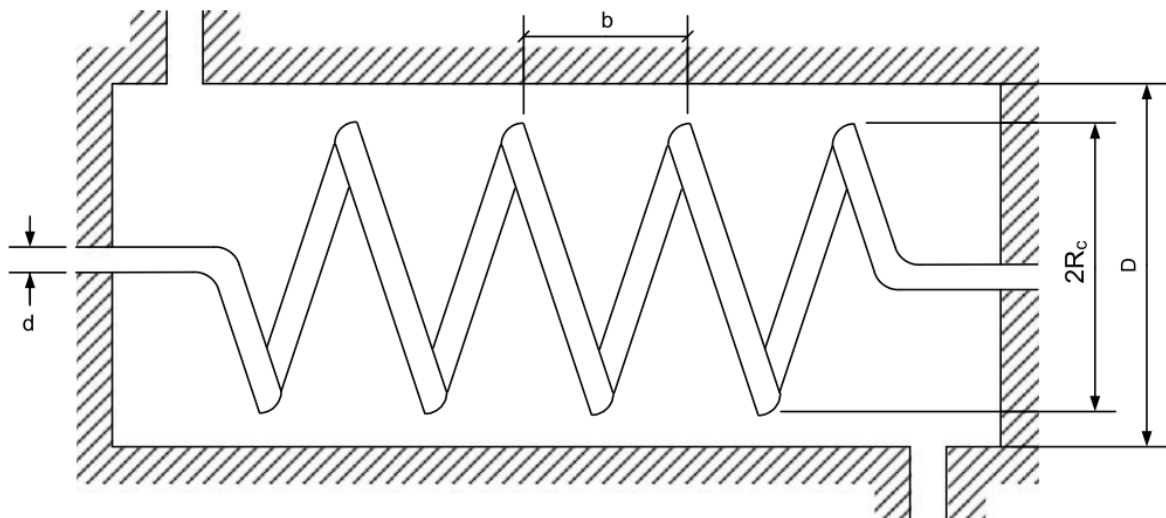


Figure 2.3 Typical coiled tube in heat exchangers [26]

Additionally, many efforts have been made to improve the thermal performance in corrugated tube. Yang et al. [29] have explored oil and water as working fluids in spirally corrugated and smooth tubes. In previous researches, spirally corrugated tube was proved to offer a higher heat transfer rate of 30-120% and a larger friction factor of 60-160% compared with smooth tube. Pethkool et al. [30] have studied helically corrugated tube with different pitch-to-diameter ratios and rib-height to diameter ratios. The two types of tubes were demonstrated in Figure 2.4. It was observed that the maximum thermal performance factor of 2.3 could be obtained at pitch-to-diameter ratio of 0.27 and rib-height to diameter ratio of 0.06. Furthermore, a comparative study has demonstrated that the helically corrugated tube performed more excellent behavior than the smooth corrugated tube for Newtonian and non-Newtonian fluids [31]. In addition, Laohalertdecha and Wongwises [32] have investigated the effects of corrugation pitch on heat transfer and pressure drop characteristic of horizontal corrugated tube in R-123a. Their results revealed that the decrease of corrugation pitch could somehow increase the heat transfer coefficient and friction factor.

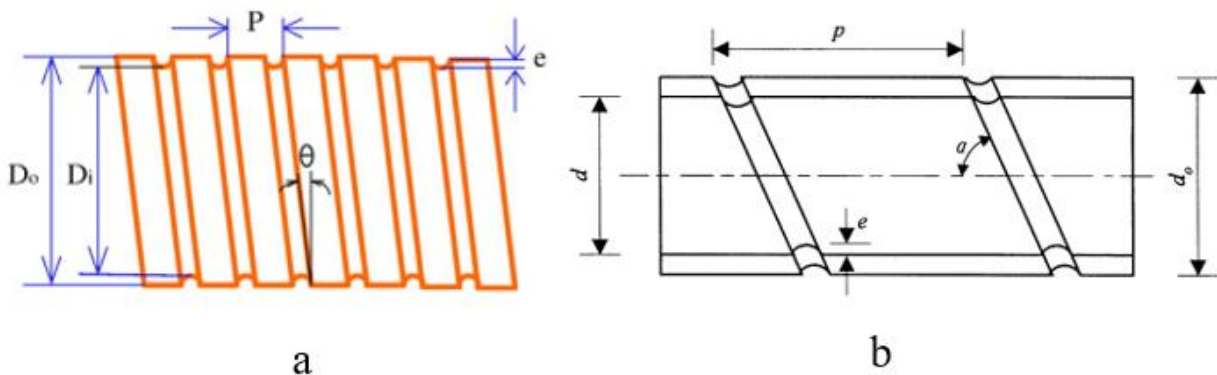


Figure 2.4 (a) Helically corrugated tube [30]; (b) Spirally corrugated tube [29]

Various fins have been widely utilized in heat transfer devices for further improvement of heat transfer rate. Sanaye and Hajabdollahi [33] have used genetic algorithm to optimize design of plat fin heat exchanger according to thermal-economic performance. An optimal solution of plat fin regarding fin pitch, fin height, fin offset length and stream flow is proposed based on results of case study. Peles et al. [34] explored the effects of microscale pin fin on performance of forced convective heat transfer. They found that relative lower thermal resistance could be achieved when using such microscale pin fins. Moreover, previous researches have studied the geometrical parameters of offset strip fin in laminar, transition and turbulence flows. Some correlations associated with geometrical parameters were proposed to predict the Colburn factor and friction factor [35]. Jang and Chen [36] have experimentally and numerically investigated the influences of variable louver angles on thermal efficiency. The optimal solution for variable louver angles could save 48.5-55.2% heat transfer area maximally.

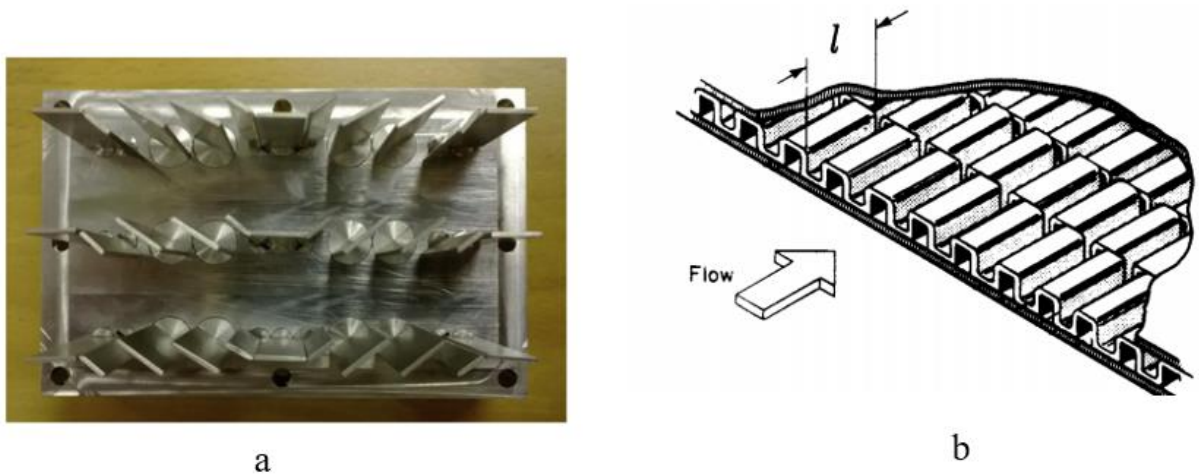


Figure 2.5 (a) louvered fin [36]; (b) typical offset strip fin [35]

Also, ribbed tubes have been considered as a feasible solution to increase the turbulence for heat transfer augmentation. Han and Park [37] have investigated rib turbulator with rib angle-of-attack of 30° , 45° , 60° and 90° in Reynolds number of 10000 to 60000. They proved that the largest heat transfer performance could be reached for rib angle-of-attack of 60° in square channel and angle-of-attack of 90° in rectangular channel. Then, Han and Zhang [38] have studied the effects of rib angle-of-attack for parallel broken and V-shaped broken ribs on thermal performance. Their results showed that the rib angle-of-attack of 60° performed greater heat transfer coefficient for both of parallel broken and V-shaped broken ribs. A numerical study investigated the thermal characteristic of a microchannel with rectangular rib at laminar flow. It was found that the maximum performance factor of 1.85 could be achieved with rib width of 0.13 and rib length of 0.5 [39]. Zheng et al. [40] have studied the flow characteristic of the tube fitted with various rib arrangements (e.g. parallel type rib and V shape type ribs, as shown in Figure 2.6). The V shape type ribs were demonstrated to be more efficient for heat transfer due to the stronger longitudinal swirl flow.

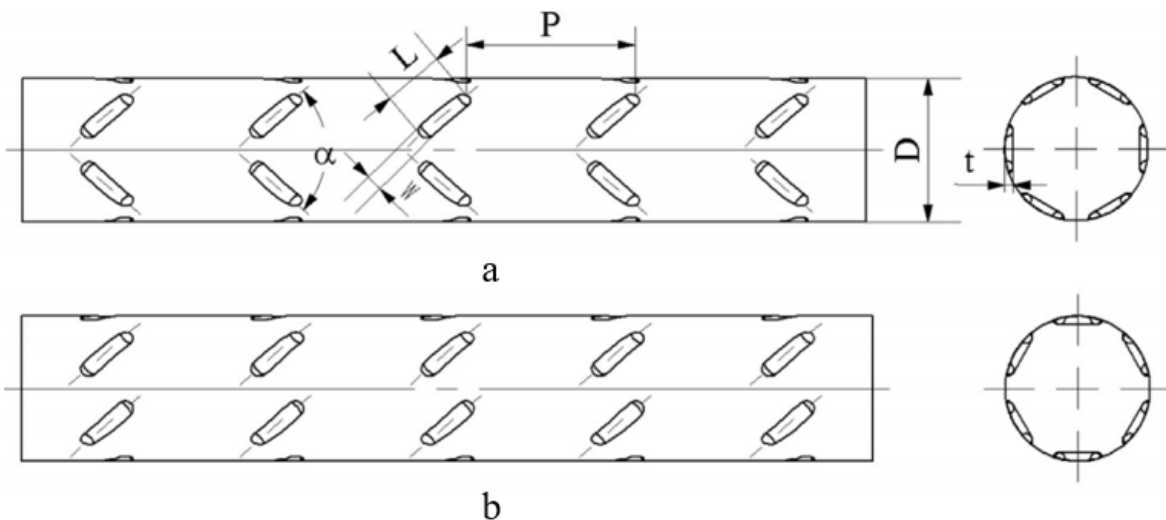


Figure 2.6 (a) V shape type ribs; (b) Parallel type rib [40]

In recent years, some researchers attempted to add nanoparticles into the base fluids for higher thermal conductivity. Xuan and Li [41] have studied the thermal properties of CuO/water with different volume concentrations. It was found that the thermal conductivity of CuO/water can be increased from 1.24 to 1.78 times of base fluids for volume concentration from 2.5% to 7.5%, as shown in Figure 2.7.

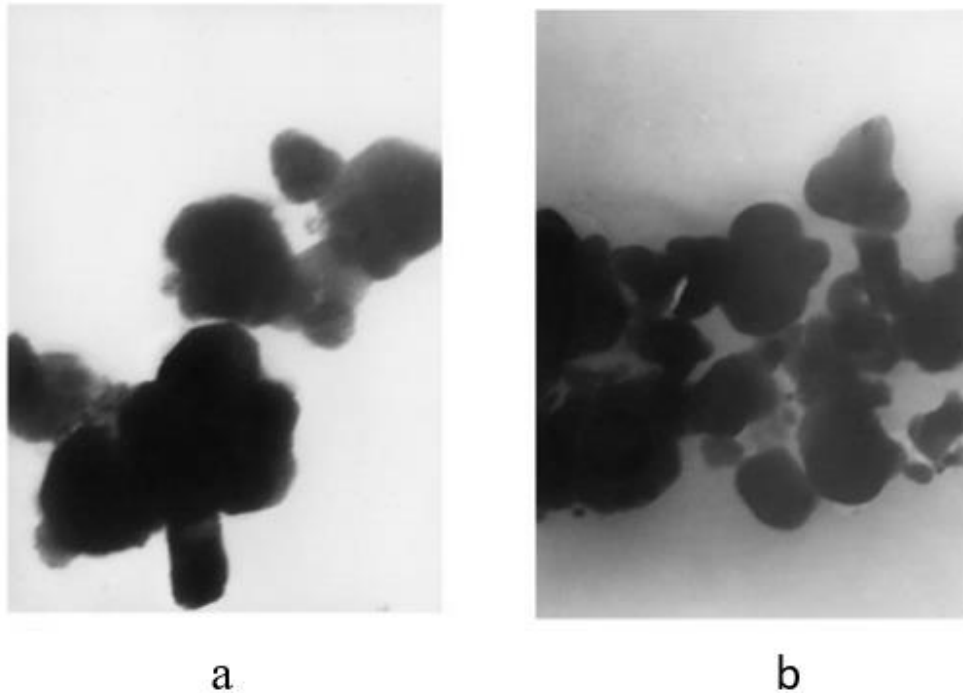


Figure 2.7 TEM micrographs: (a) CuO/water nanofluids with 5 vol%; (b) CuO/water nanofluids with 7.5 vol%. [41]

In addition, Albadr et al. [42] also conducted an experiment to investigate the convective heat transfer performance and flow characteristic in Al_2O_3 /water nanofluids. Their results represented that the friction factor and Nusselt number increased significantly with the increase of volume concentration. Similarly, Duangthongsuk and Wongwises [43] have reported that the use of TiO_2 /water with volume concentration of 0.2% could improve the heat transfer coefficient by 6-11%. Moreover, thermal performance in Fe_2O_3 /water with

different mass friction (0.1%, 0.2%, 0.3% and 0.4%) were experimentally explored. Increase of mass friction and Reynold number were demonstrated to both promote heat transfer rate [44].

2.3 Introduction of twisted tapes

2.3.1 Enhancement mechanism and performance criteria

Twisted tapes as swirl flow generator have been widely utilized to modify heat exchanger system. Researchers have attempted to understand the mechanism of heat transfer enhancement for proper utilization of twisted tapes. As presented as Figure 2.8 (a), flow pattern in plain tube is very smooth that almost no tangential velocity exists between core and near wall regions. Given the insertion of twisted tapes, it is observed that flow patterns are altered significantly due to the interaction between mainstream and a crosswise edge of tapes, as illustrated in Figure 2.8 (b). The centrifugal force generated by swirl flow along tangential direction could promote excellent fluids mixing between core and near wall regions. Such swirl flow or secondary motion could serve as inducing stronger turbulence intensity that leads to reduction of hydraulic diameter and thickness of thermal boundary layer. Due to the existence of flow blockage caused by twisted tapes, fluids velocity and residence time in near wall region increase significantly that is also responsible for augmentation of convective heat transfer.

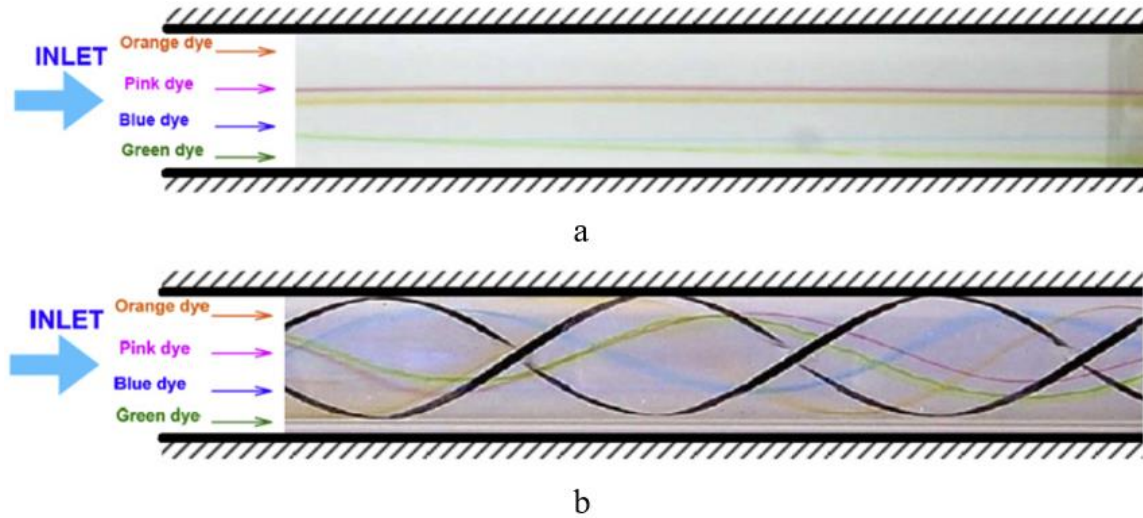


Figure 2.8 Flow pattern in (a) plain tube and (b) the tube with twisted tapes [45]

There are some non-dimensional parameters commonly used to assess different twisted tapes, such as Nusselt number, friction factor and thermal performance factor. Generally, the use of twisted tapes in heat exchanger tube could not only raise the heat transfer coefficient but also increase the friction factor. Although higher heat transfer rate could save energy or reduce heat transfer area but larger friction factor also consumed more pumping power. For overall performance appraisal, performance factor has been often adopted, which is defined as the Nusselt number ratio between the tube fitted with twisted tape and plain tube at constant pumping power. It is expressed as below:

$$\eta = \frac{h_t}{h_p} \Big|_{pp} = \frac{(Nu_t / Nu_p)}{(f_t / f_p)^{1/3}} \quad (2-1)$$

2.3.2 Various configuration of twisted tapes

A large number of studies previously focus on various configuration and dimension of twisted tapes. These researches not only examined thermal-hydraulic performance of

different twisted tapes but also provided some correlations associated with corresponding parameters for prediction of thermal performance. A main parameter of twisted tapes is twist ratio (Y), which is defined as the half of pitch length to tapes width. Some studies have investigated the thermal performance of twisted tapes with different twist ratios ($Y=3, 4.5$ and 6) in laminar and turbulence flow. They have found that heat transfer rate and pressure drop both displayed negative correlation with twist ratios [46, 47]. In addition, Naga Sarada et al. have studied effects of varying width of twisted tapes on thermal characteristic in Reynolds number of 6000-13500. Full-width twisted tapes (width=26 mm) were demonstrated to raise Nusselt number by 36-48% and 33-39% as compared with plain tube and short-width twisted tapes [48]. Also, full-length twisted tapes were shown to significantly improve Nusselt number and thermal performance factor in comparison of short-length twisted tapes [13]. Moreover, Esmailzadeh et al. [17] experimented on twisted tapes with different thickness in Al_2O_3 nanofluid. They pointed out that the increase of thickness resulted in considerably raise of heat transfer rate and friction factor.

Various configurations of twisted tapes have been investigated by experimental and numerical studies. A newly modified twisted tape with different length (600-2400 mm) have been explored experimentally. They found that such twisted tape could significantly improve Nusselt number to 1.15-1.37, 1.18-1.45, 1.23-1.55 and 1.45-1.90 times of plain tube [14]. Chang et al. [49] tried to explored broken twisted tapes with different twist ratios ($Y=1, 1.5, 2$ and 2.5), and revealed that decrease of twist ratio lead to increase of thermal performance in form of Nusselt number, friction factor and thermal performance factor. Under constant heat flux, Eiamsa-ard et al. [1] conducted an experiment on oblique delta-winglet twisted tape and straight delta-winglet twisted tape with different twist ratio in

Reynolds number of 3000-27000. Oblique delta-winglet twisted tape was found to perform greater thermal performance than straight delta-winglet twisted tape.

Additionally, Eiamsa-ard and Promvonge [50] have shown that serrated twisted tape plays more predominant effects on convective heat transfer as compared with typical twisted tapes for investigated cases. The increase of width ratio was found to improve Nusselt number, friction factor and thermal performance factor. In addition, clockwise and counter-clockwise twisted-tape inserts with different twist angles were experimentally studied under uniform heat flux conditions. The tube fitted with twist angle of 90° could achieve the highest thermal performance factor of 1.34, 1.4 and 1.43 for twist ratios of 5, 4 and 3 [51]. Piriyarungrod et al. [52] have prepared tapered twisted tape with different taper angles and twist ratios for experimental study in turbulence flow. The maximum thermal performance factor could be achieved for twist tapes with the lowest twist ratio and largest tapered angle. A numerical study have proved that use of center-cleared twisted tape could obtained higher thermal performance factor by 7-20% in comparison of conventional twisted tapes [5].

Li et al. [22] have compared cross hollow and conventional twisted tapes numerically. Cross hollow twisted tapes with smaller hollow width was considered to perform overall better thermal performance by 28.1%. Another type of twisted tapes, named regularly spaced twisted tape, were experimentally investigated with different space ratios. The results showed that the increase of space ratio leads to the increase of heat transfer rate and friction factor [53]. By using CFD simulation, the jagged twisted tapes were demonstrated to significantly increase the mean Nusselt number and thermal performance factor by 31% and 22% respectively [54]. Hong et al. [2] conducted experiments on the thermal

characteristic of overlapped multiple twisted tapes with air as working fluids. The highest thermal performance factor of 1.08 could be reached with the lowest overlapped twisted ratio.

In addition, some researchers have sought out to further improve the heat exchanger heat transfer by inserting more twisted tapes and arranging different flow pattern in heat exchanger tubes. Chokphoemphun et al. [55] have comprehensively investigated the thermal performance of the tube fitted with different numbers of twisted tapes arranged by co- and counter-twist arrangements. They reported that quadruple counter-twisted tape was considered to be more effective for convective heat transfer in turbulence flow. Similarly, double counter twisted tapes with different ratios were studied in a circular tube with air as working fluids, and the friction factor and Nusselt number could increase by 91-286% and 60-240% in comparison of plain tube [56]. Likewise, Bhuiya et al. [57] have conducted an experimental study to explore the triple twisted tapes with different twist ratios at Reynolds number of 7200-50200. It was observed that the performance indicator in form of Nusselt number, friction factor and thermal performance factor increased due to the reduction of twist ratio.

Many researchers attempted to study the effects of perforation fabrication for different twisted tapes on thermal characteristic. For example, Bhuiya et al. [10, 58] have prepared perforated typical and double-counter twisted tapes with different porosities in turbulence regime. They suggested that alternative porosities of 4.5% could provide the highest thermal performance factor. Thianpong et al. [12] have proposed some correlations regarding perforated diameter and perforated spaced-pitch length to calculate Nusselt number, friction factor and thermal performance factor. Nanan et al. [11] have studied the

tube equipped with perforated helical twisted tapes at Reynolds number of 6000-20000. They found that the maximum thermal performance factor could be achieved at diameter ratio of 0.2 and perforation pitch length ratio of 0.2.

In addition to perforation fabrication, various cut to twisted tapes have been adopted to further strengthen the heat exchanger thermal efficiency. Eiamsa-ard et al. [9] have studied the effects of peripherally-cut twisted tape in laminar and turbulence regime. It was found that the increase of peripherally-cut depth ratio and decrease of peripherally-cut width ratio could raise thermal performance. A comparative study has reported that use of V-cut could considerably reinforce heat transfer rate as compared with plain twisted tapes, and proposed some correlations associated with depth and width ratios for prediction of Nusselt number and friction factor [6]. Murugesan et al. [8] have proved that square-cut consistently performed higher heat transfer coefficient as compared with plain twisted tapes at twist ratios of 2, 4.4 and 6. Nakhchi and Esfahani [59] have numerically confirmed that existence of rectangular cut indeed improve Nusselt number and thermal performance factor. Similarly, another experimental study compared trapezoidal-cut and plain twisted tapes at different twist ratios, and utilization of trapezoidal-cut twisted tapes were verified to result in significant performance improvement [60].

2.3.3 Application of twisted tapes

Due to the multiple advantages in low cost, convent installation, easy manufacture and heat transfer enhancement, various twisted tapes have been popular to be utilized in different applications. In addition to heat exchanger system, twisted tapes have been adopted to improve efficiency of other heat transfer devices. Mokkaapati and Lin [19] have

combined twisted tape inserts and corrugated tube to improve performance of exhaust heat recovery system. They found that the use of twisted tapes and corrugated could effectively increase heat transfer rate by 235.3% annularly. Eid et al. [61] also tended to optimize a beta Stirling refrigerator by involving multiple twisted tapes. The results reported that the performance of the refrigerator could be improved by 32%, and the enhancement ratio raised with the increasing number of twisted tapes.

Also, several studies have been conducted to optimize performance efficiency of solar collector system by incorporating twisted tapes. Jaisankar et al. [62] have experimented on twisted tapes with spacer at the trailing edge used for solar water heating system. They pointed out that full-length twisted tapes with twist ratio of 3 could maximize the thermal performance. Then, Jaisankar et al. [63] have employed helical twisted tapes with different twist ratios inside solar water system. Their results revealed that lower twist ratios could strengthen the rate of heat transfer and friction factor, and some correlations regarding twist ratios also were proposed and validated based on experimental results. In addition, left–Right twisted tapes have been inserted into solar water heating system for better performance improvement, and twisted tapes equipped with rods or spaced could reduce heat transfer coefficient by 11% and 19% in comparison of full-length twisted tapes [64]. Saravanan and Jaisankar [65] have experimentally tested the thermal characteristic of diverse twisted tapes (e.g. helix twisted tape and helix twisted tape with square cut or V cut) in V trough solar collector. Helix twisted tape with V cut appeared to result in greater Nusselt number compared with those with square cut.

In order to provide the optimal solution of a parabolic solar collector with twisted tapes, Borunda et al. [66] used multi-objective genetic algorithms to evaluate design

parameter of mass flow rate and twist ratios. They pointed out smaller mass flow rate and lower twist ratio could be alternative choice to enhance thermal efficiency. Jaramillo et al. [67] have experimented on parabolic trough solar collector fitted with twisted tape inserts for low enthalpy processes. They found that insertion of twisted tapes in the tube could significantly enhance thermal efficiency as compared with plain tube. In addition, Mwesigye et al. [68] have numerically examined the performance of a parabolic trough receiver with wall-detached twisted tape inserts according to entropy generation analysis. The results reported that the maximum decrease in the entropy generation rate could be 58% by employing such twisted tapes.

2.4 Twisted tapes and other heat transfer enhancement methods

2.4.1 Twisted tapes and surface modification

In order to induce stronger swirl flow for excellent convective heat transfer, some attempts have been done to combine various twisted tapes and fabricated surfaces in heat exchanger tube. Zimparov [69, 70] has conducted some experiments to study the heat transfer and friction factor characteristic in corrugated tube fitted with twisted tapes. The model mentioned in his studies revealed that the corrugated tube and twisted tapes could strengthen wall roughness that leads to axial velocity and tangential velocity for enhancing thermal performance. Hasanpour et al. [7] have comprehensively compared the various twisted tapes (e.g. typical, perforated, V-cut and U-cut twisted tapes) in helically corrugated tube. They found that the corrugated tube fitted with all twisted tapes could

significantly improve the Nusselt number and friction factor. In the turbulence flow with Reynolds number of 10000 to 50000, Bhattacharyya et al. [71] have conducted experiments on spring tapes in corrugated tube. Their results showed that the most effective performance could be achieved with smaller spring ratio and pitch ratio. The corrugated tubes in the previous studies are shown in Figure 2.9.

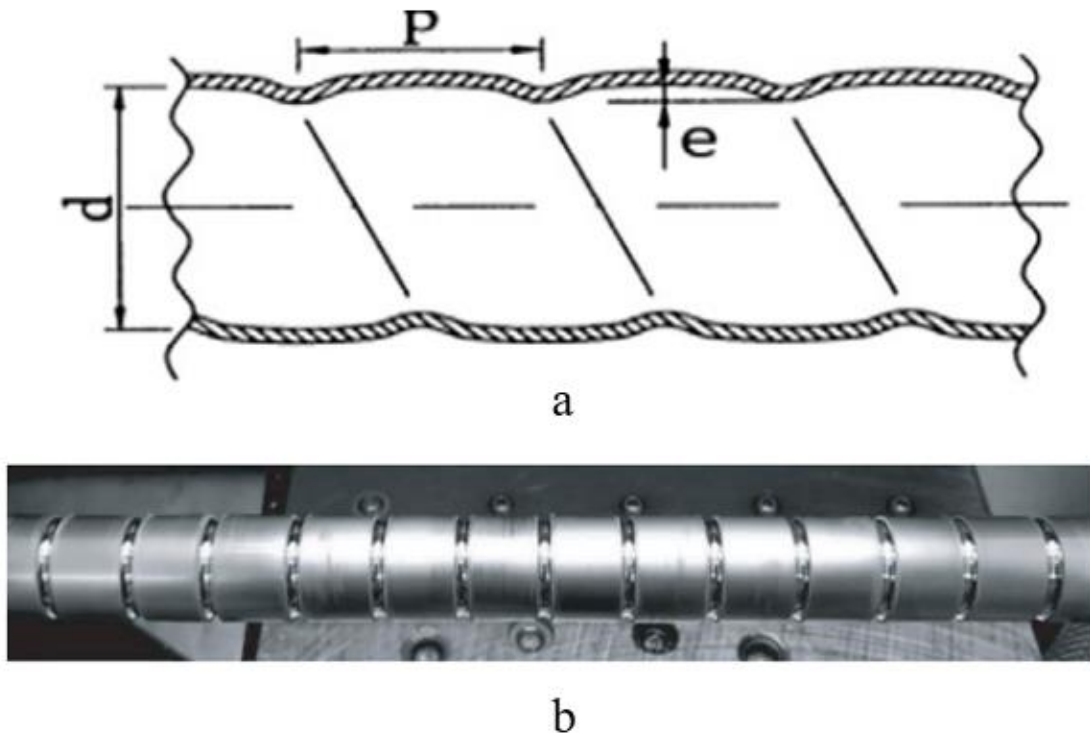


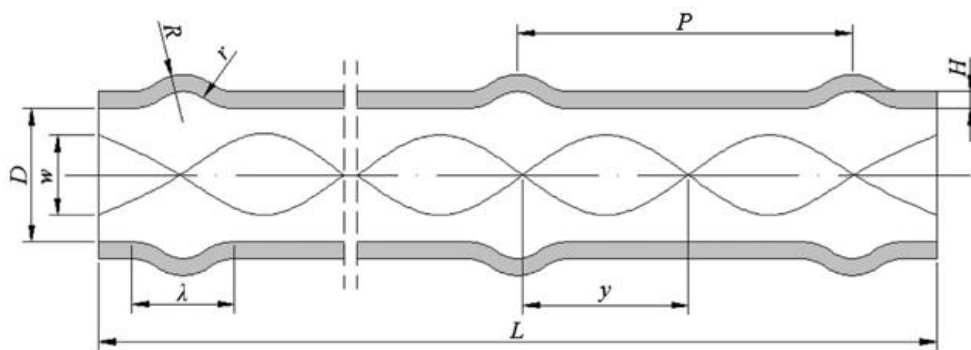
Figure 2.9 Corrugated tube: (a) Schematic diagram [7]; (b) Picture diagram [71]

Apart from corrugated tubes, researchers have attempted to manufacture heat exchanger tube with various geometries to be integrated with twisted tapes. Bharadwaj et al. [21] have explored the effects of twisted tapes in a spirally grooved tube on heat transfer and pressure drop. Such combination indeed could function in enhancing heat transfer rate as compared with smooth tube. In addition, double twisted tapes in a helical-ribbed tube have been experimentally investigated in turbulence flow. The experimental results

confirmed that employment of double twisted tapes is an effective solution for energy saving especially at low Reynolds number [72]. Hong et al. [73] also experimentally investigated the spiral grooved tube equipped with overlapped large/small twin twisted tapes. They demonstrated that such combination could improve the mean Nusselt number by 131–177%, 125–168%, 120–153%, and 113–140% for different twisted ratios in comparison of plain tube. Saha et al. have conducted several studies to investigate the center-cleared twisted-tapes in tubes prepared with axial corrugations [74], integral axial rib roughness [20] and integral helical rib roughness [75].



a



b

Figure 2.10 (a): Helical-ribbed tube and double twisted tape; (b) corrugated tube with loose-fit twisted tape

A large number of studies have been carried out to combine micro-fin tube and different types of twisted tapes for improvement of heat transfer. Al-Fahed et al. [76] firstly experimentally evaluate the micro-fin tube equipped with twisted tapes by comparing with plain tube and micro-fin tube. They found that the thermal performance could be enhanced significantly by using micro-fin tube and twisted tapes. In addition, Eiamsa-ard [77] has employed double twisted tapes in micro-fin tube for further improvement of thermal efficiency. It was seen that micro-fin tube fitted with double twisted tape in opposite direction could increase thermal performance factor by 9.3%, 6.5% and 56.4% compared with (1) micro-fin tube and double twisted tapes with co-swirl, (2) micro-fin tube and double twisted tape with opposite direction, and (3) micro-fin tube alone. Then, Eiamsa-ard and Wongcharee [78] have studied micro-fin tube and non-uniform twisted tape in Ag/water nanofluids. The highest improvement of heat transfer rate of 112.5% and thermal performance factor of 1.62 could be obtained by using uniform twisted tape with lower twist ratio and micro-fin tube. A new type of twisted tapes, named left-right twisted tapes, was also experimentally explored in micro-fin tube at range of turbulence flow. Some correlations regarding twist ratios were suggested for left-right twisted tapes used in micro-fin tube [79].

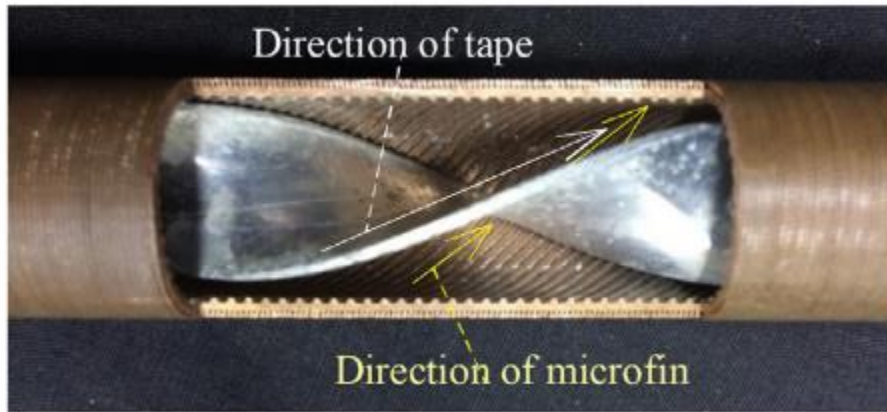


Figure 2.11 Micro-fin tube and twisted tapes [79]

2.4.2 Twisted tapes and nanofluids

Generally, heat transfer enhancement techniques mainly focus on modifying the configurations of tube surface for inducing stronger turbulence. Over past years, nanofluids have been paid much attention to be used as working fluids for heat exchanger system, which is defined by nanoparticles suspended in the base fluids. Due to higher thermal conductivity, nanofluids have been combined with twisted tapes as compound method for heat transfer augmentation. Sharma et al. have experimentally investigated thermal performance of twisted tapes in $\text{Al}_2\text{O}_3/\text{water}$ nanofluids under transition and turbulence flow [80, 81]. They found that the use of twisted tapes and nanofluids could significantly improve heat transfer rate compared with twisted tapes and $\text{Al}_2\text{O}_3/\text{water}$ alone, and some correlations associated with twist ratio and volume concentration were suggested to calculate Nusselt number and friction factor. Dimpled twisted tapes with different arrangements have been studied numerically in $\text{Al}_2\text{O}_3/\text{water}$ nanofluids. For all

investigated cases, numerical results showed that such combination could enhance the rate of heat transfer by 58.96%, and the maximum friction factor of 5.05% could be obtained [16]. In range of turbulence flow, Maddah et al. have investigated the thermal behavior in the tube equipped with modified twisted tapes and Al_2O_3 /water nanofluids. It is observed that the increase of 12% to 52% and 5% to 28% for Nusselt number and friction factor could be achieved in comparison of those with typical twisted tapes and Al_2O_3 /water [82].

Additionally, some other metal oxide as nanoparticles have been added to base fluids for heat transfer enhancement. For example, Wongcharee and Eiamsa-ard [83] have employed twisted tapes with alternate axis in CuO /water nanofluids at Reynolds number of 830-1990. It is found that highest thermal performance factor of 5.53 could be reached with twisted tape with alternate axis and volume concentration of 0.7%. Full-length twisted tapes have been employed in Fe_3O_4 magnetic nanofluids for compound effects on heat transfer enhancement. Heat transfer and pressure drop augmentation by 51.88% and 1.231 times could be found in comparison of pure water in plain tube [84]. Azmi et al. [85] also have investigated thermal characteristic of SiO_2 /water in a tube equipped with twisted tape inerts. They found that the maximum increase in heat transfer rate of 94.1% could be reached at twist ratio of 5 and volume concentration of 3%. Moreover, Eiamsa-ard and Kiatkittipong [86] have tried to use TiO_2 /water in a tube equipped with different multiple twisted tape inserts for enhancement in heat transfer. The quadruple counter tapes in the cross directions and volume concentration of 0.21% could offer largest thermal performance factor of 1.59. The SEM or TEM images of various nanoparticles combined with twisted tapes were shown in Figure 2.12.

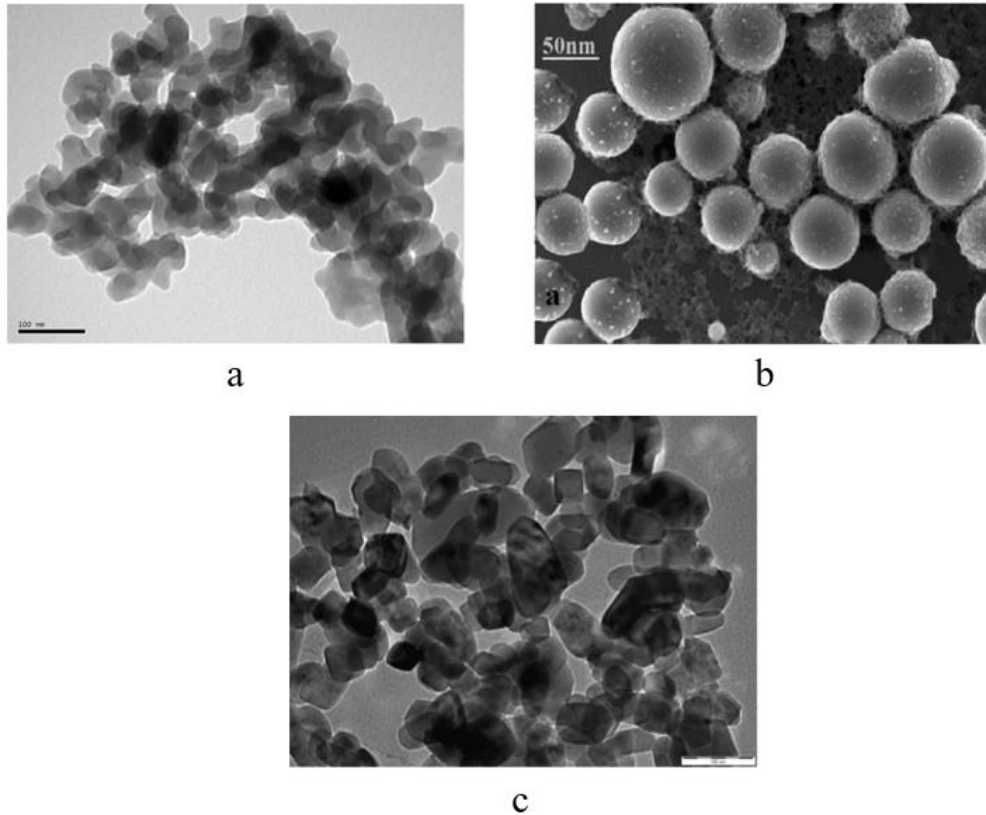


Figure 2.12 SEM or TEM images of various nanoparticles to be combined with twisted tapes: (a) CuO/water [83]; (b) Al₂O₃/water [82]; (c) TiO₂/water [86]

2.5 Research methodology on twisted tapes

Experimental-based method and numerical simulation are the main methods that often adopted to study twisted tapes by previous research. Some algorithms are also used to optimize design parameters of twisted tapes.

2.5.1 Experimental study

A large number of experimental studies have been conducted to explore various twisted tapes. Most experimental work used water or air as working fluids, and controlled operation conditions in laminar and turbulence regimes. They sought out to study the relationship between thermal performance and dimensional or non-dimensional parameters of various twisted tapes experimentally. For example, Esmailzadeh et al. [17] have prepared twisted tapes with different thickness (0.5 mm, 1 mm and 2 mm) utilized in $\text{Al}_2\text{O}_3/\text{water}$ nanofluids. Their results reported that increase in twisted tapes width could significantly increase rate of heat transfer and pressure drop in laminar flow with Reynolds number of 150-1600.

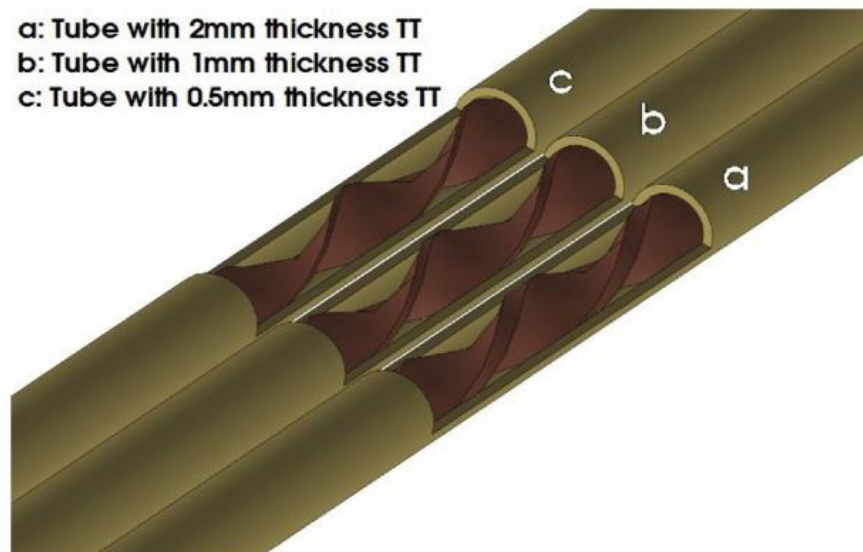


Figure 2.13 Schematic view of twisted tapes with different thickness [17]

Eiamsa-ard et al. [88] attempted to evaluate twisted tapes with centre wings and alternate-axes (WT-A) in turbulence flow. All used WT-As have the constant twist ratio of 3, and they were fabricated with three angles of attack ($\beta=43^\circ$, 53° and 74°). Their results

indicated that larger angles of attack could enhance Nusselt number, friction factor and thermal performance factor. The maximum thermal performance factor of 1.4 could be obtained at lower Reynolds number.

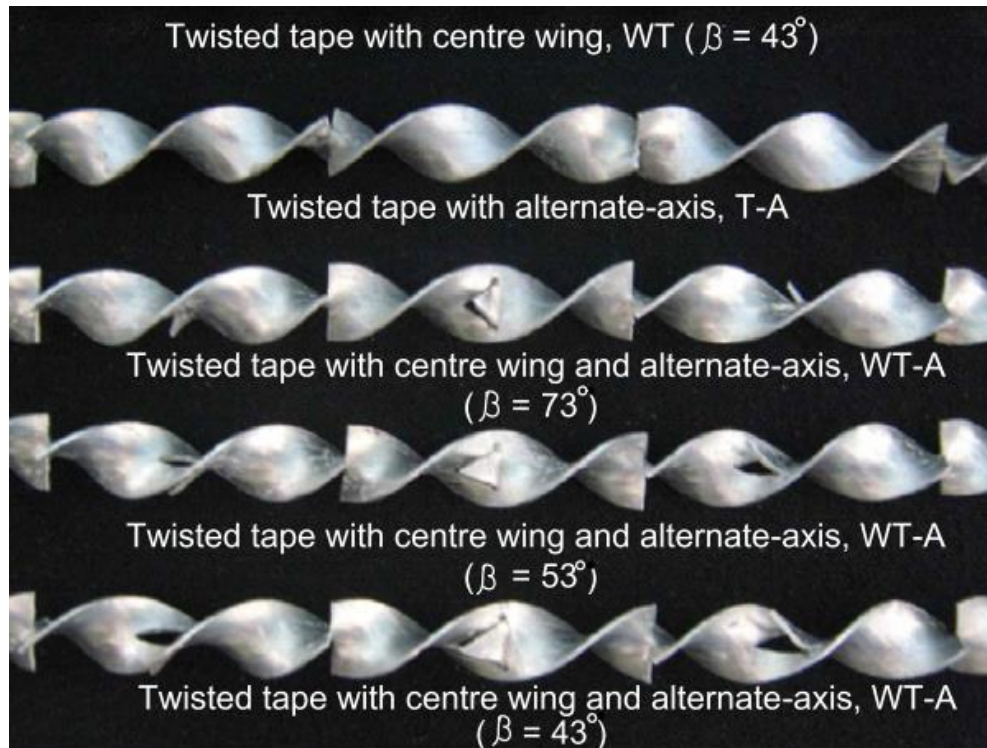


Figure 2.14 Photograph of twisted centre wings and alternate-axes [88]

In addition, an experimental study was conducted to investigate the cross hollow twisted tape with hollow width $C=6$ mm, 8 mm and 10 mm at Reynolds number of 5600-18000 [3]. Reduction of hollow width was found to significantly improve the heat transfer coefficient and thermal efficiency. Increase in Nusselt number and pressure drop by 93%–120% and 883%–1042% could be achieved by using cross hollow twisted tape with hollow width of 6 mm as compared with plain tube.

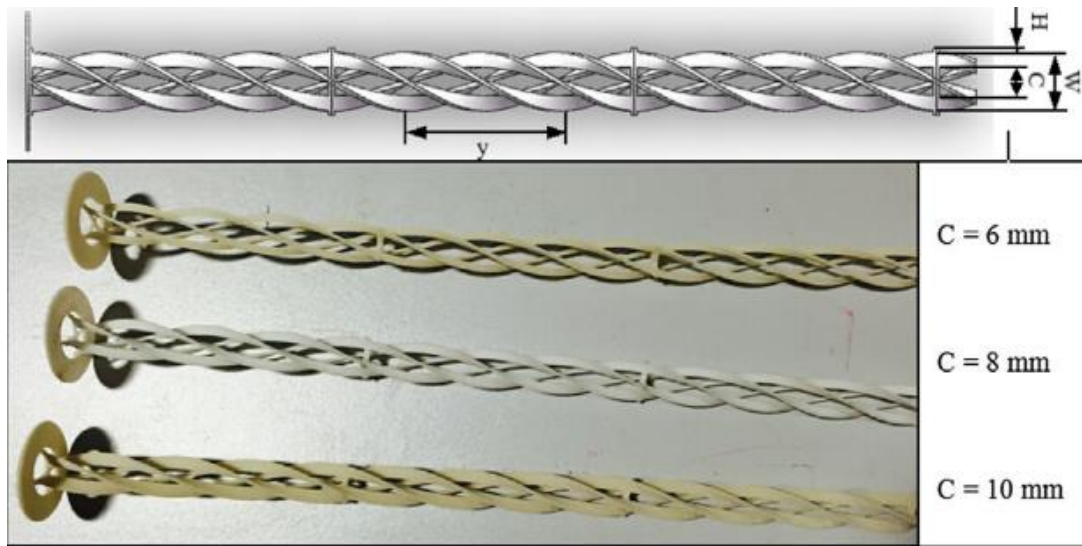


Figure 2.15 Sketch map of cross hollow twisted tape with different hollow width

Besides, Piriyarungrod et al. [52] have designed a tapered twisted tapes with different taper angle ($\theta=0.3^\circ$, 0.6° and 0.9°) for experimental study. The experiment was conducted in turbulence regime with air as working fluids. The results demonstrated larger taper angle resulted in higher thermal performance, and maximum thermal performance factor could be achieved with taper angle of 0.9° .

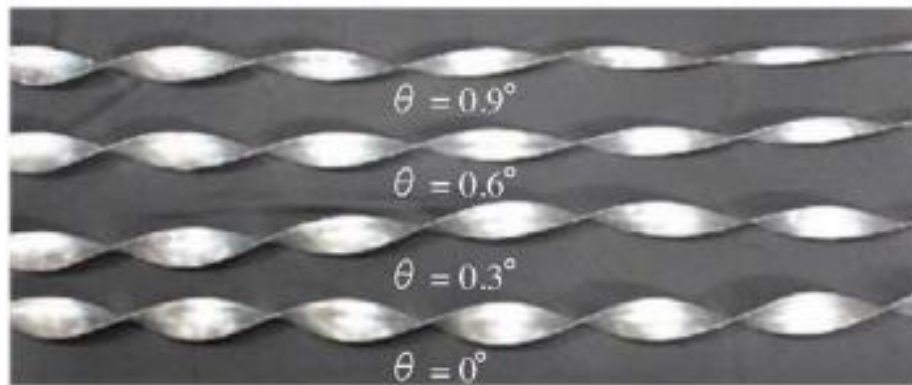


Figure 2.16 Photograph of tapered twisted tapes different with taper angle [52]

Moreover, serrated twisted tapes with serration depth ratio (d/W) and serration width ratio (w/W) were fabricated for improvement of heat transfer enhancement [50]. It is observed that the heat transfer rate could be promoted with reduction in serration width ratio and increase in serration depth ratio. While, higher thermal performance factor could be reached with the smallest depth ratio and width ratio. The maximum thermal performance factor at given Reynolds number was found to be lower than jagged twisted tapes but higher than notched, serrated and perforated twisted tapes.

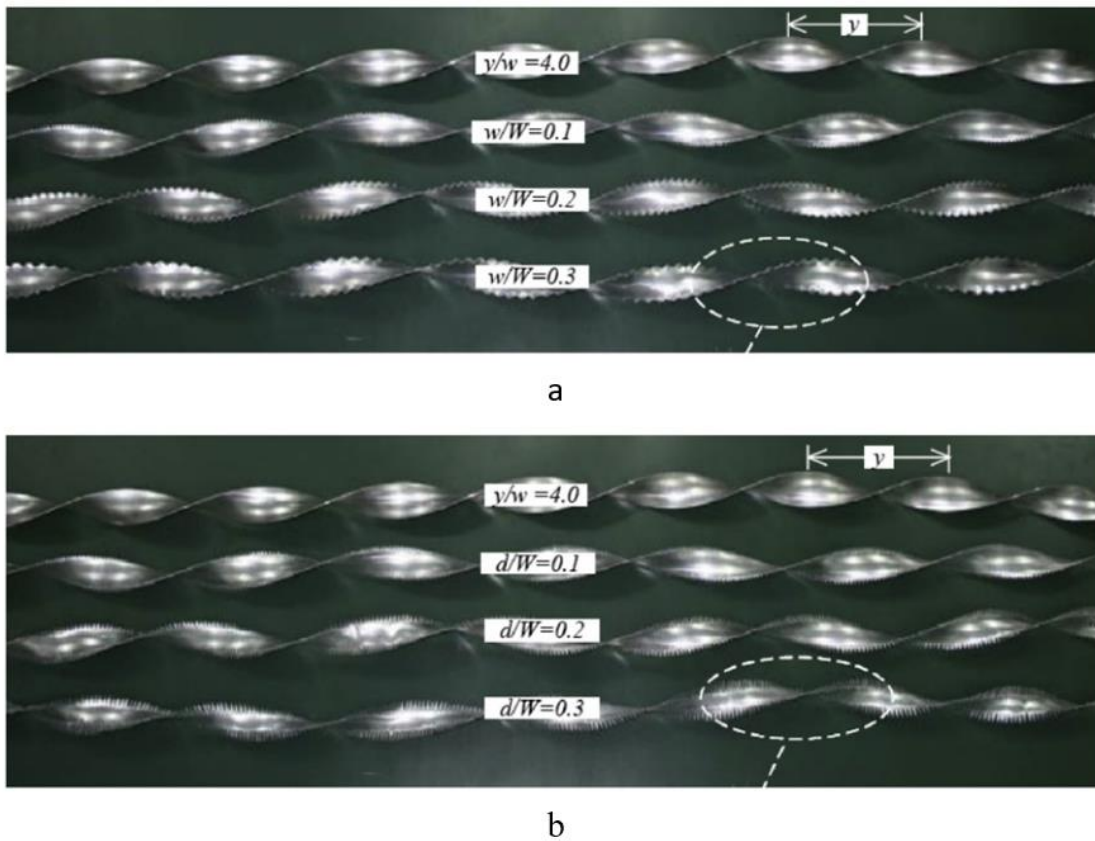


Figure 2.17 Serrated twisted tapes: (a) serration width ratio, (b) serration depth ratio

2.5.2 Numerical study

As the development of computational technology during past years, numerical analysis has been widely used to solve complicated mathematical equations, in particular Computational Fluid Dynamic (CFD). Some govern equations, such as Navier–Stokes equations, are involved to model heat transfer process in numerical analysis. There are several numerical studies implemented to investigate the heat transfer and flow characteristic of the tube fitted with twisted tapes. For example, Eiamsa-ard et al. [89] studied the thermal behavior of loose-fit twisted tapes by using 3D numerical simulation. They presented flow structure of the tube fitted with loos-fit twisted tapes at different clearance ratios ($CR=0, 0.1, 0.2$ and 0.3), as seen in Figure 2.18. The numerical results showed that lower clearance ratios could significantly reduce mean Nusselt number.

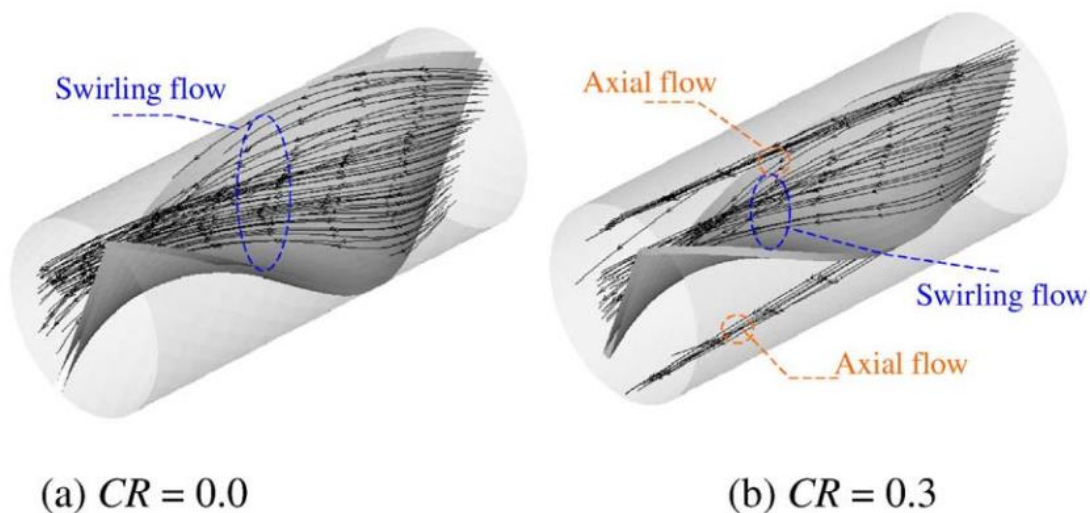


Figure 2.18 Contour plots of flow structure at different clearance ratios [89]

Guo et al. [5] tended to evaluate the thermal-hydraulic performance of center-cleared twisted tapes with central clearance ratio (c). They provided contour plots of velocity and temperature with different width ratios as displayed in Figure 2.19. Also, decrease in

central clearance ratio were found to strengthen heat transfer rate and overall thermal efficiency. Similarly, Li et al. [22] numerically evaluate thermal and flow behavior of central hollow narrow twisted tapes with different hollow width (C) and clearance. The velocity distribution in the tube fitted with this twisted tapes was illustrated as Figure 2.20. Their results have shown that central hollow narrow twisted tapes could perform more excellent thermal performance in comparison of conventional twisted tapes.

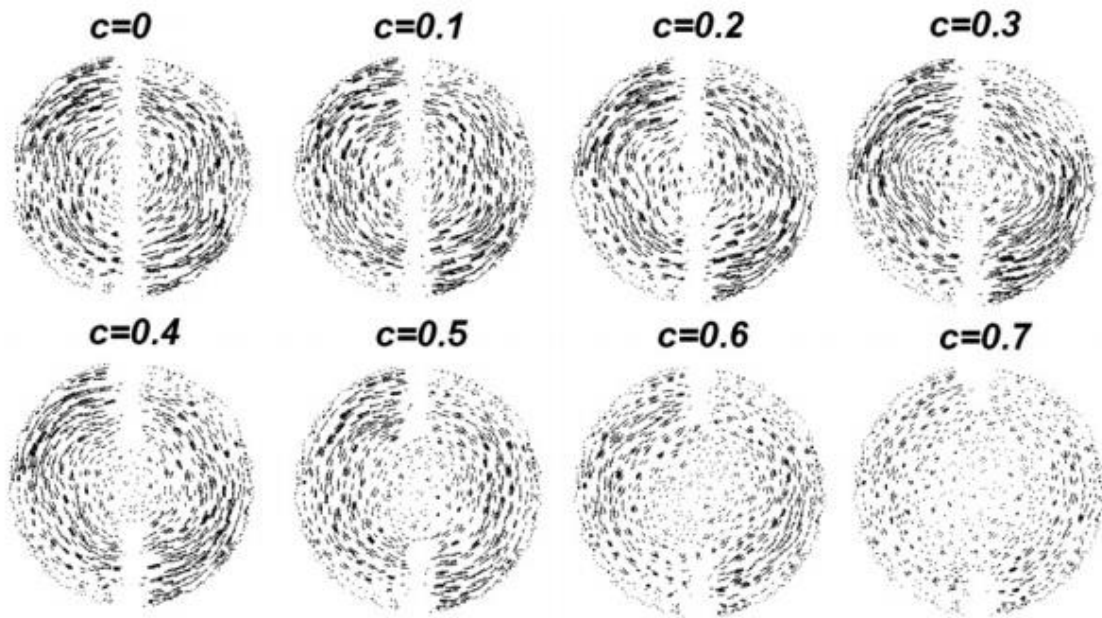


Figure 2.19 Contour plots of tangential velocity for the tube fitted with center-cleared twisted tapes at different central clearance ratios [5]

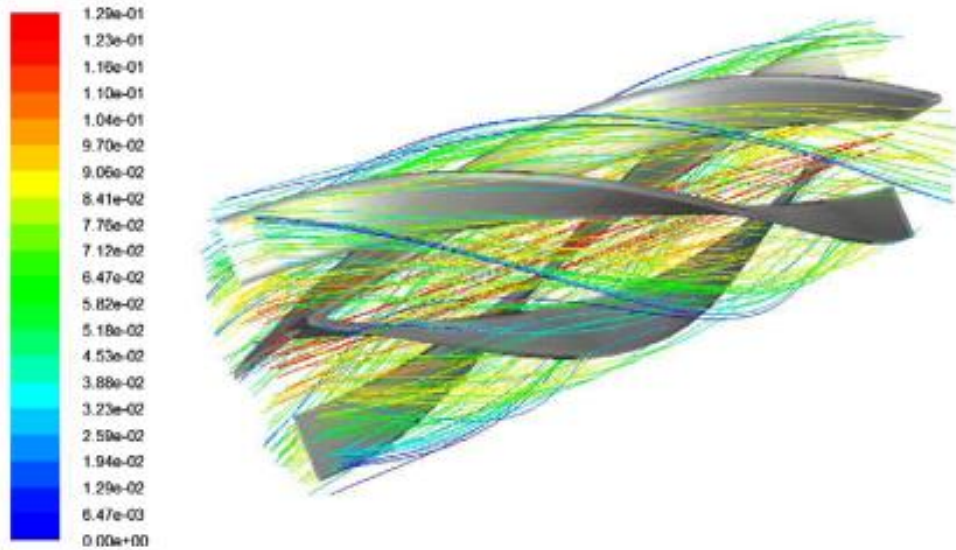


Figure 2.20 Velocity streamline distribution in the cross hollow twisted tapes [22]

In addition, Wang et al. [90] attempted to optimize the configuration parameters (e.g. space ratio, twist ratio and rotated angle) of regularly spaced short-length twisted tapes by using CFD simulation. They suggested that twist ratio of 4.25-4.75, rotated angle of 180° and spaced ratio of 28-33 could be an alternative solution for heat transfer enhancement. Zhang et al. [91] have numerically assessed flow resistance and thermal characteristic of multiple regularly spaced twisted tapes in laminar flow. The velocity profiles of triple twisted tapes with different clearance ratios were displayed in Figure 2.21. The numerical results revealed that Nusselt number could be improved by 171% and 181% by using triple and quadruple twisted tapes as compared with plain tube.

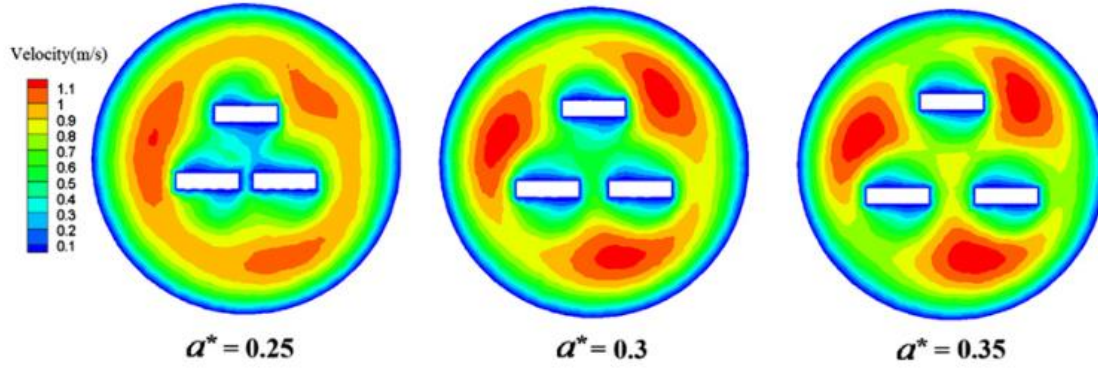


Figure 2.21 Velocity distribution in triple twisted tapes with different clearance ratios [91]

2.5.3 Optimization of twisted tapes based on different algorithms

Thermal design of heat exchangers focuses more on maximizing the heat transfer coefficient with less increase in pressure drop. Many algorithms have been previously utilized to improve overall thermal efficiency of the heat exchanger tube fitted with different twisted tapes. For instance, Karami et al. [23] have investigated the heat transfer characteristic of typical twisted tapes with different ratios from 1.76 to 3.53 in laminar flow. By involving cost function in Imperialist Competitive Algorithm (ICA) as presented in Figure 2.22, the maximum value of Nusselt number could be achieved with the lowest twist ratio of 1.76 according to computational results. Similarly, perforated twisted tapes with variables of hole diameter ratio, twist ratio and free spacing ratio in heat exchanger tube have been studied for optimization and prediction of thermal design by using artificial neural network (ANN) as presented in Figure 2.22 [24]. Their results showed that the correlations from ANN method seem to be more prior than other empirical correlations.

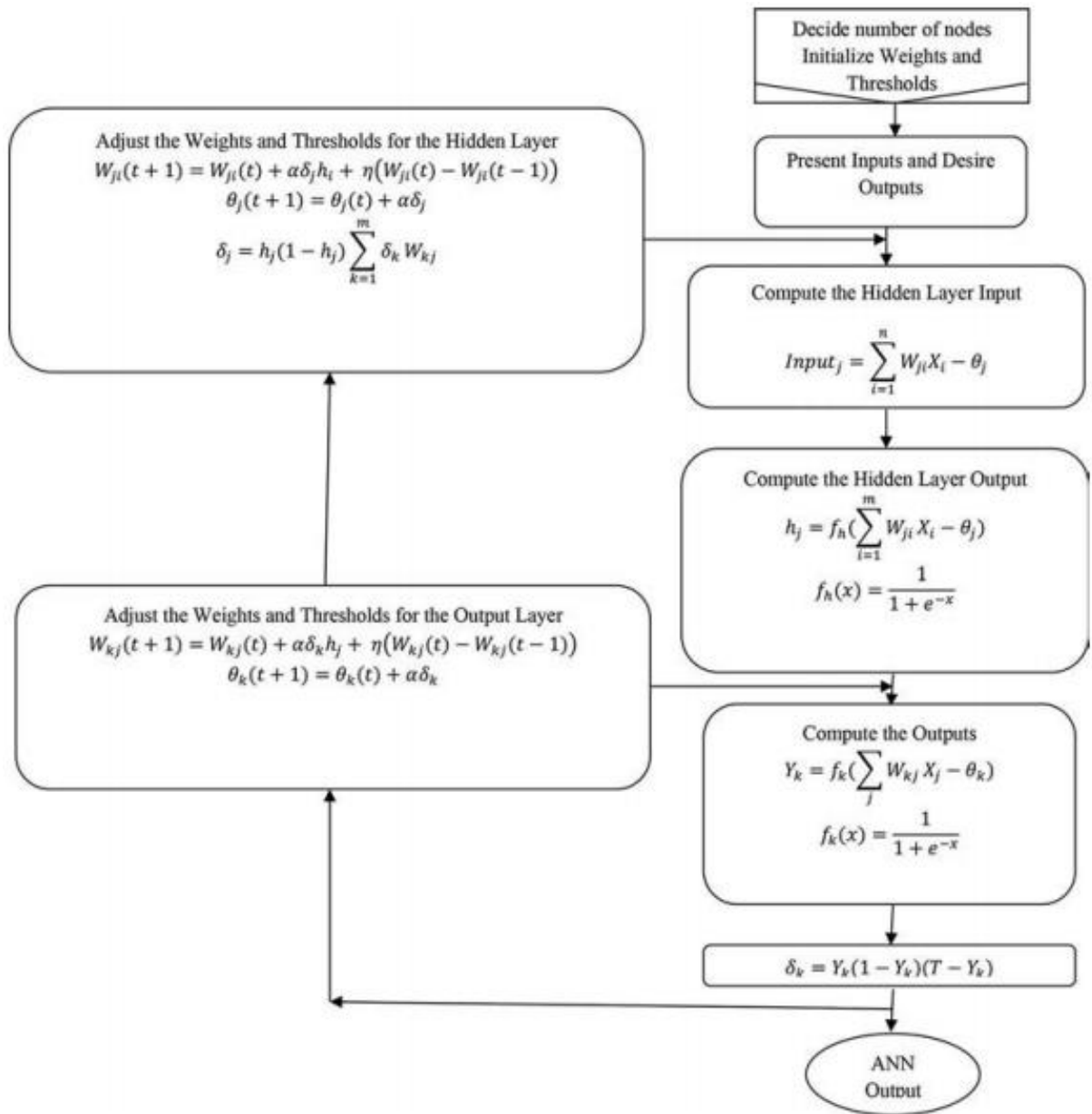


Figure 2.22 Flowchart of ANN method [24]

Han et al. [92] attempted to optimize the corrugated tube equipped with multi-channel twisted tapes by involving Response Surface Methodology (RSM) and Non-dominated Sorting Genetic Algorithm (NSGA-II). The entire procedure to optimize three variables of channel number, twist ratio and Reynolds number are displayed in Figure 2.23. The optimal

design with Reynolds number of 20344, twist ratio of 3.271 and channel number of 5 were suggested based on objective functions related to thermal performance.

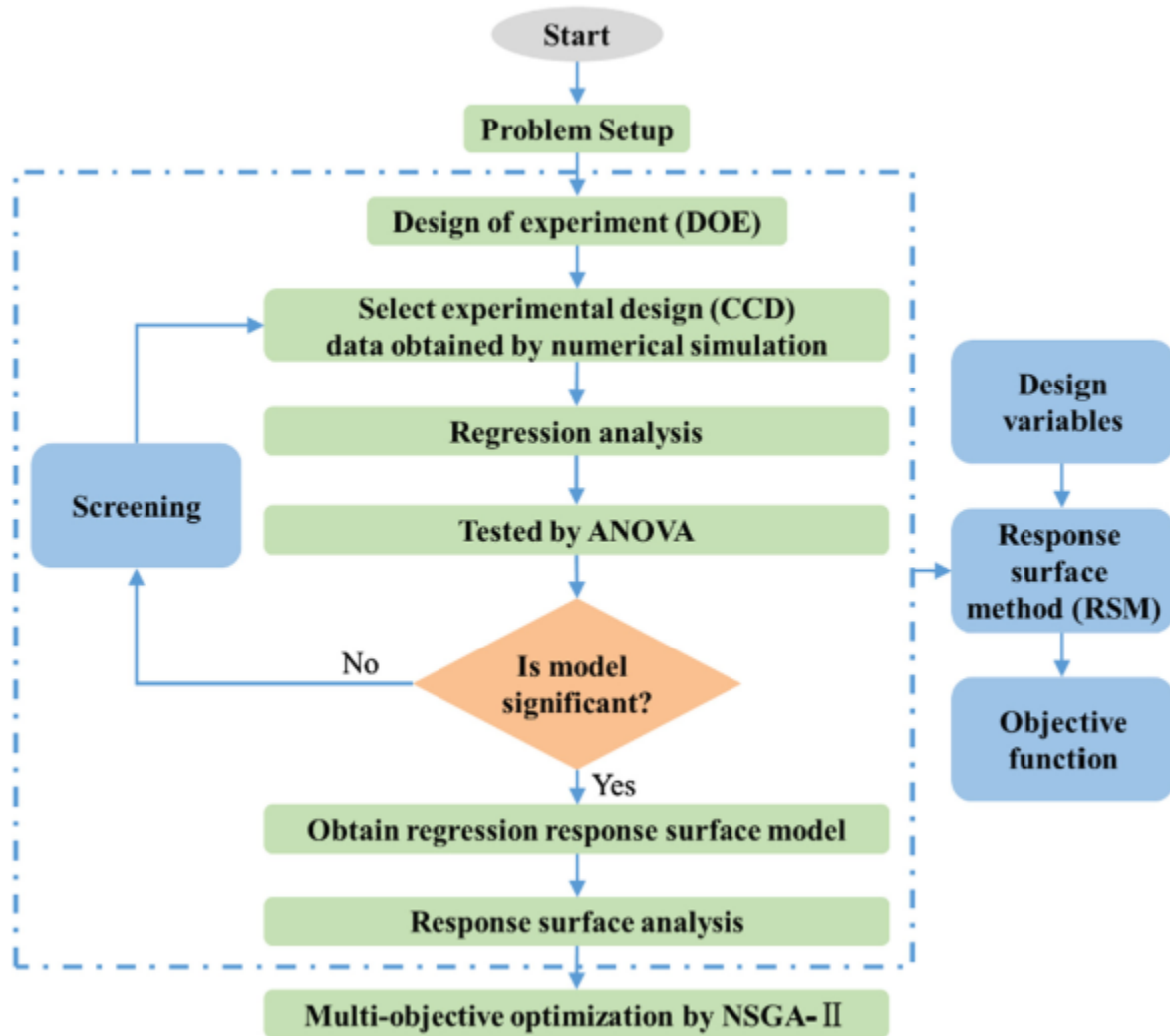


Figure 2.22 Flowchart of optimal design of multi-channel twisted tapes [92]

Additionally, Artificial Neural Network (ANN) is an alternative approach to previously be used for investigation of twisted tapes in corrugated tube [93] and modified twisted tapes in nanofluids [94]. The ANN models used in these studies have been demonstrated to be reliable with less error percentage for prediction of heat transfer and flow resistance characteristic.

2.6 Research gaps and research methodology

As stated above, an amount of previous literatures have been carried out to investigate the various configuration and applications of twisted tapes used for heat transfer enhancement of heat exchangers equipped with twisted tapes. Although previous researches were done to evaluate and optimize the twisted tapes, some research gaps have not been bridged in this research field.

The theoretical gaps in the field have been concluded and listed as below:

- (1) Most twisted tapes investigated in previous work are stationary twisted tapes (STTs). Recently, a new twisted tapes, named self-rotating twisted tapes (SRTTs), have been invented to be widely utilized in heat transfer devices. However, a few studies were conducted to experimentally compare thermal and flow characteristic of SRTTs and STTs in double-pipe heat exchanger.
- (2) Twist ratios as an important parameter have been considered for optimal design of twisted tapes. To best of my knowledge, there were few research implemented to investigate effects of twist ratios on thermal performance in double-pipe heat exchangers.
- (3) Perforation fabrication is a feasible solution to secondary improvement of heat transfer. However, few attentions have been given to combine perforation fabrication and SRTTs to improve thermal efficiency of a double-pipe heat exchangers.
- (4) Short-length fabrication previously has been employed for various twisted tapes to enhance rate of heat transfer within allowable increase of pressure

drop. Nevertheless, a few studies focused on applying short-length fabrication in SRTTs for optimizing thermal performance.

In order to address the mentioned research gaps, experimental studies were carried out to comprehensively explore the various configurations of SRTTs. Theoretical study was also conducted to derive some useful correlations for evaluating the thermal-hydraulic behaviors based on the experimental data. The research flow chart is illustrated in Figure 2.23 to give a brief introduction of this thesis.

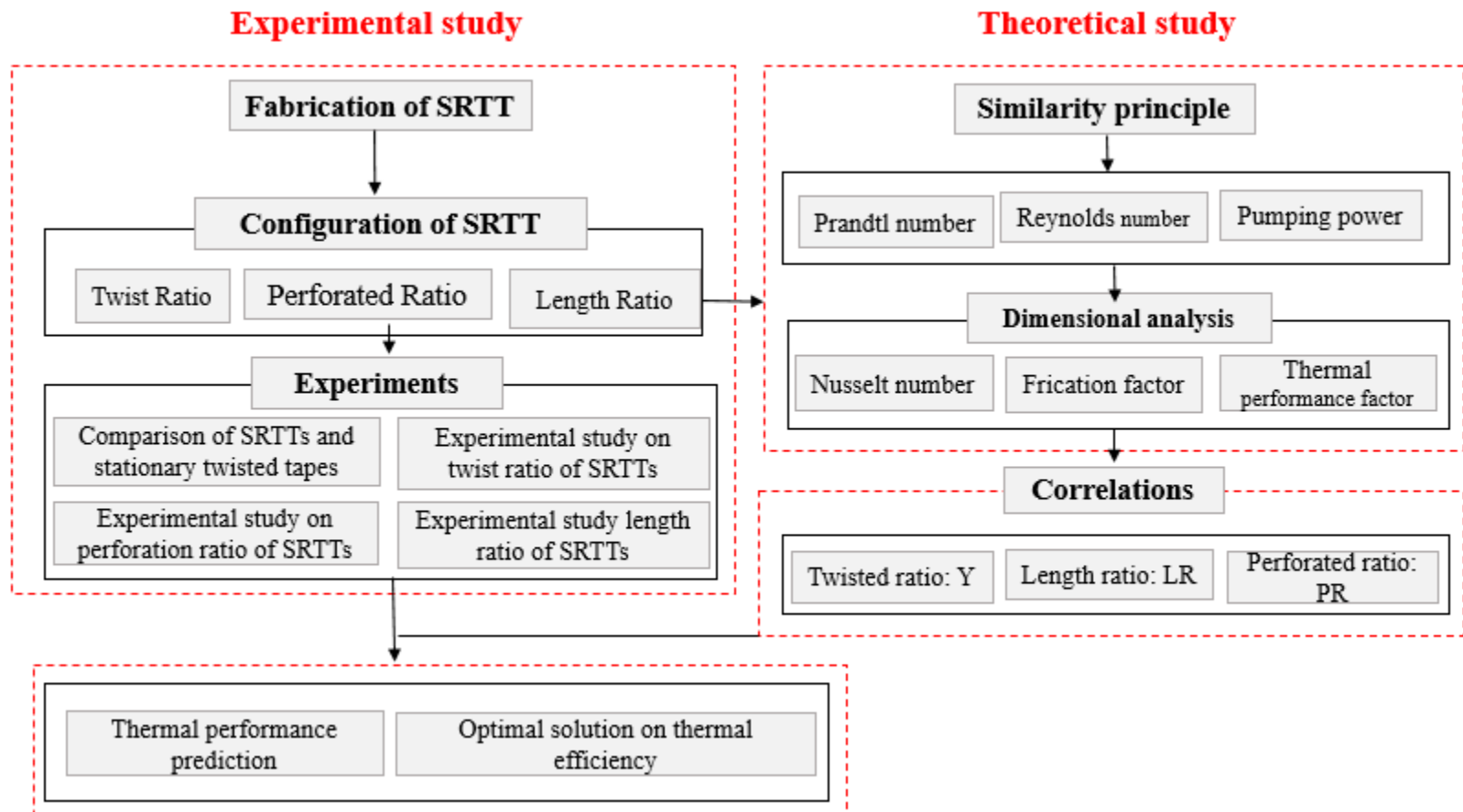


Figure 2.23 Research flowchart of this thesis

First of all, a test bed with a double-pipe heat exchanger, measurement devices, a water tank and a heat sink was prepared. The double-pipe heat exchanger as test section consists of inner tube and outer tube in which hot water and cold water flow through, respectively. In order to compare the thermal performance of SRTTs and STTs, both of them needed to be fabricated with same twist ratio, thickness and length. Then, SRTTs and STTs were employed in double-pipe heat exchanger to be examined at given Reynolds number. Comparison of SRTTs and STTs regarding thermal performance under stationary and rotating conditions is discussed, respectively.

As a main parameter of twisted tapes, the effects of twist ratio on thermal characteristic are analyzed based on the experimental results. The SRTTs used in this experiment are fabricated with different twist ratios ($Y=2.2, 3, 4$ and 6). Also, the rotational speed of SRTTs with different twist ratios are recorded through observational section of test section at investigated Reynolds number. The influences of rotational speed of rotating behavior on the enhancement in heat transfer are discussed. According to the experimental data, some useful correlations in regard of twist ratios are established to calculate the Nusselt number and friction factor.

Afterwards, SRTTs with twist ratio of four are perforated with four perforation ratios ($PR= 0\%, 1.16\%, 3.63\%, 6.46\%$, and 10.1%). Similarly, the rotational speed of SRTTs with different perforations ratios are measured. The mechanism of heat transfer enhancement by perforation and the rotating behavior are investigated experimentally. Two correlations varying with perforation ratios are proposed as well.

Finally, short-length SRTTs with different length ratios are made for heat transfer enhancement within acceptable level of pressure drop. How the length ratios influence the

rotational speed are investigated. In addition, the effects of length ratio and rotational speed on Nusselt number, friction factor and thermal performance factor are studied.

CHAPTER 3

COMPARISON OF THERMAL PERFORMANCE OF SELF-ROTATING AND STATIONARY TWISTED TAPES IN A CIRCULAR TUBE

According to the literature review in Chapter 2, mostly used twisted tapes are stationary, which are usually fixed at the inlet of the tubes. However, there is less research focus on a new type of twisted tapes, i.e. self-rotating twisted tapes (SRTTs). Therefore, this chapter introduces this new type of twisted tapes and investigates the thermal performance of SRTTs and stationary twisted tapes (STTs) in a circular tube experimentally. The main objectives include: (1) comparing the thermal performance of SRTTs and STTs with same geometry in a double-pipe heat exchanger experimentally; and (2) exploring the effects of twist ratios on rotational speed and thermal performance for all given cases.

Section 3.1 introduces the definition and advantages of SRTTs, and reviews the studies related to the main parameters of twisted tapes (twist ratio). Then, Section 3.2 gives detailed information on all SRTTs with different twist ratios and test bed with double-pipe heat exchangers used in the experiment. In addition, experimental procedure to collect experimental data is also given in Section 3.2. Afterwards, Section 3.3 illustrates the

formulas to calculate the desired parameters, including Reynolds number, Nusselt number, friction factor and thermal performance factor. Section 3.4 shows the experimental results from present study. Comparison of thermal performance between SRTTs and STTs is demonstrated, and the influences of twist ratios on rotational speed and thermal performance is explored. Some correlations regarding twist ratio are proposed to estimate Nusselt number and friction factor, and the calculated results from these correlations are compared with empirical correlations in Section 3.4. Finally, a summary is outlined in Section 3.5.

3.1 Introduction

Recently, a novel type of twisted tapes, named self-rotating twisted tapes (SRTTs), have been commercialized to be widely utilized for heat exchanger system. SRTTs are made of a special polymer material with the same density of water that can help suspend in the water. As water velocity reaches to a certain value, driving force of water can make SRTTs rotate automatically. A review study pointed out rotating behavior of SRTTs could alter fluids pattern that leads to rotational flow, which contributes to extra swirl flow for greater convective heat transfer [95] Although SRTTs previously have been reported to play positive role in solving anti-scaling and descaling problem, few studies have been carried out to investigate SRTTs with focus on heat transfer enhancement by comparing with stationary twisted tapes (STTs).

In addition, the twist ratio which is defined as the ratio of half pitch length to twisted tapes width is considered as a main geometry parameter used to optimize various twisted tapes, as presented in Table 3.1. Jaisankar et al. [63] have adopted helical twisted tapes with different twist ratios of 3, 4, 5 and 6 used in solar water system. Their experimental results demonstrated that smaller twist ratios promote the heat transfer coefficient and pressure drop in comparison of larger twist ratios. They also offered some correlations associated with twist ratios as below:

$$Nu = 0.000115 Re^{1.169} Pr^{2.424} Y^{-0.511} \quad (3-1)$$

$$f = 271.1 Re^{-0.947} Y^{-0.584} \quad (3-2)$$

Chang et al. [49] have designed a new twisted tapes with different twist ratios from 1 to ∞ , named broken twisted tapes. They found that increase in twist ratio could reduce mean value of pressure drop, but less enhancement of heat transfer rate could be provided. In addition, Bhuiya et al. [57] have studied triple twisted tapes with different twist ratios in turbulence regime. The experimental results have revealed thermal indicators in form of Nusselt number, friction factor and thermal performance factor all increase significantly with decrease of twist ratio. They also proposed some correlations associated with twist ratio to predict thermal performance as below:

$$Nu = C Re^{0.00002y^3+0.0013y^2-0.0094y+0.5746} Pr^{0.33} \quad (3-3)$$

$$f = C_1 Re^{0.00005y^3+0.0017y^2-0.0164y-0.5193} \quad (3-4)$$

$$\eta = 41.176C * C_1^{-0.6802} Re^{0.000014y^3+0.000144y^2-0.001755y-0.1138} \quad (3-5)$$

where $C = -0.0017y^3 + 0.0179y^2 - 0.0962y + 0.7734$ and $C_1 = -0.0388y^3 + 0.2484y^2 - 0.8462y + 17.685$.

Chang et al. have experimented on thermal characteristic of serrated twisted tape with twist ratios in range of 1.56 to ∞ . Their results showed that all serrated twisted tapes used in this experiment could improve the heat transfer rate by 250-480%, and the decrease in twist ratio also could increase heat transfer rate and thermal performance factor. Some correlations regard of twist ratio are suggested for this type of twisted tapes.

$$Nu = (0.118 + 5.84e^{-1.83y}) Re^{(0.73 - 0.695e^{-1.26y})} Pr^{1/3} \quad (3-6)$$

$$f = (0.033 + 0.756e^{-0.765y}) Re^{(0.166 - 0.235e^{-0.524y})} \quad (3-7)$$

Moreover, Bhuiya et al. [56] have explored double counter twisted tapes with twisted ratios of 1.95, 3.85, 5.92 and 7.75 in turbulence flow. Their findings revealed all double counter twisted tapes could increase Nusselt number and pressure drop by 60-240% and 91-286% respectively in comparison of plain tube. The highest thermal performance factor of 1.34 could be obtained with lowest twist ratio of 1.95. Some correlations in terms of twist ratio have been also indicated as followings:

$$Nu = C Re^{-0.0002y^3 + 0.0021y^2 + 0.0047y + 0.5894} Pr^{0.33} \quad (3-8)$$

$$f = C_1 Re^{0.00004y^3 + 0.0015y^2 - 0.0165y - 0.4722} \quad (3-9)$$

$$\eta = 41.176C * C_1^{-0.6802} Re^{0.0002272y^3 + 0.0031203y^2 + 0.015923y - 0.13103} \quad (3-10)$$

where $C = -0.0007y^3 + 0.0077y^2 - 0.0385y + 0.4777$ and $C_1 = -0.0009y^3 - 0.1015y^2 + 1.0842y + 8.685$.

Eiamsa-ard et al. [96] have investigated thermal characteristic of twin counter and twin co-twisted tapes with different twist ratios of 2.5, 3, 3.5 and 4 in a circular tube. At similar operation condition, twin counter twisted tapes were proven to be an alternative choice for heat transfer enhancement based on experimental results of thermal performance.

Besides, decrease in twisted ratio has been demonstrated to improve Nusselt number and thermal performance factor for given cases. Some correlations related to the twist ratios were also given for twin counter twisted tapes as below:


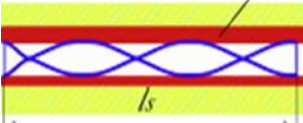














$$Nu = 0.473 Re^{0.66} Pr^{0.4} y^{-0.9} \quad (3-11)$$

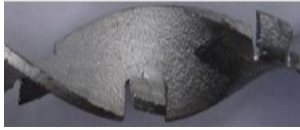
$$f = 72.29 Re^{-0.53} y^{-1.01} \quad (3-12)$$

$$\eta = 41.176 C * C_1^{-0.6802} Re^{0.0002272y^3 + 0.0031203y^2 + 0.015923y - 0.13103} \quad (3-13)$$

Hence, this study aims to experimentally compare the thermal performance of SRTTs and STTs in a double-pipe heat exchanger, and to examine the influences of twist ratio and rotational speed on thermal characteristic in form of Nusselt number, friction factor and thermal performance factor.

Table 3.1: Various Configurations of twisted tapes

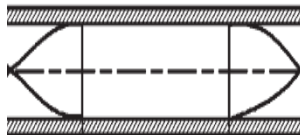
Configuration	Type of twisted tape	Reference	Configuration	Type of twisted tape	Reference
	Double counter twisted tapes	[56]		Short-length twisted tapes	[13]
	Perforated twisted tapes	[10], [12]		Centre-wings twisted tapes	[88]
	Delta-winglet twisted tapes	[1]		Hollow twisted tapes	[3]
	Serrated twisted tapes	[97]		Broken twisted tapes	[49]
	Helical screw tapes	[98], [99]		A new twisted tapes	[14]
	V-cut twisted tapes	[6]		Peripherally-cut twisted tapes	[9]
	Square-cut twisted tapes	[100]		Multiple twisted-tapes	[4]
	U-cut twisted tapes	[7]		Center-cleared twisted tapes	[5]



Jagged twisted tape [54]



Triple twisted tape [57]



Regularly spaced twisted tape [53]



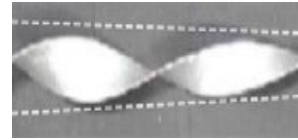
Perforated double counter twisted tape [58]



Perforated twisted tapes with alternate axis [102]



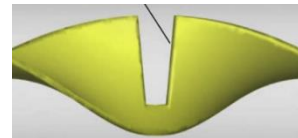
Alternate clockwise and counter clockwise twisted tapes [51]



Tapered twisted tape [52]



Alternative axis twisted tape [101]



Rectangular-cut twisted tape [59]

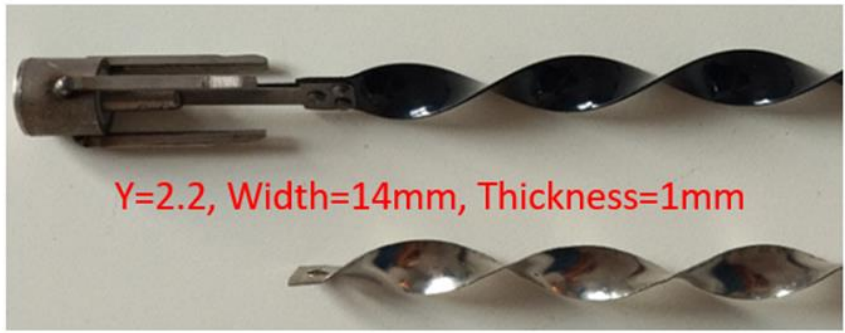


Multiple twisted-tape [55]

3.2. Experimental methodology

3.2.1 Experimental facilities

In our experiment, all SRTTs are made of special polymer materials with a dimension of 2000 mm length, 14 mm width and 1 mm thickness. The special polymer materials have the same density of water that they can suspend in water for smooth rotation. The thermal conductivity of the polymer material is approximately 0.28 W/m*K. Prior to conducting the experiment, STTs were fabricated with the same geometry (e.g., twist ratio, thickness, and width) as the SRTTs, as shown in Figure 3.1(a). In addition, SRTTs were prepared using four twisted ratios ($Y = 2.2, 3, 4, \text{ and } 6$), as presented in Figure 3.1(b). The definition of twist ratio (Y) is the ratio of pitch length to tapes width.



a



b

Figure 3.1 (a) SRTTs and STTs with the same geometry; (b) Pictorial view of SRTTs with different twist ratios

As displayed in Figure 3.2 (a), the test tube with observational sections made of transparent materials was designed to observe the rotating behavior of SRTTs. From Figure 3.2 (b), a Digital Tachometer RPM Meter with contactless mode was used to measure the rotational speed of SRTTs through the observational section. The test rig consisted of the following as presented in Figure 3.2 (c): (1) an electrical heater with temperature control by a variac transformer for heating water; (2) a water pump for circulating water; (3) two resistance temperature detector (RTDs) for recording water temperature at the inlet and

outlet of the test tube; (4) a double-pipe heat exchanger with a 2000-mm length as a test section; (5) a heat sink with an electrical fan; (6) pressure taps for measuring pressure drop across the test tube; (7) two rotameters for recording the volumetric flow rate of water in the test tube (inner tube) and outer tube; (8) Thirty thermocouples attached at 10 positions alongside the test tube; and (9) a data logger connected to a PC.

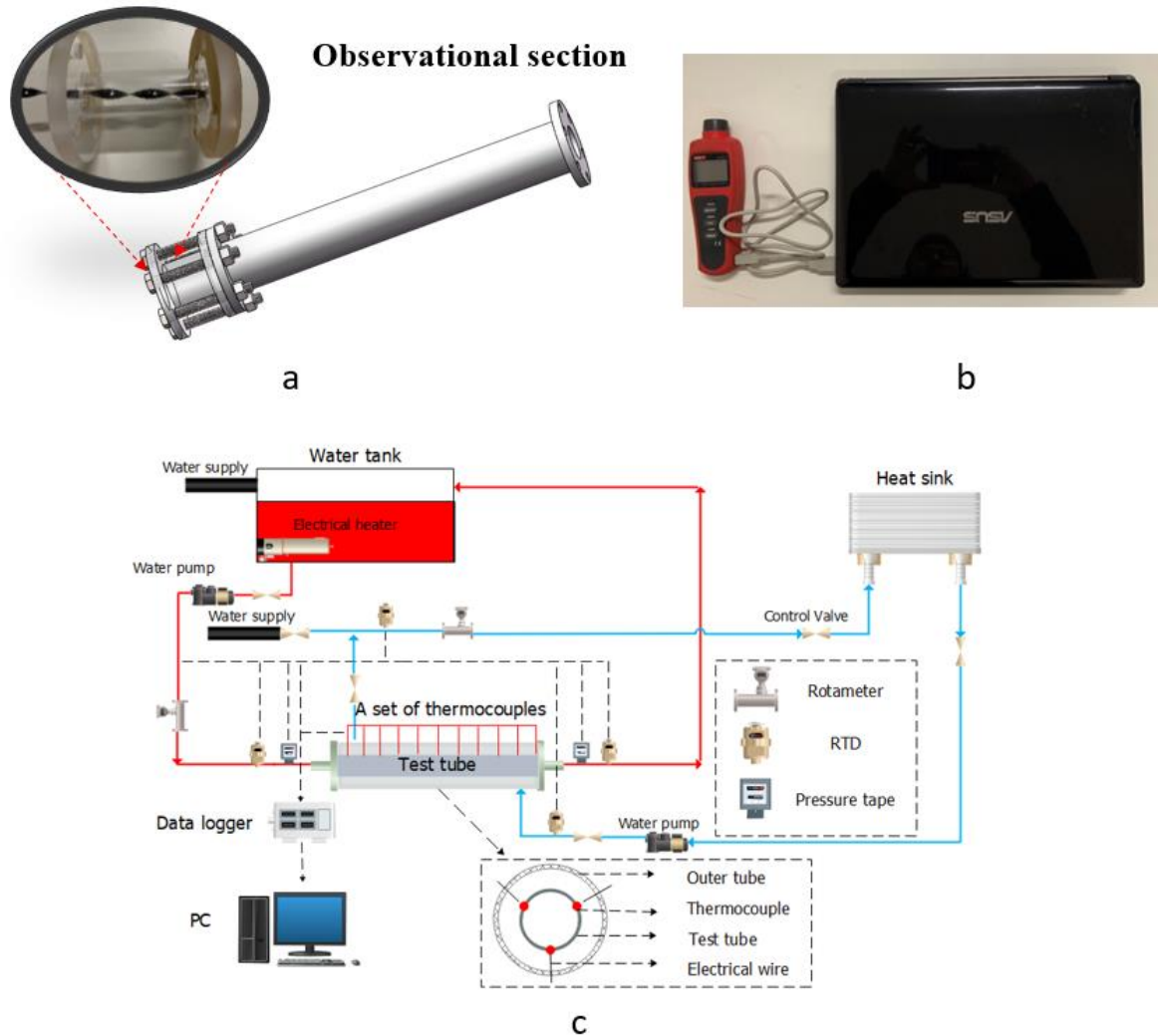


Figure 3.2 (a) Test tube with observational section; (b) Digital Tachometer RPM Meter with contactless mode; (c) Schematic of test rig used

3.2.2 Experimental procedure

In this experiment, the Reynolds numbers of working fluids were controlled from 12000 to 45000. The Pr was estimated based on the average temperature of working fluids at the inlet and outlet of the test tube. The rotational speeds of SRTTs at stable state were measured by using a Digital Tachometer RPM Meter with contactless mode through the observational section of the test tube for 5 minutes. The volumetric flow rate of water could be adjusted by controlling the power output of the water pump. The double-pipe heat exchanger consisted of an outer tube and test tube (inner tube). Hot water was flowed through the test tube while cold water entered the outer tube for convective heat transfer. After the heat transfer process, hot water was returned to the water tank for secondary heating. Cold water was pumped to the heat sink to release heat to the ambient environment, which can be controlled using an electrical fan. It should be noted hot water was maintained at $40\text{ }^{\circ}\text{C}$ ($\pm 0.5\text{ }^{\circ}\text{C}$) at the inlet of the test tube, and cold water was maintained at $21.8\text{ }^{\circ}\text{C}$ ($\pm 0.2\text{ }^{\circ}\text{C}$) at the inlet of the outer tube. The average bulk temperature of water was calculated based on the bulk temperatures of water before and after the heat transfer process. The average temperatures of the local wall were recorded by the thermocouples along the test tube. In addition, the pressure drop between inlet and outlet of test tube was measured by two pressure tapes, which is delivered to a personal computer. Detailed information of the experimental setup is shown as Table 3.2.

Table 3.2: Details of experimental setup

	STTs	SRTTs
Tape width	14 mm	14 mm
Twisted ratio	2.2	2.2, 3, 4 and 6
Tape thickness	1 mm	1 mm
Inner diameter of test tube	20 mm	20 mm
Inner diameter of outer tube	65 mm	65 mm
Working fluid	Water	Water
Range of Reynolds number	12000-45000	12000-45000
Inlet temperature of inner tube	40 °C	40 °C
Inlet temperature of outer tube	21.8 °C	21.8 °C

3.3 Data reduction

The measured data were collected to estimate the Nussle number, friction factor, and thermal performance factor at given Reynolds numbers. The data reduction of experimental results are displayed as following section.

The transferred heat to cold water should be equal to the convective heat loss from the test tube expressed as follows:

$$Q_w = Q_{conv} \quad (3-14)$$

where

$$Q_w = m_w C_{p,w} (T_{w,in} - T_{w,out}) \quad (3-15)$$

The heat balance between the input power (Q_{VI}) and the convective heat transfer rate of water (Q_w) was found to be less than 5% for all experimental runs which can be calculated by

$$\left| \frac{Q_{VI} - Q_w}{Q_{VI}} * 100\% \right| \leq 5\% \quad (3-16)$$

The convective heat transfer performance from the hot water is defined as

$$Q_{conv} = hA_i(\bar{T}_s - T_b) \quad (3-17)$$

These parameters can be written as

$$A_i = \pi D_i L \quad (3-18)$$

$$T_b = (T_{out} + T_{in}) / 2 \quad (3-19)$$

$$\bar{T}_s = \sum T_s / 10 \quad (3-20)$$

Then

$$h = Q_w / A_i(\bar{T}_s - T_b) \quad (3-21)$$

The heat transfer rate in terms of the Nusselt number can be calculated as

$$Nu = \frac{hD_i}{\lambda} \quad (3-22)$$

The friction factor is given by

$$f = \frac{\Delta P}{\left(\frac{L}{D_i}\right)\left(\rho \frac{v^2}{2}\right)} \quad (3-23)$$

The situation of working fluids can be expressed by Reynolds number that is defined as

$$\text{Re} = \frac{\rho v D_i}{\mu} \quad (3-24)$$

Based on previous research [4, 12, 98], the thermal performance factor used as the overall assessment of heat exchangers with different twisted tapes was applied in this study.

It can be derived by the following equations:

$$(\bar{V}\Delta P)_p = (\bar{V}\Delta P)_t \quad (3-25)$$

The previous equation means that the pumping power of the tube with twisted tapes is equal to that of the plain tube.

$$\bar{V} = \frac{m}{\rho} \quad (3-26)$$

$$\Delta p = f\left(\frac{L}{D}\right)\left(\frac{\rho v^2}{2}\right) \quad (3-27)$$

$$\text{Re} = \frac{m}{\pi D^2} \quad (3-28)$$

where the representation of Reynolds number and friction factor are given. By combining above equations:

$$\left[\frac{m}{\rho} * f\left(\frac{L}{D}\right)\left(\frac{\rho v^2}{2}\right)\right]_p = \left[\frac{m}{\rho} * f\left(\frac{L}{D}\right)\left(\frac{\rho v^2}{2}\right)\right]_t \quad (3-29)$$

$$(f \text{Re}^3)_p = (f \text{Re}^3)_t \quad (3-30)$$

Then,

$$\text{Re}_p = \text{Re}_t \left(\frac{f_t}{f_p} \right)^{1/3} \quad (3-31)$$

Thus, the thermal performance factor defined as the ratio of the heat transfer rate of the tube with twisted tapes to the plain tube at the same pumping power can be expressed as

$$\eta = \frac{h_t}{h_p} \Big|_{pp} = \frac{(Nu_t / Nu_p)}{(f_t / f_p)^{1/3}} \quad (3-32)$$

The uncertainties of non-dimensional variables (Nusselt number, friction factor and Reynolds number) were calculated based on the measured variables with known uncertainties from Equation (3-22), (3-24) and (3-28). Prior to the experiment, thermocouples used to measure the temperatures were calibrated with an accuracy of ± 0.1 °C, and the rotameter was calibrated with ± 0.1 g rated accuracy. According to the least counts and sensitivities of the measured data, the maximum error of inner diameter of the test tube is ± 0.0001 m. The uncertainties of desired variables could be estimated by ANSI/ASME standard [103]:

$$\delta_y = \pm \sqrt{\sum_{i=1}^N \left(\frac{\partial Y}{\partial x_i} \delta x_i \right)^2} \quad (3-33)$$

where δY is the combined uncertainties of desired variables Y . δx_i is the uncertainties of the i_{th} measured variables.

In the uncertainty analysis, the maximum uncertainty was calculated to be within $\pm 3.4\%$ for the Reynolds number, $\pm 8.8\%$ for the Nusselt number, and $\pm 9.2\%$ for the friction factor.

3.4 Results and Discussion

3.4.1 Validation test of plain tube

Prior to investigating the thermal behavior of SRTTs, the experimental results were verified from the plain tube with empirical correlations, including the Dittus-Boelter (Eq. (3-34)) or Gnielinski (Eq. (3-35)) equations for the Nusselt number, and Blasius (Eq. (3-36)) or first Petukhov (Eq. (3-37)) equations for the friction factor [8]. As presented in Figure 3.3, experimental data were validated to match the Dittus-Boelter ($\pm 9.9\%$) and Gnielinski ($\pm 7.8\%$) equations. In addition, the data obtained from this study for the friction factor was compared with the Blasius and first Petukhov equations, showing variations of $\pm 9.6\%$ and $\pm 11.6\%$, as indicated in Figure 3.4. The correlations of (3-34) and (3-26) were used to formula empirical correlations of Nusselt number and friction factor for heat exchanger tube fitted with SRTTs in Section 3.4.4.

$$Nu = 0.023 Re^{0.8} Pr^{0.3} \quad (3-34)$$

$$Nu = \frac{(f/8)(Re-1000)Pr}{1+12.7(f/8)^{0.5}(Pr^{2/3}-1)} \quad (3-35)$$

$$f = 0.316 Re^{-0.25} \quad (3-36)$$

$$f = (0.79 \ln Re - 1.64)^{-2} \quad (3-37)$$

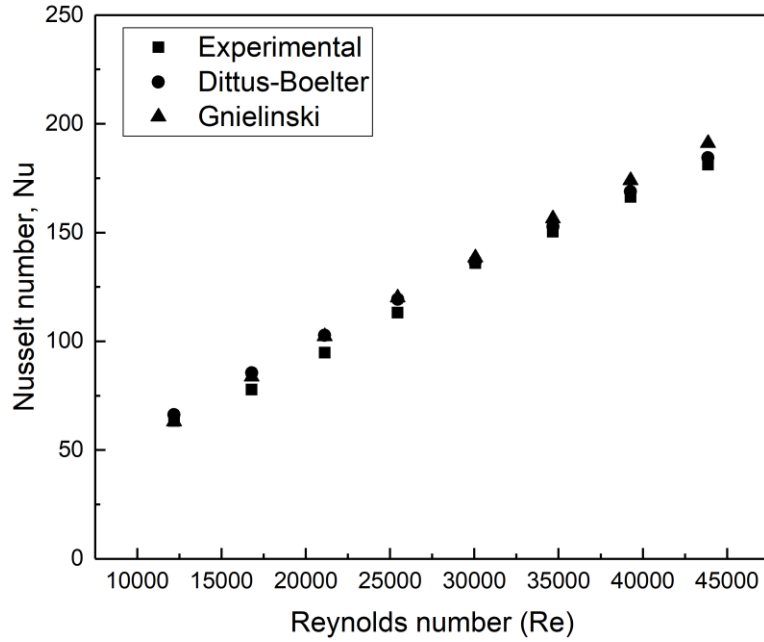


Figure 3.3 Validation of experimental Nu in plain tube

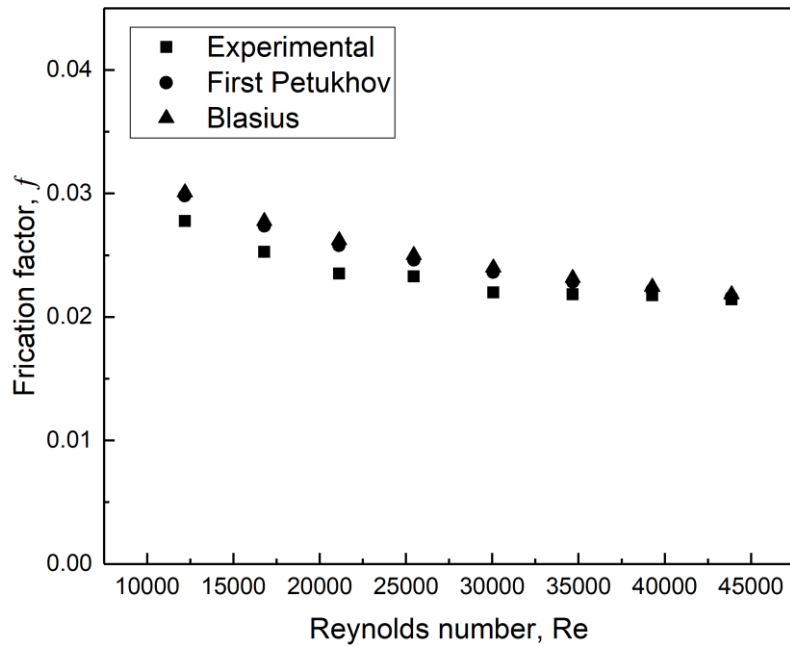


Figure 3.4 Validation of experimental f in plain tube

3.4.2 Effects of twist ratio on rotational speed

Prior to reaching the initial stages of rotating behavior, SRTTs remain at a stationary condition and then begin to rotate automatically due to the force of working fluids. As displayed in Figure 3.5, the initial stages of the rotating behavior begin at $Re = 17874$ (water velocity = 0.58 m/s) for $Y = 6$, $Re = 18687$ (water velocity = 0.61 m/s) for $Y = 3$ and $Y = 4$, and $Re = 18958$ (water velocity = 0.62 m/s) for $Y = 2.2$. The twist ratios appear to have less influence on the initial stages of the rotating behavior. However, a lower twisted ratio ($Y = 2.2$) can increase rotational speed at similar operating conditions as compared with higher twist ratios ($Y = 3, 4$, and 6). It is likely that with a larger contact surface area, SRTTs with a smaller twisted ratio lead to significant increase in rotational speed.

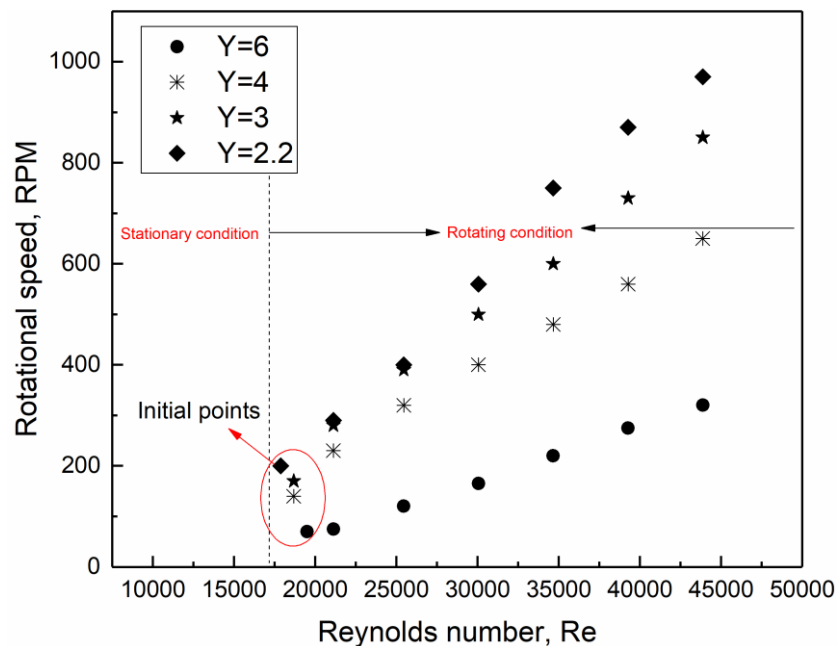
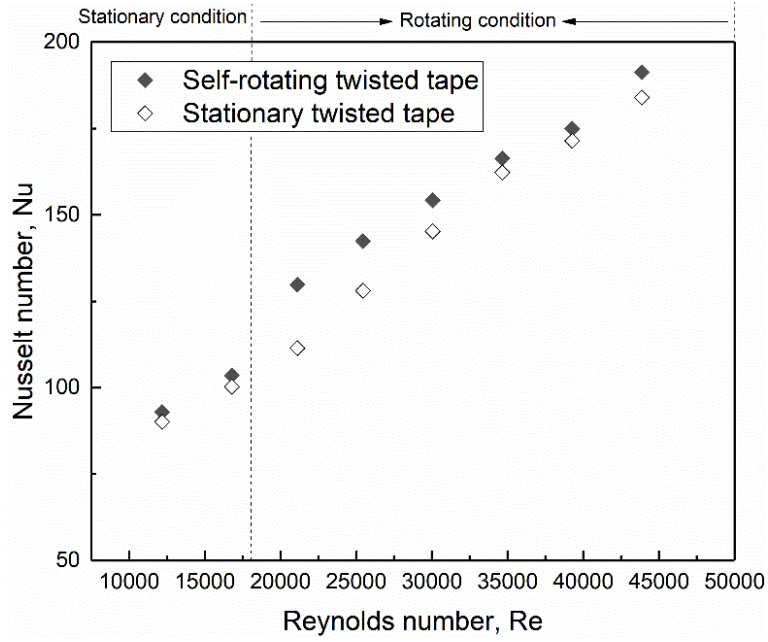


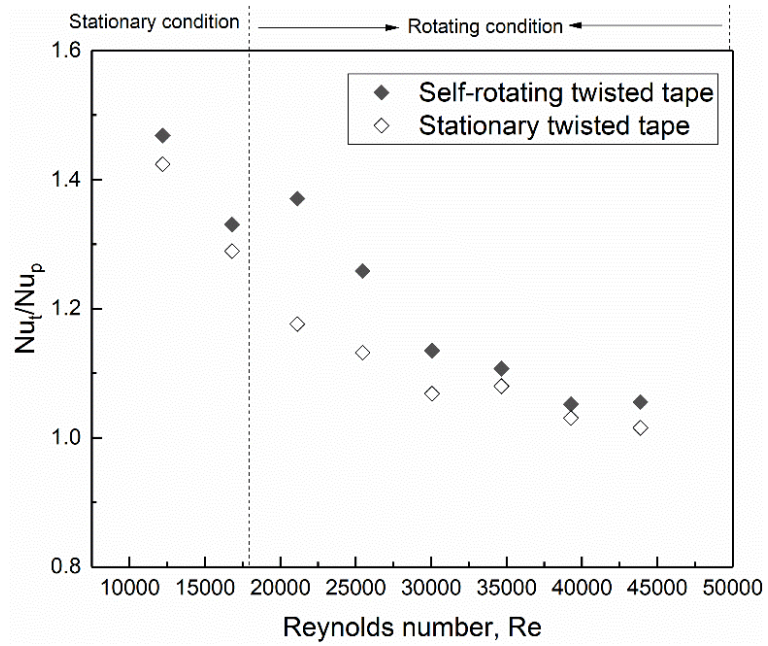
Figure 3.5 Variation of rotational speed (RPM) with Reynolds number

3.4.3 Comparison between SRTTs and STTs

Figures 3.6–3.8 illustrate the variations of thermal performance based on Nusselt number, friction factor, and thermal performance factor with Reynolds numbers of 12000-45000 for SRTTs and STTs. In stationary conditions, the tube fitted with SRTTs can provide a slightly higher heat transfer rate as compared to that fitted with STTs. This can be explained by the fact that additional turbulence can be generated from the vibration-like effect when water velocity is low. As illustrated in Figure 3.8, little discrepancy in the thermal performance factor was found for SRTTs and STTs in stationary conditions. From Figure 3.5, SRTTs keep stationary under conditions of Reynolds number smaller than 12000. It means that no rotating behavior exists in such situation. As stated above, no significant discrepancies of thermal characteristic between SRTTs and STTs are found. Hence, SRTTs can be considered to perform similar thermal performance as stationary twisted tapes with the same geometry when Reynolds number is lower than 12000.



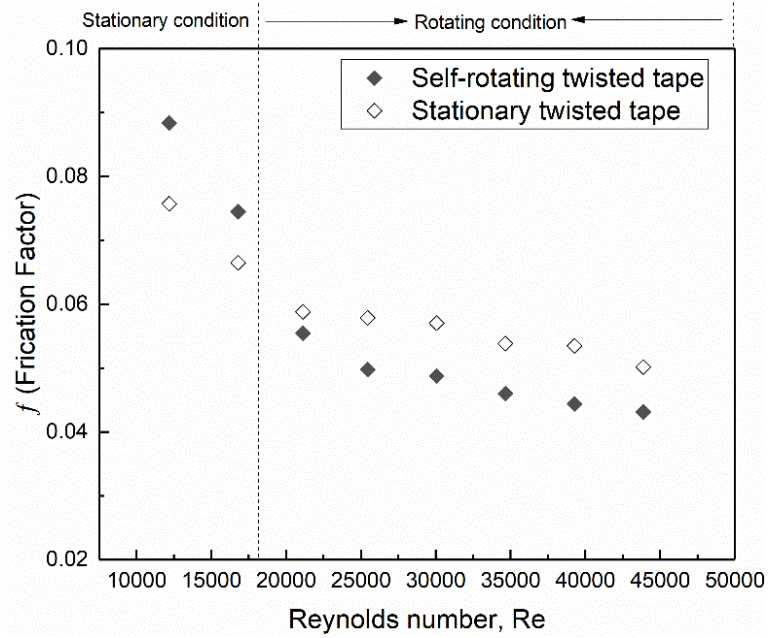
(a)



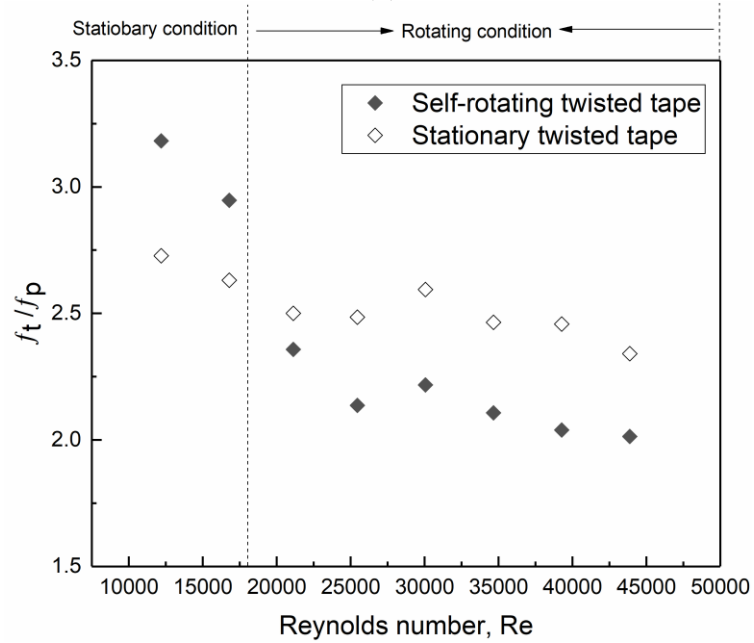
(b)

Figure 3.6 Variation of (a) Nu and (b) Nu_t/Nu_p at given Reynolds for STTs and SRTTs

At a given Reynolds number in the rotating condition, SRTTs can effectively raise the heat transfer rate by 16.5% maximally as compared with STTs. This can be attributed to the effects of rotating behavior in promoting centrifugal force to tangential flow, which induces more turbulence in a tangential direction to produce excellent mixing of flow between the core and wall region. Figure 3.7 shows that the friction factor for SRTTs was significantly lower than that for STTs in the rotating condition. It is possible that the rotating behavior smoothens the contact surface between working fluids and twisted tapes, effectively reducing the flow resistance. In addition, Figure 3.8 reveals that the thermal performance factor of SRTTs was demonstrated to be 8–18.8% higher than that of STTs for all investigated cases in the rotating condition. This can be attributed to the effects of rotating behaviour on improving heat transfer rate and reducing flow blockage in comparison of STTs.



(a)



(b)

Figure 3.7 Variation of (a) f and (b) f_t/f_p at given Reynolds number for STTs and SRTTs

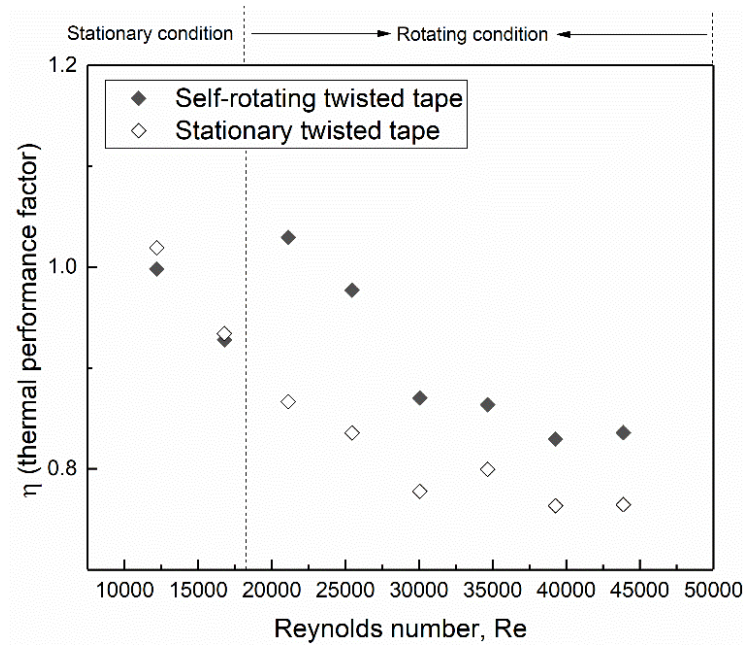
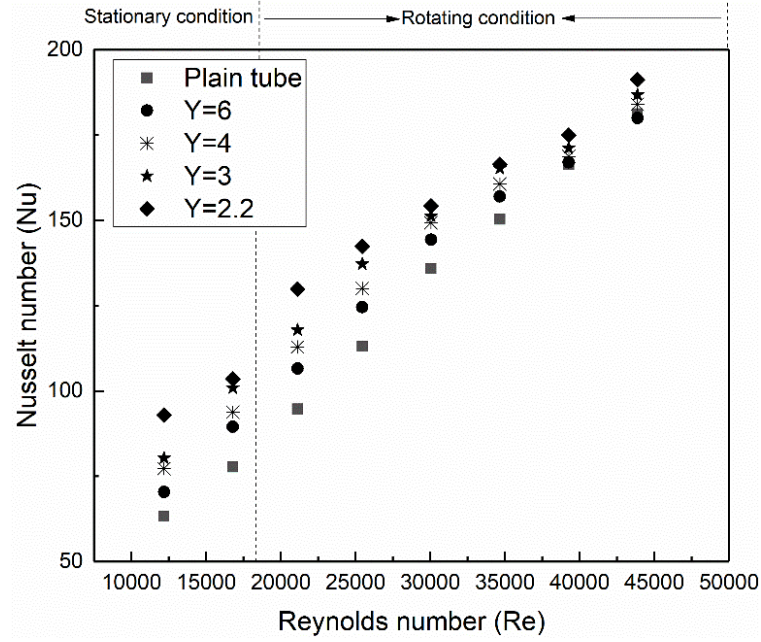


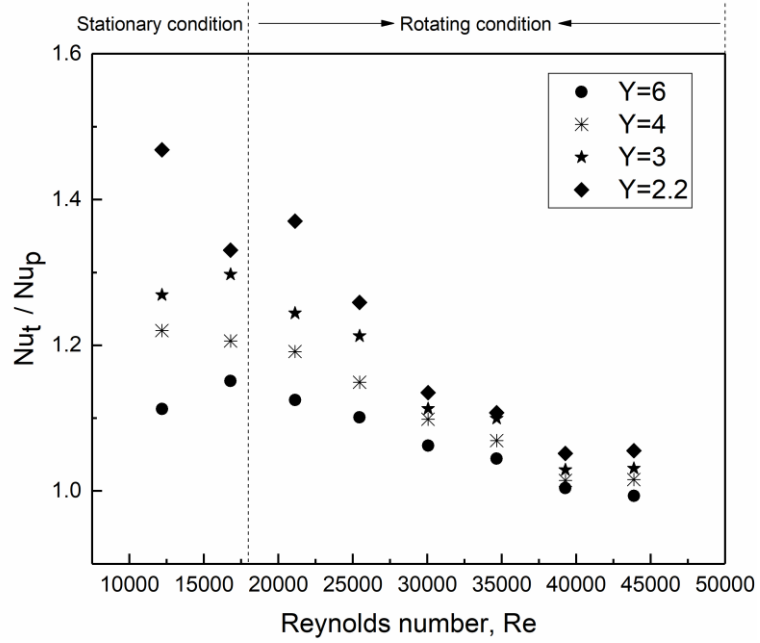
Figure 3.8 Variation of thermal performance factor at given Reynolds number for STTs and SRTTs

3.4.4 Effect of twist ratios (Y) on thermal performance

The effect of a tube fitted with twist ratios ($Y = 2.2, 3, 4,$ and 6) on thermal characteristics in terms of the Nusselt number is presented in Figure 3.9. The Nusselt number generally rises with each increase in Reynolds number because of the higher turbulence intensity at higher Reynolds numbers. Moreover, a tube fitted with SRTTs was found to have a much higher heat transfer rate than that of the plain tube, and SRTTs with a lower twist ratio ($Y = 2.2$) enhanced the heat transfer rate as compared with those with higher twist ratios ($Y = 3, 4,$ and 6). This agrees with some previous research that has revealed that the heat transfer rate with a small twist ratio was higher than those with a larger twist ratio [49, 56].



(a)

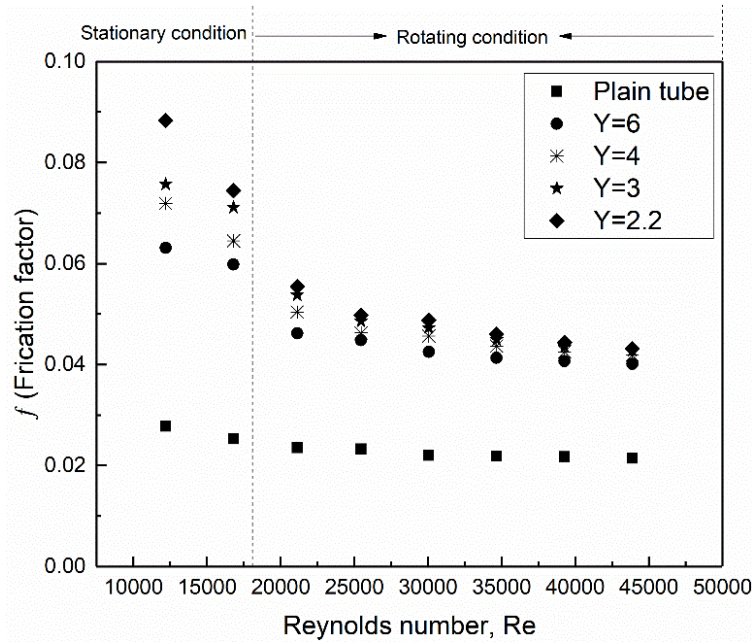


(b)

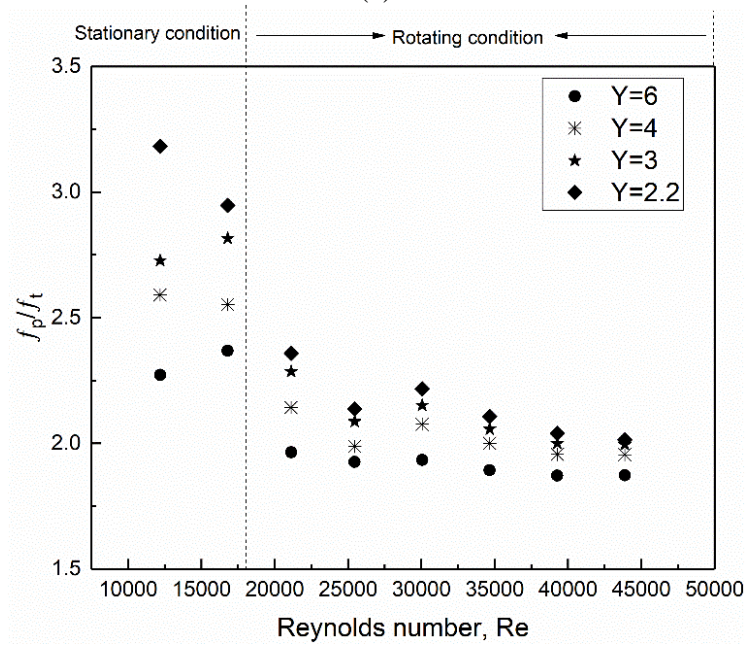
Figure 3.9 Variation of (a) Nu and (b) Nu_t / Nu_p at given Reynolds number

As discussed in Section 3.4.3, the rotating behavior produces additional swirl flow or turbulence along the tangential direction to promote heat transfer. Figure 3.5 shows that SRTTs with lower twist ratios consistently rotate faster than twisted tapes with higher twist ratios at given Reynolds numbers. It seems that not only a lower twist ratio can induce a greater amount of swirl flow but also rotating behavior at a high speed enhances turbulence level, resulting in a reduction in thickness of thermal boundary layer for greater convective heat transfer.

Variations in the friction factor for SRTTs with different twist ratios are presented in Figure 3.10. The figure illustrates that the friction factor in the tube fitted with SRTTs at a low twist ratio is consistently higher than those at a high twist ratio. This is attributed to higher viscous loss along the test tube generated by stronger turbulence or swirl flow. It is also consistent with previous results on the consequences of the twist ratio on the pressure drop for various twisted tapes [56, 97]. Moreover, it is clearly observed that the friction factor decreases ($Y = 2.2$, from 0.0744 to 0.055; $Y = 3$, from 0.0711 to 0.054; $Y = 4$, from 0.072 to 0.0645; $Y = 6$, from 0.0598 to 0.0462) when SRTTs change from stationary to rotating conditions. A possible explanation for this is that the smooth flow surface produced by the rotating behavior can decrease the flow resistance considerably. In addition, rotational flow generated by the existence of rotating behaviour performs function to reduce the flow blockage along the flow path.



(a)



(b)

Figure 3.10 Variation of (a) f and (b) f_t/f_p at given Reynolds number

The relationship of thermal performance factor versus Reynolds number for SRTTs with different twist ratios is shown in Figure 3.11. It shows that the thermal performance factor increases sharply after switching from stationary to rotating conditions, that is, from 0.928 to 1.03, 0.919 to 0.944, 0.882 to 0.924, and 0.863 to 0.898 for $Y = 2.2, 3, 4,$ and $6,$ respectively. This can be attributed to the influences of high rotational speed (218 RPM for $Y = 6,$ 230 RPM for $Y = 4,$ 281 RPM for $Y = 3,$ and 292 RPM for $Y = 2.2$) at initial stages of rotating behavior when enhancing heat transfer coefficient and decreasing friction factor significantly. Furthermore, the general trend of the thermal performance factor reduces as the Reynolds number increases in the rotating condition (from $Re = 20000$ to $Re = 45000$). Experimental results revealed that a lower twist ratio ($Y = 2.2$) can promote the thermal performance factor as compared to higher twist ratios ($Y = 3, 4,$ and 6). In the experimental cases, the maximum thermal performance factor could be obtained in the test tube fitted with SRTTs at a twist ratio of $Y = 2.2$ and Reynolds number of 21124 (i.e., the initial stage of rotating behavior).

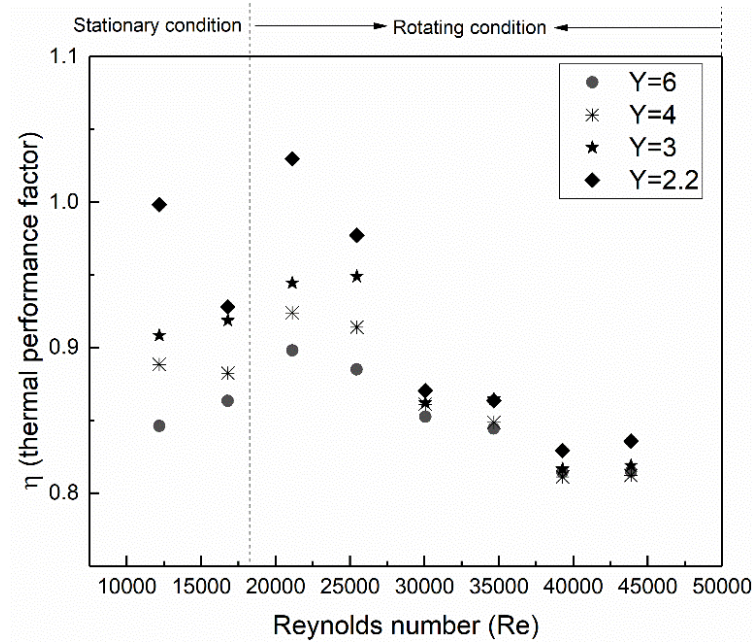


Figure 3.11 Variation of thermal performance factor at given Reynolds number

Proposed correlations for the Nusselt number (Nu) and friction factor (f) are established from measured data of the tube fitted with SRTTs at Reynolds numbers in the range of 12000–45000 and four twist ratios ($Y = 2.2, 3, 4,$ and 6). These are expressed by the following two equations:

$$Nu_{SRTTs} = 0.12634 Re^{0.6469} Pr^{0.3421} Y^{-0.0923} \quad (3-25)$$

$$f_{SRTTs} = 11.6228 Re^{-0.5112} Y^{-0.1919} \quad (3-26)$$

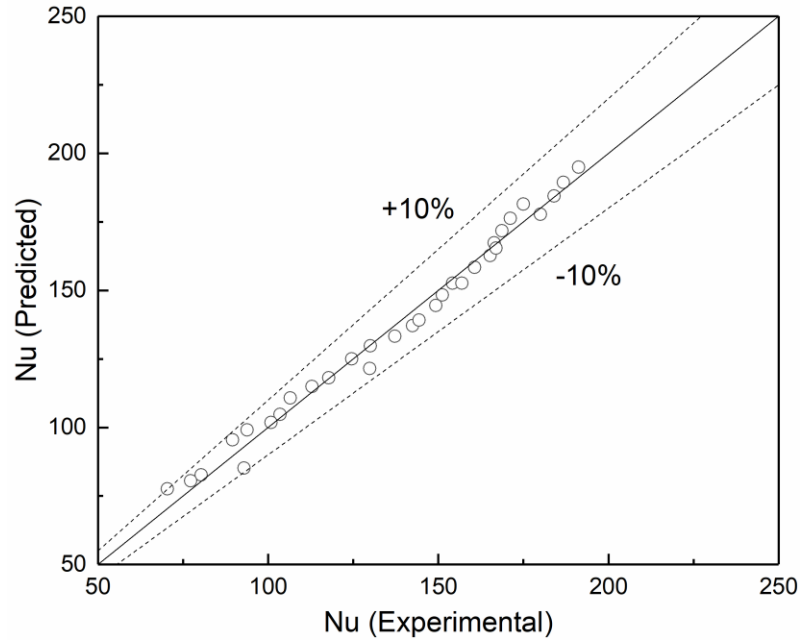


Figure 3.12 Experimental value versus prediction of Nusselt number

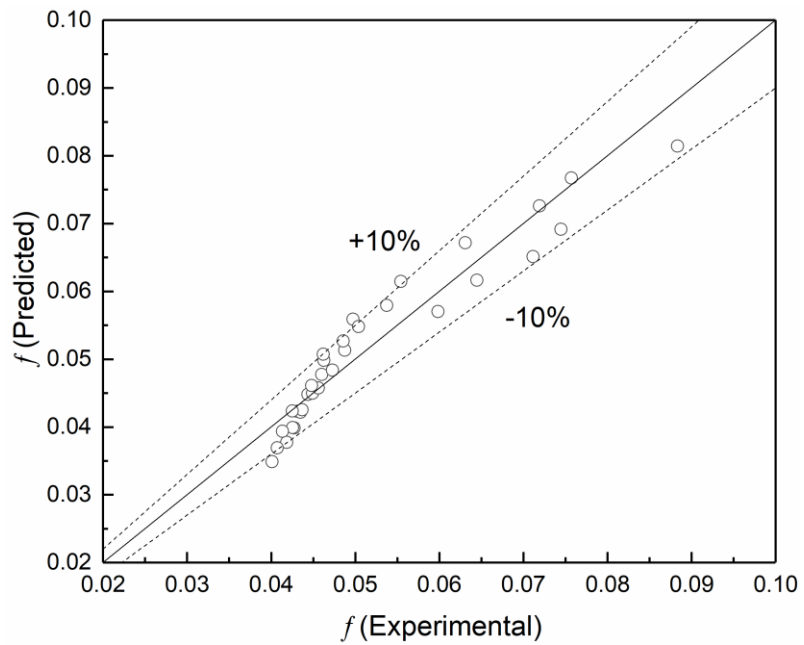


Figure 3.13 Experimental value versus prediction of friction factor

The relationships between experimental and predicted results for the Nusselt number and friction factor are presented in Figures 3.12 and 3.13. It is found that the predicted values of the Nusselt number and friction factor were in excellent agreement with experimental results to within $\pm 10\%$.

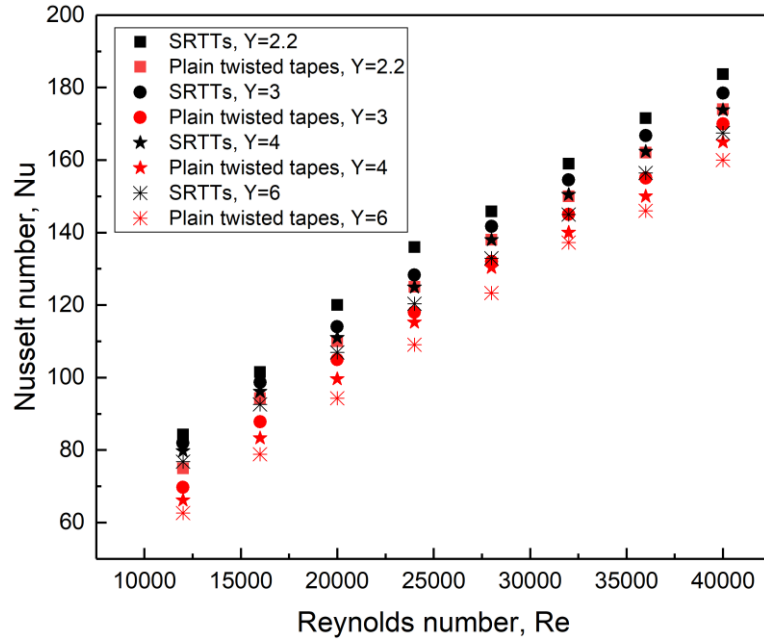
3.4.5 Comparison between SRTTs and previous work

The results of the thermal performance from above correlations of SRTTs are compared with the ones of plain twisted tapes proposed by previous work [46]. The empirical correlations used for predicting the Nusselt number and friction factor of plain twisted tapes are shown as below:

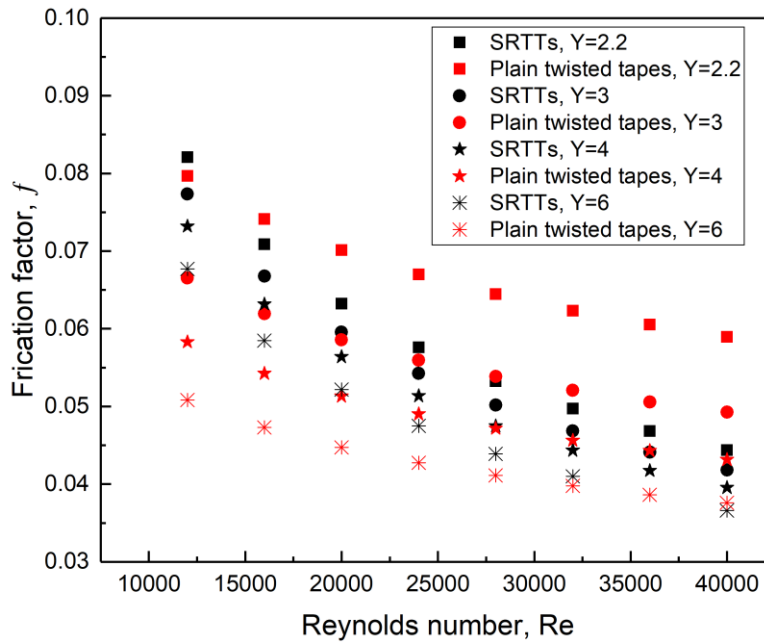
$$Nu = 0.023 Re^{0.8} Pr^{0.4} \left(\frac{\pi}{\pi - 4\varepsilon / D_i} \right)^{0.8} \left(\frac{\pi + 2 - 2\varepsilon / D_i}{\pi - 4\varepsilon / D_i} \right)^{0.2} (1 + 0.769 / Y) \quad (3-27)$$

$$f = 0.079 Re^{-0.25} \left(\frac{\pi}{\pi - 4\varepsilon / D_i} \right)^{1.75} \left(\frac{\pi + 2 - 2\varepsilon / D_i}{\pi - 4\varepsilon / D_i} \right)^{1.25} (1 + 2.752 / Y^{1.29}) \quad (3-28)$$

As illustrated in Figure 3.14 (a), SRTTs appear to excel with higher heat transfer rate as compared with plain twisted tapes at the same twisted ratio. This can be explained by the positive effects of rotating behavior on enhancing the fluids mixing along the tangential direction for convective heat transfer. At the same twist ratio, Figure 3.14 (b) reveals that the tube fitted with SRTTs has larger friction factor than that with plain twisted tapes at the range of low Reynolds number. Then, the friction factor generated by SRTTs becomes lower than that by plain twisted tapes with the increasing Reynolds number. This can be attributed to the rotating behavior at large Reynolds number is featured by high rotational speed that allows water to flow through the heat exchanger tube with less pressure drop.



(a)



(b)

Figure 3.14 SRTTs versus plain twisted tapes at the Reynolds number of 12000-45000: (a) Nusselt number and (b) Friction factor

3.5 Summary

This chapter experimentally examined the thermal characteristics of a heat exchanger tube equipped with SRTTs at different twist ratios of 2.2, 3, 4, and 6. The following conclusions can be drawn:

- Under stationary conditions, no significant discrepancies in thermal performance were found for SRTTs and STTs. Because of their rotating behavior, SRTTs facilitate thermal performance in form of the friction factor, Nusselt number and thermal performance factor as compared to STTs.
- Twist ratios were found to have less effect on the initial stages of rotating behavior. However, a lower twist ratio ($Y = 2.2$) resulted in a higher rotational speed as compared to higher twist ratios ($Y = 3, 4, \text{ and } 6$) under the same operating conditions. As expected, SRTTs with lower twist ratios performed better thermal behavior than did STTs. For given cases of four twist ratios, the maximum thermal performance factor could be obtained at the start of rotating behavior.
- The correlations for Nusselt number and friction factor against the Reynolds number and twist ratio were established. The proposed correlations were validated by the experimental results, and within $\pm 10\%$ deviation was reported.

To sum up, this study demonstrated that the rotating behavior of SRTTs is another main factor to enhance the heat transfer of heat exchanger tube with little increase of pressure drop. This study can offer useful information for researchers for the further investigations of SRTTs, and the experimental results and correlations are also used for industrial applications.

CHAPTER 4

THERMAL CHARACTERISTIC OF PERFORATED SELF-ROTATING TWISTED TAPES

As mentioned in Chapter 3, SRTTs have been demonstrated to be more efficient for thermal performance in comparison of STTs. Previous researches also demonstrated perforated fabrication is an alternative approach to improve heat transfer. Hence, this chapter investigates the compound effects of perforated twisted tapes on the enhancement in thermal performance. Section 4.1 mainly reviews previous studies that examine the thermal behavior of various perforated twisted tapes in heat exchanger tubes. Section 4.2 prepares the perforated twisted tapes with different perforation ratios, and illustrates the experimental procedure to measure the experimental variables. Then, Section 4.3 derives equations for calculating the thermal indicators, and conducting uncertain analysis. Section 4.4 reveals the findings from the experimental results, and it shows the relationship between perforation ratio and thermal performance. In addition, variation of rotational speed with Reynolds number for SRTTs with different perforated ratios is presented. Two correlations associated with perforation ratio are also given to predict heat transfer and friction factor characteristic. At the end, a summary is outlined to provide the major findings of this chapter.

4.1 Introduction

According to the literature review in Chapter 2, many researchers sought out to induce stronger swirl flow between core and near wall region by means of utilizing various fabrication to twisted tapes (e.g. V-cut, U-cut, broken and alternate axes twisted tapes), as displayed in Table 4.1. They found that such fabrication indeed could function in improving the heat transfer coefficient in comparison of original twisted tapes. Also, these modified twisted tapes were designed with non-dimensional parameters. The relationship between thermal performance and these non-dimensional parameters have been given for further application of corresponding twisted tapes used in heat exchanger system.

Among these modified twisted tapes, perforated twisted tapes have been investigated by several studies. For example, some studies have comprehensively explored perforated twisted tapes by comparing with other twisted tapes (e.g. typical, V-cut and U-cut twisted tapes) [7, 52, 102]. In addition, Nanan et al. [11] have studied the perforated helical twisted tapes with different perforation pitch ratios (s/w) and diameters ratios (d/w). Their results demonstrated that the tube fitted with perforated helical twisted tapes with s/w of 2 and d/w of 0.2 could have the largest thermal performance factor of 1.28. Some correlations to predict Nusselt number and friction factor have been also given:

$$Nu = 0.035Re^{0.795} Pr^{0.4} (d/w)^{-0.068} (s/w)^{0.086} \quad (4-1)$$

$$f = 1.915Re^{-0.299} (d/w)^{-0.068} (s/w)^{0.094} \quad (4-2)$$

$$\eta = 4.058Re^{-0.145} (d/w)^{-0.045} (s/w)^{0.054} \quad (4-3)$$

In addition, Bhuiya et al. [10] have experimentally studied the perforated twisted tapes with different porosities ($R_p=1.6, 4.5, 8.9$ and 14.7%) in a circular tube. Their results

indicated that the utilization of perforated twisted tapes could enhance the pressure drop, rate of heat transfer and thermal performance by 110 –360, 110 –340, and 28–59%. The perforated twisted tapes with R_p of 4.5% was considered as an optimal solution because of the higher thermal performance factor. They also provided some correlations for further application of perforated twisted tapes, as expressed as below:

$$Nu = C Re^{0.00005R_p^3 - 0.0013R_p^2 + 0.0073R_p + 0.5501} Pr^{0.33} \quad (4-4)$$

$$f = C_1 Re^{0.00009R_p^3 - 0.0022R_p^2 + 0.012R_p - 0.6006} \quad (4-5)$$

$$\eta = 36.995CC_1^{-0.676} Re^{-0.000011y^3 + 0.000187y^2 - 0.000808y - 0.07168} \quad (4-6)$$

where $C = 0.0002R_p^3 - 0.0046R_p^2 + 0.0334R_p + 0.6569$ and

$$C_1 = 0.0027R_p^3 + 0.0583R_p^2 + 0.0455R_p + 24.536 .$$

Then, Bhuiya et al. [58] have perforated double counter twisted tapes with different porosities ($R_p=1.2, 4.6, 10.4$ and 18.6%). The insertion of perforated double counter twisted tapes were all found to perform much higher thermal performance than the plain tube. The highest thermal performance factor of 1.44 could be achieved at porosities of 4.6%. Some correlations associated with porosities were established as followings:

$$Nu = C Re^{-0.000004y^3 + 0.0002y^2 - 0.0001y + 0.546} Pr^{0.33} \quad (4-7)$$

$$f = C_1 Re^{-0.00004y^3 - 0.0012y^2 - 0.0108y - 0.5579} \quad (4-8)$$

$$\eta = 41.176CC_1^{-0.6802} Re^{-0.0000312y^3 + 0.001016y^2 - 0.00745y - 0.11614} \quad (4-9)$$

where $C = 0.0003y^3 - 0.0093y^2 + 0.0556y + 0.6194$ and $C_1 = 0.0008y^3 - 0.0231y^2 - 0.1877y + 16.659$.

Similarly, Thianpong et al. [12] have comprehensively investigated the perforated twisted tapes with different twist ratio (y/W), hole diameter ratio (d/W) and perforated ratio (s/W) at Reynolds number of 5000-20000. They found that the decrease in twist ratio and perforated ratio as well as the increase in hole diameter ratio could improve thermal efficiency. Some related correlations were illustrated as below:

$$Nu = 0.09 Re^{0.768} Pr^{0.4} (y/W)^{-0.325} (s/W)^{-0.133} (d/W)^{0.114} \quad (4-10)$$

$$f = 9.03 Re^{-0.272} (y/W)^{-0.631} (s/W)^{-0.204} (d/W)^{0.428} \quad (4-11)$$







$$\eta = 1.764 Re^{-0.059} (y/W)^{-0.114} (s/W)^{-0.065} (d/W)^{-0.028} \quad (4-12)$$

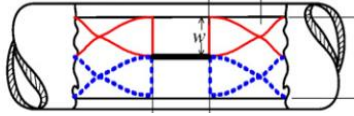
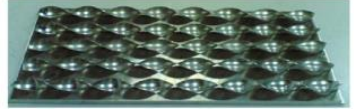
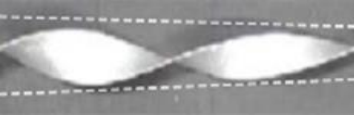

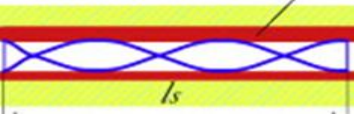

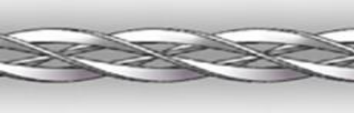
In summary, perforation fabrication to various twisted tapes previously have been proved to be an effective solution for further improvement of heat transfer rate. Hence, this chapter aims to combine the perforation fabrication with SRTTs for compound method to improve the tube heat transfer in turbulence regime.




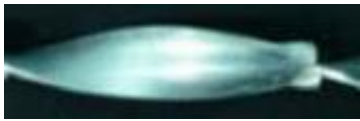



Some main contributions of this chapter are listed as below:

- Perforated SRTTs with five perforation ratios (PR=0%, 1.16%, 3.63%, 6.46%, and 10.1%) are prepared.
- Effects of perforation ratio on rotational speed, Nusselt number, friction factor and thermal performance factor are illustrated.
- Two correlations regarding perforation ratio are proposed to calculate the Nusselt number and friction factor.

Table 4.1: Previous studies on the correlations of twisted tape

Twisted tapes type	Geometry	Fabrication parameters	Proposed correlations	Reference
Peripherally-cut twisted tape		Depth ratio: (d/W) Width ratio: (w/W)	$Nu = 0.244Re^{0.625} Pr^{0.4} (d/W)^{0.168} (w/W)^{-0.112}$ $f = 39.46Re^{-0.591} (d/W)^{0.195} (w/W)^{-0.201}$ $\eta = 4.509Re^{-0.152} (d/W)^{0.102} (w/W)^{-0.054}$	[9]
V-cut twisted tape		Depth ratio: (d/W) Width ratio: (w/W) Twisted ratio: (y)	$Nu = 0.0296Re^{0.853} y^{-0.222} Pr^{0.33} (1+d/W)^{1.148} (1+w/W)^{-0.75}$ $f = 8.632Re^{-0.615} y^{-0.269} (1+d/W)^{2.477} (1+w/W)^{-1.914}$ $\eta = 1.392Re^{-0.01} y^{-0.124} (1+d/W)^{0.252} (1+w/W)^{-0.058}$	[6]
Square-cut twisted tape		Twisted ratio: (y)	$Nu = 0.041Re^{0.826} Pr^{0.33} y^{-0.228}$ $f = 6.936Re^{-0.579} y^{-0.259}$	[8]
Perforated twisted tape		Hole ratio: (d/W) Pitch ratio: (s/W) Twist ratio: (y/W)	$Nu = 0.09Re^{0.768} Pr^{0.4} (y/W)^{-0.325} (s/W)^{-0.133} (d/W)^{0.114}$ $f = 9.03Re^{-0.272} (y/W)^{-0.631} (s/W)^{-0.204} (d/W)^{0.428}$ $\eta = 1.764Re^{-0.059} (y/W)^{-0.114} (s/W)^{0.065} (d/W)^{-0.028}$	[12]
Perforated helical twisted tape		Diameter ratio: (d/w) Pitch ratio: (s/w)	$Nu = 0.035Re^{0.795} Pr^{0.4} (d/w)^{-0.068} (s/w)^{0.086}$ $f = 1.915Re^{-0.299} (d/w)^{-0.068} (s/w)^{-0.094}$ $\eta = 4.058Re^{-0.145} (d/w)^{-0.045} (s/w)^{0.054}$	[11]
Perforated twisted tape		Porosity: (R_p) Twist ratio: (y)	$Nu = C Re^{0.00005R_p^3 - 0.0013R_p^2 + 0.0073R_p + 0.5501} Pr^{0.33}$ $f = C_1 Re^{0.00009R_p^3 - 0.0022R_p^2 + 0.012R_p - 0.6006}$ $\eta = 36.995CC_1^{-0.676} Re^{-0.000011y^3 + 0.000187y^2 - 0.000808y - 0.07168}$ <p>Where, $C = 0.0002R_p^3 - 0.0046R_p^2 + 0.0334R_p + 0.6569$ $C_1 = 0.0027R_p^3 + 0.0583R_p^2 + 0.0455R_p + 24.536$</p>	[10]

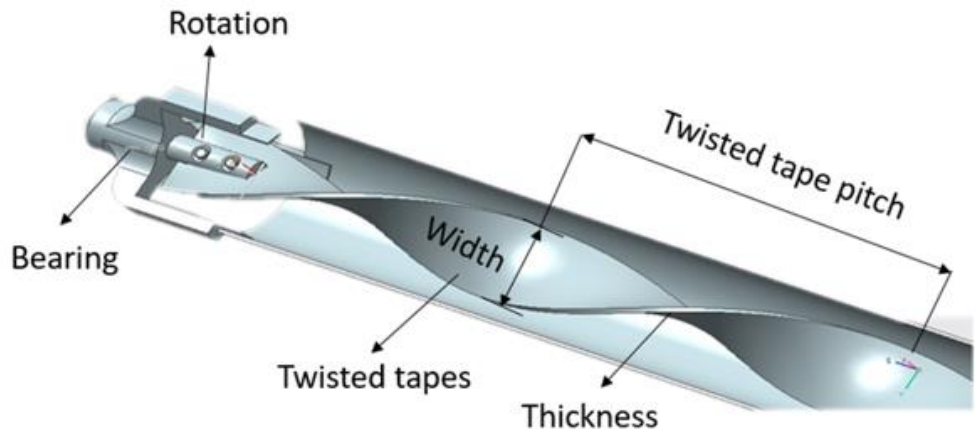
Regularly-spaced dual twisted tapes		Twist ratio: y/w Space ratio: s/D	$Nu = 0.069 Re^{0.74} Pr^{0.4} (y/w)^{-0.26} (1.5(s/D) + 1)^{-0.1}$ $f = 30.5 Re^{-0.56} (y/w)^{-0.54} (1.5(s/D) + 1)^{-0.2}$ $\eta = 1.9 Re^{-0.05} (y/w)^{-0.08} (1.5(s/D) + 1)^{-0.034}$	[104]
Multiple twisted tape		Twist ratio: y/w Space ratio: s/w	$Nu = 0.203 Re^{0.71} Pr^{0.4} (y/w)^{-0.79} (s/w)^{-0.63}$ $f = 207.77 Re^{-0.71} (y/w)^{-0.99} (s/w)^{-1.25}$	[105]
Tapered twisted tapes		Twist ratio: y/W Taper angle: θ	$Nu = 0.076 Re^{0.75} Pr^{0.4} (y/W)^{-0.39} (1 + \theta)^{-0.1}$ $f = 16.559 Re^{-0.49} (y/W)^{-0.51} (1 + \theta)^{-0.53}$ $\eta = 1.871 Re^{-0.04} (y/W)^{-0.22} (1 + \theta)^{-0.08}$	[52]
Regularly spaced twisted tape		Space ratio: S	$Nu = 0.01014 Re^{0.929} Pr^{1/3} (1 + S)^{-0.266}$ $f = 4.143 Re^{-0.398} (1 + S)^{-0.376}$	[53]
Short-length twisted tapes		Length ratio: LR	$Nu = 0.0664 Re^{0.693} Pr^{0.4} LR^{0.122}$ $f = 2.8 Re^{-0.398} LR^{0.19}$ $\eta = 1.82 Re^{-0.068} LR^{0.067}$	[13]
Trapezoidal-cut twisted tapes		Twist ratio: y	$Nu = 0.034 Re^{0.841} Pr^{0.33} y^{-0.226}$ $f = 7.401 Re^{-0.587} y^{-0.278}$ $\eta = 1.71 Re^{-0.032} y^{-0.126}$	[60]
Cross hollow twisted tape		Hollow width: C	$Nu = 0.34 Re^{0.59} Pr^{0.32} (0.91C^3 + 0.54C^2 - 1.35C + 1.27)$ $f = 9.348 Re^{-0.3959} (5.53C^3 + 2.578C^2 - 7.307C + 3.499)$	[3]

Twisted tapes consisting of centre wings and alternate-axes		Angle of attack: β	$Nu = 0.385 Re^{0.568} Pr^{0.4} (1 + \tan \beta)^{0.129}$ $f = 20.445 Re^{-0.504} (1 + \tan \beta)^{0.283}$ $\eta = 6.772 Re^{-0.194} (1 + \tan \beta)^{0.035}$	[106]
Peripherally-cut twisted tape		Depth ratio: d/W Width ratio: w/W	$Nu = 0.244 Re^{0.625} Pr^{0.4} (d/W)^{0.168} (w/W)^{-0.112}$ $f = 39.46 Re^{-0.591} (d/W)^{0.195} (w/W)^{-0.201}$ $\eta = 4.509 Re^{-0.152} (d/W)^{0.102} (w/W)^{-0.054}$	[9]
Oblique delta-winglet twisted tape		Twist ratio: y/W Wing cut ratios: d/W	$Nu = 0.184 Re^{0.67} Pr^{0.4} (y/W)^{-0.423} (1 + (d/W))^{0.982}$ $f = 24.8 Re^{-0.51} (y/W)^{0.566} (1 + (d/W))^{1.87}$ $\eta = 2.04 Re^{-0.042} Pr^{0.4} (y/W)^{-0.261} (1 + (d/W))^{0.45}$	[1]
Straight delta-winglet twisted tape		Twist ratio: y/W Wing cut ratios: d/W	$Nu = 0.184 Re^{0.675} Pr^{0.4} (y/W)^{-0.465} (1 + (d/W))^{0.76}$ $f = 21.7 Re^{-0.45} (y/W)^{0.564} (1 + (d/W))^{1.41}$ $\eta = 2.164 Re^{-0.0435} Pr^{0.4} (y/W)^{-0.304} (1 + (d/W))^{0.356}$	[1]
Helically twisted tapes		Twist ratio: y/W Helical pitch ratios: p/D	$Nu = 0.053 Re^{0.796} Pr^{0.4} (y/W)^{-0.127} (p/D)^{-0.188}$ $f = 12.653 Re^{-0.295} Pr^{0.4} (y/W)^{-0.652} (p/D)^{-1.513}$ $\eta = 3.377 Re^{-0.148} (y/W)^{0.091} (p/D)^{0.317}$	[107]
A new kind of twisted tape		Length ratio: L/l	$Nu = 0.2247 Re^{0.6285} Pr^{0.3} (L/l)^{0.19}$ $f = 286.3 Re^{-0.7886} (L/l)$	[14]
Triple twisted tape		Twist ratio: y	$Nu = C Re^{(0.00002y^3 + 0.0013y^2 - 0.0094y + 0.5746)} Pr^{0.33}$ $f = C_1 Re^{(0.00005y^3 + 0.0017y^2 - 0.0164y - 0.5193)}$ $f = 41.176 C C_1^{-0.6802} Re^{(0.000014y^3 + 0.000144y^2 + 0.001755y - 0.11379)}$ <p>Where</p> $C = -0.0017y^3 + 0.0179y^2 + 0.0962y + 0.7734$ $C_1 = -0.0388y^3 + 0.2484y^2 - 0.8462y + 17.685$	[57]

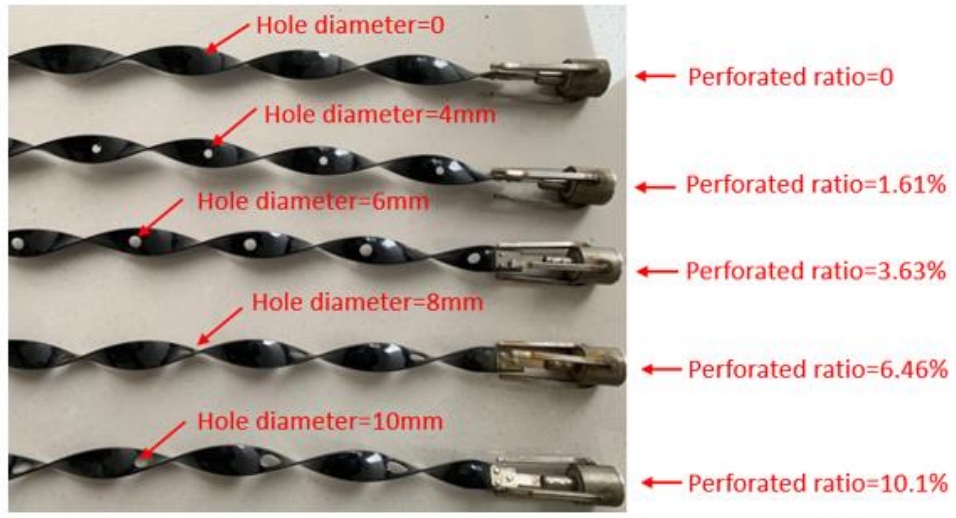
4.2 Experimental methodology

4.2.1 Experimental facilities

SRTTs were made from 2000-mm-long, 1-mm-thick, and 14-mm-wide polymer straight tapes, and were equipped with rotation and bearing, as shown in Figure 4.1(a). Bearing fixes the twisted tape at the inlet of inner tube, and rotation can help the twisted tape rotate along the axial center of the inner tube. In this experiment, five perforated SRTTs with different perforation ratios (PR = 0%, 1.61%, 3.63%, 6.46%, and 10.1%) were prepared, as shown as Figure 4.1(b). The tapes had different perforation hole diameters. The definition of PR was a ratio of the perforation area to the total area of a twisted tape. It should be noted that all SRTTs used in this experiment had a constant twist ratio of four.



a

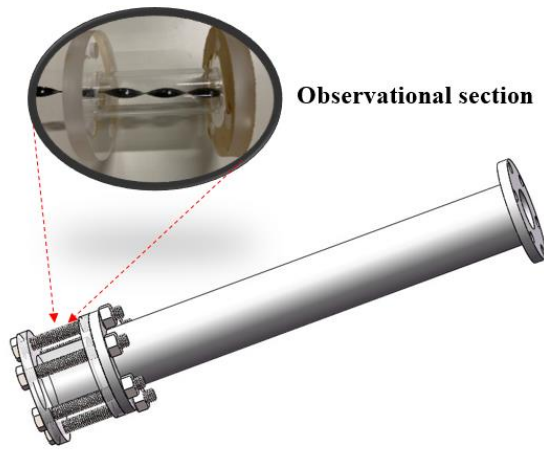


b

Figure 4.1 (a) Structure of SRTTs; (b) Perforated SRTTs, for different PRs

A double-pipe heat tube with an observational section was modified for measuring the rotation speed of the SRTTs (Figure 4.1(a)). The rotation speed was recorded by a digital tachometer RPM meter in the contactless mode (Figure 4.2(b)). The test bed mainly consisted of a test section, a data collection system and a heat sink, as shown in Figure 3. The test section (a double-pipe heat exchanger) contained an inner tube and an outer tube. The inner diameter and outer diameter of inner tube are 20 mm and 25 mm, respectively. The inner diameter and outer diameter of outer tube are 65 mm and 70 mm. In addition,

outer tube was made of stainless steel, and inner tube was manufactured from copper with full length of 2000 mm. In order to reach convective heat transfer in the countercurrent manner, hot water (40 °C at the inlet of the inner tube) was circulated through the inner tube, and cold water (21.8 °C at the inlet of the outer tube) flowed through the outer tube, respectively. The water volume flow rate was controlled by adjusting the power capacity of a water pump. It should be noted that water volume flow rate was maintained at 0.55 m³/h in outer tube, and varied from 0.45 m³/h to 1.62 m³/h in inner tube for the study cases. To maintain a constant water temperature, hot water was pumped back to a water tank and was re-heated using an electrical heater with a constant heat flux, while cold water was discharged to the heat sink for releasing heat to the outdoors. As for the data collection system, two temperature sensors (RTDs) were installed at the inlet and the outlet of the inner tube for estimating the bulk temperature of water. Some thermocouples were tapped on 10 positions along the inner tube for recording the local wall temperature. Two pressure tapes were placed at the inlet and the outlet of the inner tube for measuring the pressure drop across the inner tube. All of the experimental data, including the water temperature, pressure drop and volume water flow rate were steadily monitored using a data logger. For example, the inlet temperature at inner tube was kept at 40 °C (± 0.5 °C), and the inlet temperature at outer tube was controlled at 21.8 °C (± 0.2 °C).



a



b

Figure 4.2 (a) Fabricated tube with an observational section; (b) Digital tachometer

RPM meter in the contactless mode

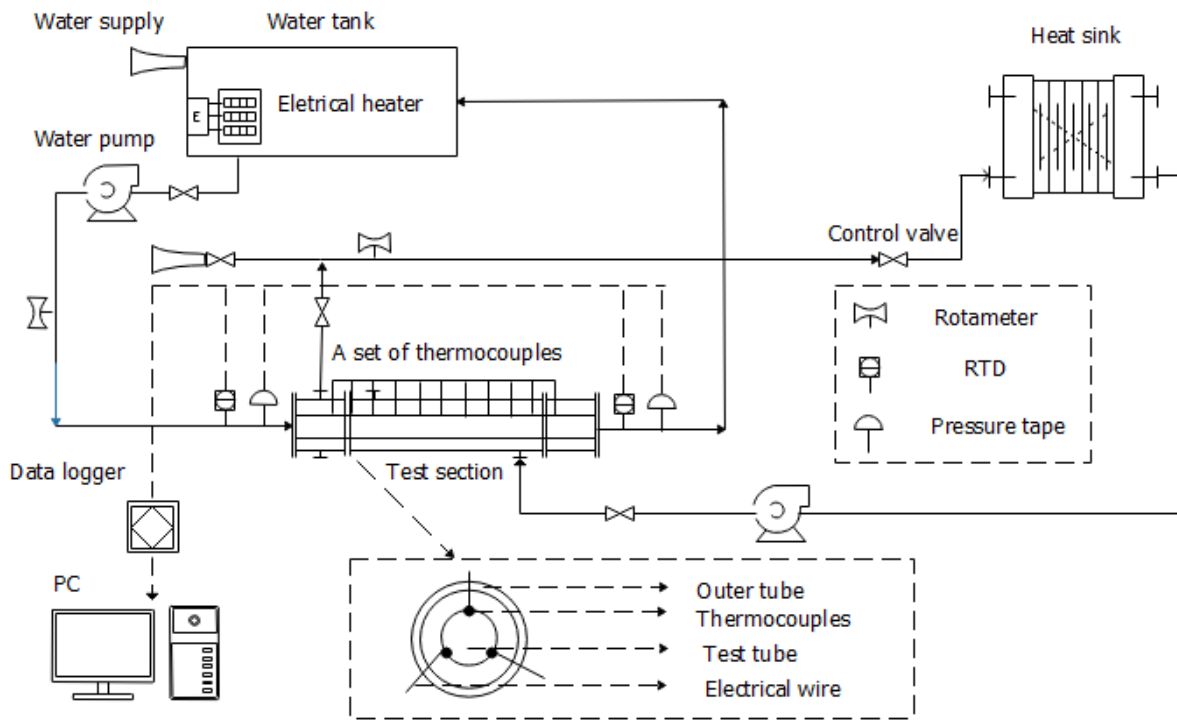


Figure 4.3 Diagrammatic sketch of the test bed

4.3 Data processing

Below, we describe the procedure of calculating the Nusselt number, friction factor, and thermal performance factor for the tube with the SRTTs at the Reynolds number of 12000–45000. The details are summarized below.

4.3.1 Heat transfer characteristic

The heat transfer loss by the hot water across the inner tube is

$$Q_w = m_w C_{p,w} (T_{w,in} - T_{w,out}) \quad (4-13)$$

The transferred heat from the inner tube to outer tube is supposed to be the same as the convective heat transfer, as shown below:

$$Q_w = Q_{conv} \quad (4-14)$$

For all experimental runs, the above two quantities should be in an excellent agreement owing to the thermal equilibrium between the heat supply and transferred heat, as follows:

$$\left| \frac{Q_{VI} - Q_w}{Q_{VI}} * 100\% \right| \leq 5\% \quad (4-15)$$

The convective heat transfer in this experiment was

$$Q_{conv} = hA_i (\bar{T}_s - T_b) \quad (4-16)$$

where

$$T_b = (T_{out} + T_{in}) / 2 \quad (4-17)$$

$$\bar{T}_s = \sum T_s / 10 \quad (4-18)$$

The heat transfer coefficient of local tube wall was

$$h_i = Q_w / A_i (\bar{T}_s - T_b) \quad (4-19)$$

The heat transfer rate of inner tube was indicated by Nusselt number as below:

$$Nu = \frac{hD_i}{\lambda} \quad (4-20)$$

4.3.2 Friction factor characteristics

The friction factor was estimated from the differential pressure across the entire inner tube:

$$f = \frac{\Delta P}{\left(\frac{L}{D_i}\right)\left(\rho \frac{v^2}{2}\right)} \quad (4-21)$$

The Reynolds number, which indicates the working fluid's condition, is

$$Re = \frac{\rho v D_i}{\mu} \quad (4-22)$$

4.3.3 Thermal performance factor

In order to assess the potential of twisted tapes for energy saving, the thermal performance factor has been commonly used previously to quantify the thermal efficiency of heat exchangers [1, 4,108]. This parameter is defined by the relationship between the Nusselt number ratio and the friction factor ratio at a constant pumping power, which can be expressed as

$$\eta = \frac{h_t}{h_p} \Big|_{pp} = \frac{(Nu_t / Nu_p)}{(f_t / f_p)^{1/3}} \quad (4-23)$$

4.3.4 Uncertainty analysis

Uncertainty in the experimental results was estimated according to ANSI/ASME standard [103]. The measured quantities, such as the volume flow rate, the water temperature, and the pressure drop, were used for estimating the combined uncertainties of non-dimensional parameters. The maximal uncertainties in these parameters were estimated to be within $\pm 3.4\%$ for the Reynolds number, $\pm 8.8\%$ for the Nusselt number, and $\pm 9.2\%$ for the friction factor. The equations that were used to estimate these uncertainties were

$$\left(\frac{\Delta Nu}{Nu}\right) = \left[\left(\frac{\Delta h}{h}\right)^2 + \left(\frac{\Delta D}{D}\right)^2\right]^{0.5} \quad (4-24)$$

$$\left(\frac{\Delta f}{f}\right) = \left[\left(\frac{\Delta(\Delta p)}{\Delta p}\right)^2 + \left(\frac{3\Delta D}{D}\right)^2 + \left(\frac{2Re}{Re}\right)^2 + \left(\frac{\Delta L}{L}\right)^2\right]^{0.5} \quad (4-25)$$

$$\left(\frac{\Delta Re}{Re}\right) = \left[\left(\frac{\Delta m}{m}\right)^2 + \left(\frac{\Delta D}{D}\right)^2\right]^{0.5} \quad (4-26)$$

4.4 Results and Discussion

4.4.1 Verification test: plain tube

The experimental data for the Nusselt number and friction factor of the plain tube were verified by some correlations that are frequently observed for single-phase fluids and straight tubes [8]; these correlations are listed below.

The correlation of Dittus–Boelter (Eq. 4-27):

$$Nu = 0.023 Re^{0.8} Pr^{0.3} \quad (4-27)$$

The correlation of Gnielinski (Eq. 4-28):

$$Nu = \frac{(f/8)(Re-1000)Pr}{1+12.7(f/8)^{0.5}(Pr^{2/3}-1)} \quad (4-28)$$

The correlation of Blasius (Eq. 4-29):

$$f = 0.316 Re^{-0.25} \quad (4-29)$$

The correlation of first Petukhov (Eq. 4-30):

$$f = (0.79 \ln Re - 1.64)^{-2} \quad (4-30)$$

The results of the validation test are shown in Figures 4.4 and 4.5. The experimental data were observed to reach a great agreement with the Dittus–Boelter ($\pm 9.9\%$) and Gnielinski ($\pm 7.8\%$) equations. In addition, the results obtained in the present work for the friction factor were validated by the equations of Blasius and Petukhov with deviation of $\pm 9.6\%$ and $\pm 11.6\%$. Eqns. 4-27 and 4-29 are proposed to predict the Nusselt number and the friction factor for the SRTTs in Section 4.4.

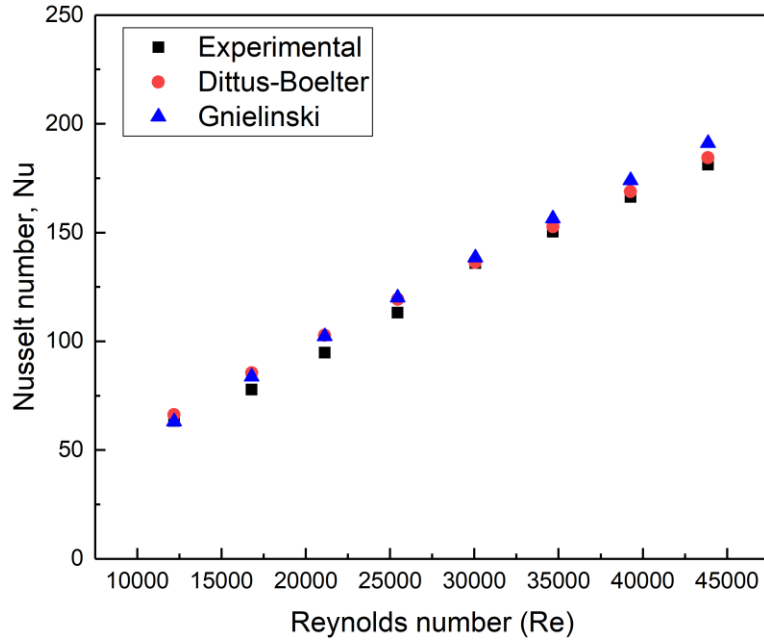


Figure 4.4 Experimental results versus empirical correlations results: Nu

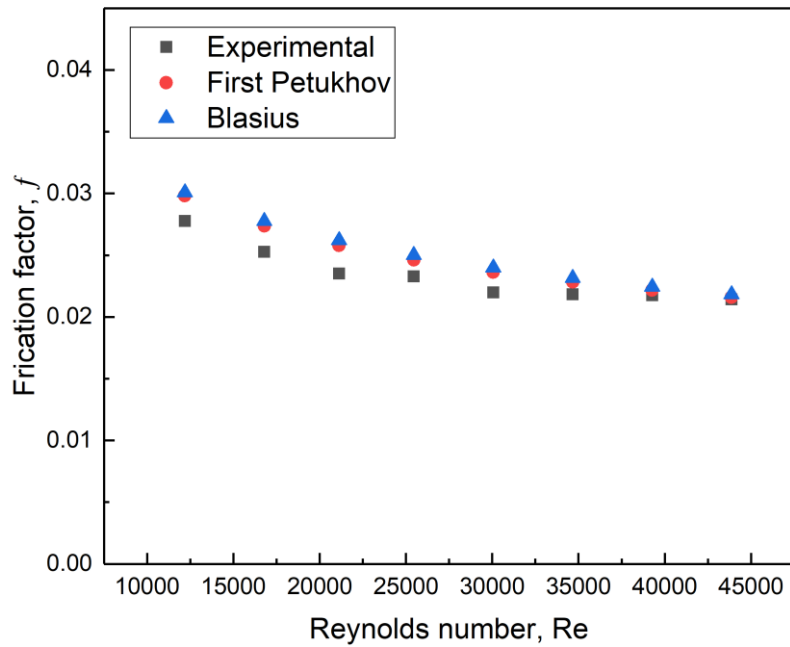


Figure 4.5 Experimental results versus empirical correlation results: f

4.4.2 Effect of the PR on the rotation speed

SRTTs are stationary at low water velocities, and exhibit rotation behavior that is enforced by the working fluid at higher water velocities. Figure 4.6 demonstrates that the PR significantly affects the initial stage of rotation behavior, and lower PRs induce SRTTs rotation behavior at lower Reynolds numbers and/or lower water velocity. In addition, the speed of rotation behavior increases sharply with increasing the Reynolds number, and the SRTTs with lower PRs (PR = 0) rotate faster than those with higher PR (PR = 1.61%, 3.63%, 6.45%, and 10.1%). This can be attributed to reason that reducing the perforation area raises the contact surface area between the working fluid and the twisted tape, which allows SRTTs rotation behavior at higher rates.

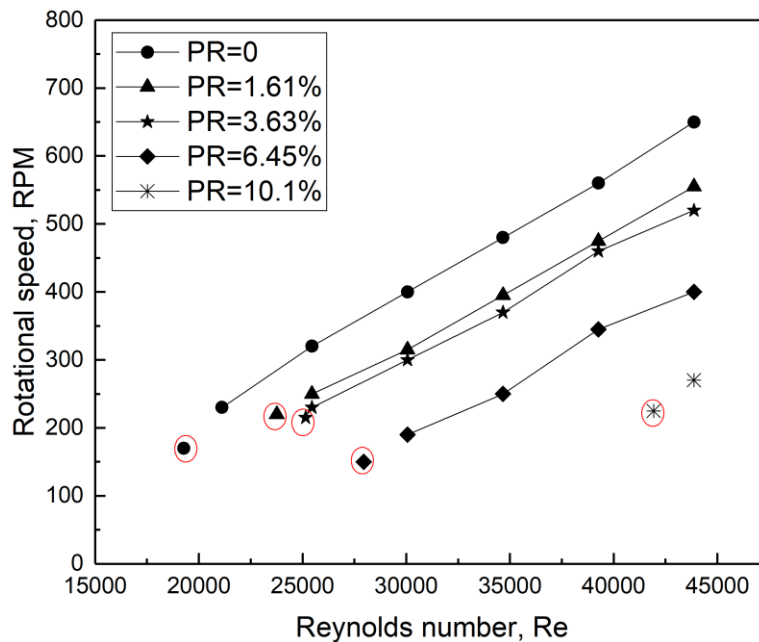
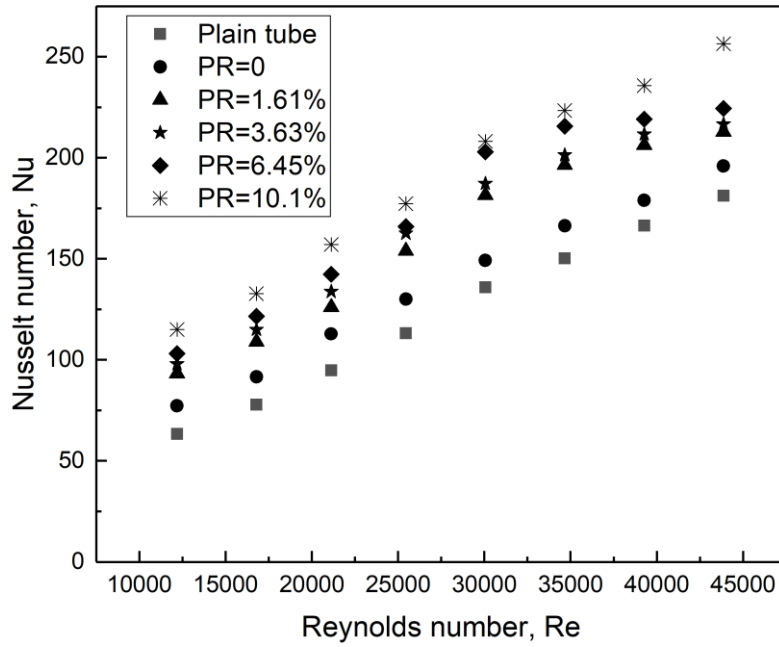


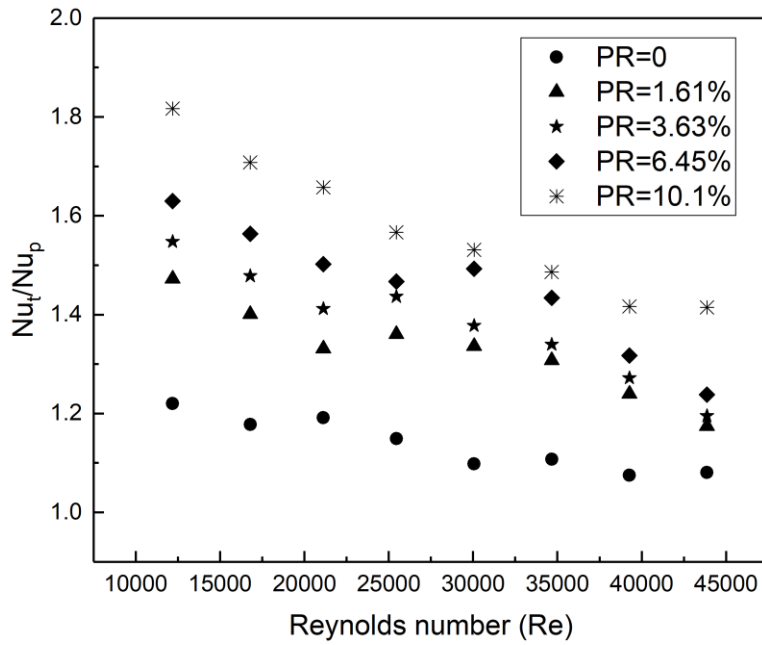
Figure 4.6 Relationship between the rotation speed (RPM) and the Reynolds number (The red circles denote the initial phase of rotation behavior)

4.4.3 Effect of the PR on the heat transfer characteristic

Figure 4.7 presents the variation of the Nusselt number, friction factor, and thermal performance factor with the Reynolds number in the 12000–45000 range, for the SRTTs with different PRs. These results show that the tube fitted with the different SRTTs yields much higher Nusselt number, compared with the plain tube. This can be explained by the stronger swirl flow induced by the insertion of the SRTTs, which improves the motion of working fluid between the core region and the near wall surface. Moreover, lower PRs can significantly enhance the Nusselt number, compared with higher PRs. These results are somewhat different from previously reported results regarding the effect of the perforation area on heat transfer [10, 12]. It is possible that perforated modification (multiple perforated hole) used in previous research is somehow different from the perforated modification (single perforated holes) used in this study. Increasing perforated area can disturb thermal boundary layer to improve heat transfer coefficient between working fluids and local wall. As mentioned in Section 4.4.2, an increase in the perforation area reduces the rotation speed. It also implies that the perforation fabrication method is stronger than the rotation speed in terms of disrupting the thermal boundary layer and increasing the residence time along the tangential direction. As shown in Figure 4.7(b), the Nu_t/Nu_p ratio decreased from 1.22 to 1.08, 1.47 to 1.27, 1.55 to 1.2, 1.63 to 1.24, and 1.82 to 1.41, for PR = 0%, 1.61%, 3.63%, 6.46%, and 10.1%, respectively, with increasing the Reynolds number. It turns out that the perforation fabrication method plays a more dominant role in inducing extra turbulence for effective convective heat transfer at lower Reynolds numbers, compared with higher-Reynolds-number flows.



(a)

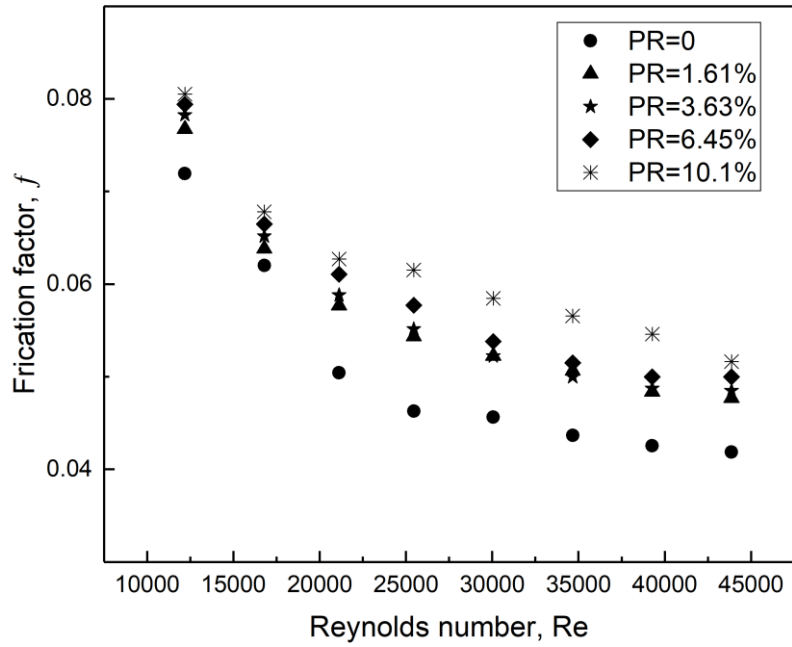


(b)

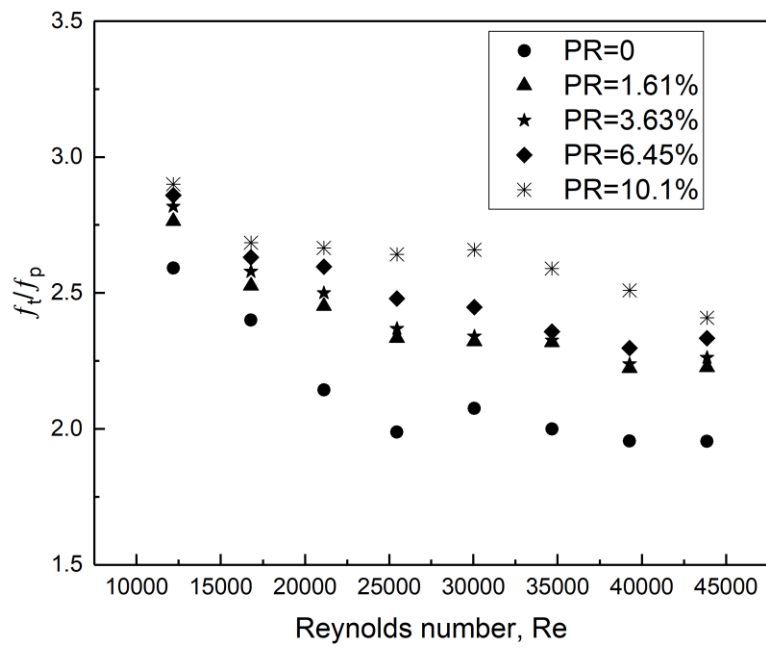
Figure 4.7 Variation of (a) the Nu and (b) the Nu_t/Nu_p ratio with Re for the SRTTs with different PRs

4.4.4 Effect of the PRs on the friction factor characteristic

The effect of the PRs on the friction factor characteristic is summarized in Figure 8. Figure 8(a) shows that the friction factor of the SRTTs with higher PRs is higher than that of the SRTTs with lower PRs for given operating conditions. A possible explanation is that stronger turbulence intensity generated by higher PR increases the viscous loss along the inner tube, resulting in a considerable differential pressure. Moreover, SRTTs with lower PRs can rotate faster than those with higher PRs. Hence, high rotational speed is likely to promote rotational flow that significantly reduces flow resistance and smoothen heat transfer surface. As presented in Figure 8(b), the f_t/f_p ratio overall tends to decrease gradually with the increase of Reynolds number. This might be partially owing to the higher rotation speed caused by higher water velocity and larger Reynolds numbers, which can mitigate the flow blockage and resistance along the flow path.



(a)



(b)

Figure 4.8 Variation of (a) the f and (b) the f_t/f_p ratio with Re for the SRTTs with different PRs

4.4.5 Effect of the PR on the thermal performance factor

Figure 4.9 illustrates the dependence of the thermal performance factor on the Reynolds number for different PRs. Interestingly, the thermal performance factors of all SRTTs were found to increase significantly (0.862 to 0.924, 0.987 to 1.025, 1.04 to 1.078, 1.084 to 1.101, and 1.042 to 1.055, for PR = 0%, 1.61%, 3.63%, 6.46%, and 10.1%, respectively) when the SRTTs started to rotate. A possible explanation is that rotation behavior increases the heat transfer rate by enhancing the turbulence intensity along the tangential direction, while it reduces the friction factor by smoothening the fluid motion. Augmentation of the heat transfer and reduction of the pressure drop can both remarkably increase the thermal performance factor. Moreover, it is seen that the tube fitted with the SRTTs with higher PR exhibits a higher thermal performance factor than those with lower PRs. It is likely that an increase in the perforation area is responsible for considerably enhancing the fluid motion along the longer flow path, which generate stronger turbulence intensity along tangential direction.

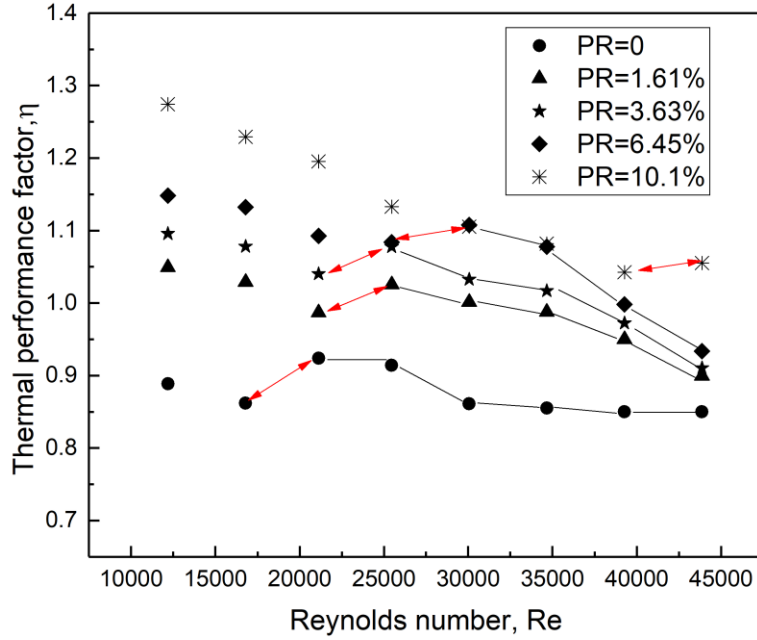


Figure 4.9 Variation of the η with the Re for SRTTs with different PRs (Red arrow denotes the change of the SRTTs from the stationary to rotation condition)

4.4.6 Proposed correlations

The derived correlations for the Nu and the f were developed for the heat exchanger tube fitted with SRTTs at the Reynolds number in the 12000–45000 range and PRs of 0%, 1.61%, 3.63%, 6.46%, and 10.1%. They are expressed in the following Eqns. (4-31) and (4-32):

$$Nu_{SRTTs} = 0.1775 Re^{0.7193} Pr^{0.2254} (0.008 + PR)^{0.10905} \quad (4-31)$$

$$f_{SRTTs} = 3.3127 Re^{-0.3832} (0.0041 + PR)^{0.0526} \quad (4-32)$$

The Comparison between the experimental and predicted values are displayed in Figures 4.10 and 4.11 for Nusselt number and friction factor, respectively. The results

showed that there are 10% discrepancy between experimental and correlations values for Nusselt number and friction factor.

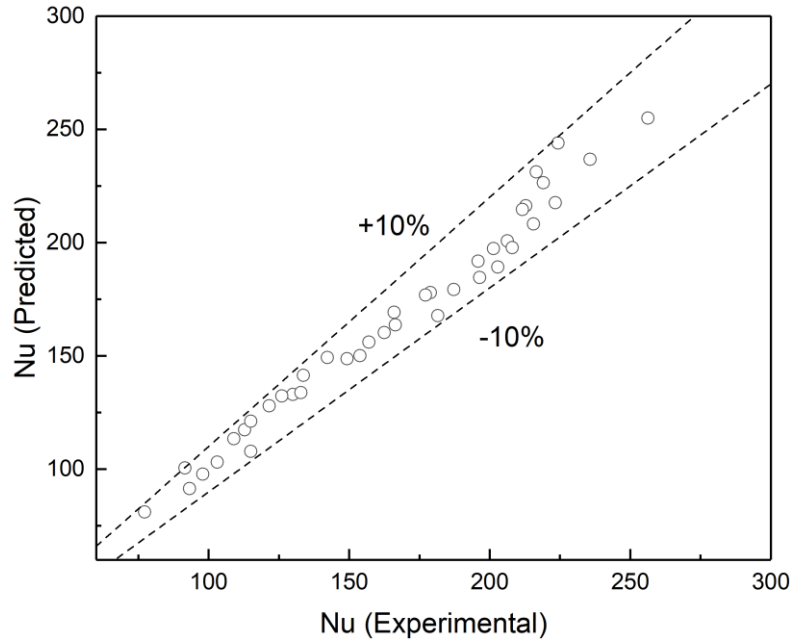


Figure 4.10 Comparison of the experimental and predicted Nusselt numbers for the SRTTs with different PRs

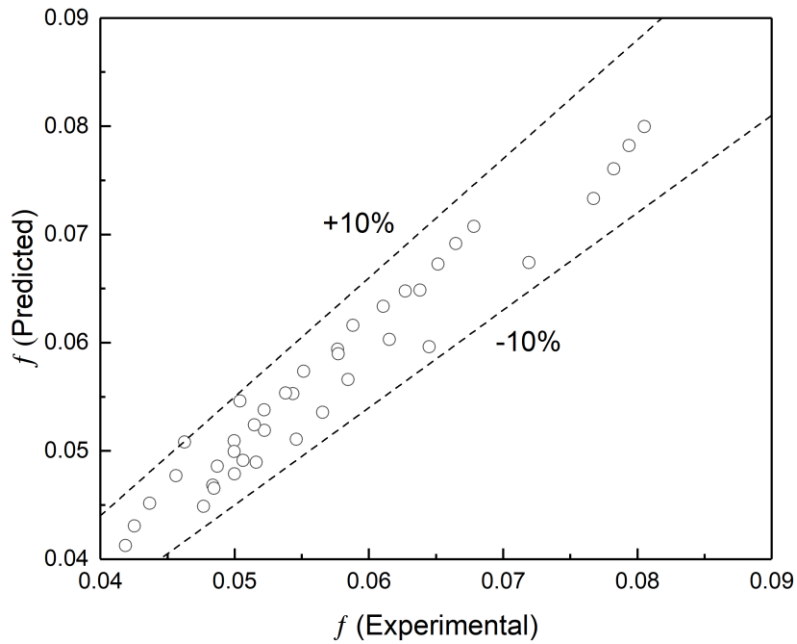


Figure 4.11 Comparison of the experimental and predicted friction factors for the SRTTs with different PRs

4.4.7 Comparison of perforated SRTTs and perforated twisted tapes

Perforated SRTTs were compared with perforated twisted tapes (PTTs) used in a previous study, in terms of the thermal performance factor [12]. From Figure 4.12, the tube with the perforated SRTTs evidently has a larger thermal performance factor than those with the PTTs for the same PR. This is because of the vital influences of rotation behavior on producing extra residence time of the heat transfer process and decreasing the flow blockage. In addition, large perforation diameter of SRTTs was examined for improving the thermal performance factor, which was not consistent with the results for PTTs [12]. It seems possible that such perforation fabrication to SRTTs is more dominant than the Reynolds number as for affecting the thermal performance factor in comparison of PTTs.

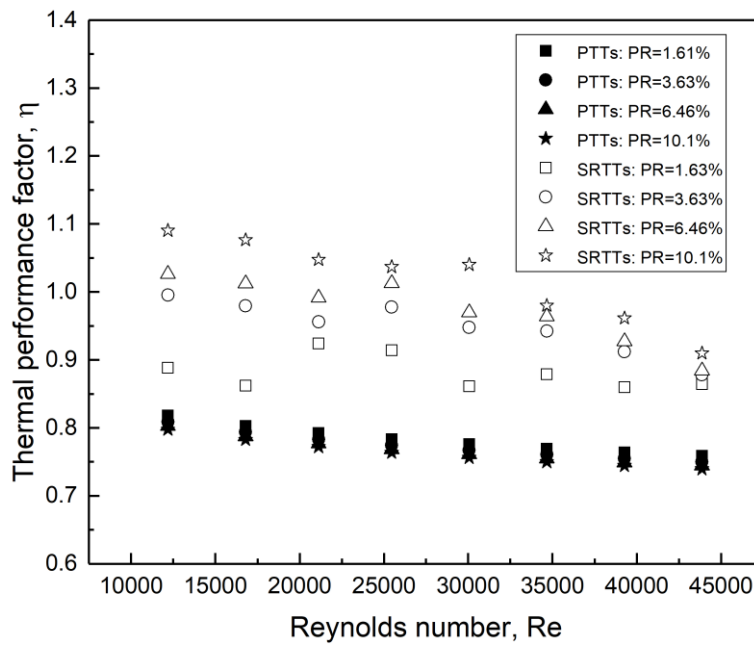


Figure 4.12 Comparison of f of perforated SRTTs and those of perforated PTTs

4.5 Summary

The thermal characteristics of SRTTs with different PRs in the double-pipe heat exchanger were experimentally investigated in this chapter. Some of the major conclusions drawn in this study are listed as below:

- For SRTTs with smaller PRs, rotation behavior starts at lower water velocities or Reynolds numbers. Moreover, SRTTs with larger PRs seem to rotate slower than those with smaller PR.
- Increasing the PR of SRTTs can significantly increase the Nusselt number and the friction factor, by 13.8% to 57.5%, and by 116% to 163%, respectively. For all given cases, the tube fitted with larger-PR SRTTs has a much better thermal performance than those with lower-PR SRTTs. The thermal performance factor increases sharply when the SRTTs start to rotate from the stationary condition.
- Some correlations for SRTTs associated with the PRs were formulated to accurately establish the Nusselt number and the friction factor. The predicted value from the proposed correlations was validated to be within 10% of experimental data.

In summary, the present study revealed that the perforation fabrication of SRTTs with large PRs can significantly improve their thermal performance. The derived empirical correlations associated with the PR could be employed to accurately estimate the Nusselt number and the friction factor of SRTTs. The findings of the present study are likely to provide valuable guidelines for further application of SRTTs in heat exchangers.

CHAPTER 5

THERMO-HYDRAULICS CHARACTERISTIC OF THE TUBE FITTED WITH SHORT-LENGTH SELF-ROTATING TWISTED TAPES

In addition to the perforated SRTTs introduced in Chapter 4, short-length SRTTs might be able to enhance rate of heat transfer with allowable pressure drop as well. This chapter aims to investigate the heat transfer and friction factor characteristic of short-length SRTTs in the double-pipe heat exchanger. Section 5.1 introduces the significance of pressure drop in heat exchanger system, and reviews previous studies on reducing increase of pressure drop by using short-length SRTTs. Then, short-length SRTTs with four length ratios are fabricated in Section 5.2. Section 5.2 also introduces the experimental procedure to control the operation condition and collect the measured parameter values. Section 5.3 describes the theoretical step to calculate the thermal performance factor and analyze the uncertainties. In Section 5.4, the effects of length ratio on rotational speed of rotating behavior and thermal behavior are analyzed and some correlations varying with length ratio are presented. Also, the short-length SRTTs are compared with other short-length twisted tapes in terms of thermal performance factor depending on related correlations. A brief conclusion of this chapter is also drawn in Section 5.5.

5.1 Introduction

Twisted tapes in group as a swirl flow generator are popularly employed to improve the thermal performance of heat exchangers, as presented in Table 5.1. However, regarding the thermal design of heat exchanger, pressure drop or friction factor is another main consideration. The increase in pressure drop of fluids flowing through heat exchangers will cause more pumping power consumption that decreases the overall energy efficiency of heat exchangers. Therefore, the pressure drop should be managed with an allowable level of pumping power consumption. Although the utilization of twisted tapes can induce stronger swirl flow and enhance the heat transfer behavior, extra pressure drop could be generated simultaneously due to the enlarged fitting and viscous losses. Some previous studies have proposed some alternative approaches to improve the heat transfer rate with less increase of friction factor, particularly by short-length fabrication.

Eiamsa-ard et al. [13] firstly proposed that the short-length twisted tapes might be feasible to increase the heat transfer rate with less increase of pressure drop. Their results revealed that short-length fabrication could decrease the pressure drop to some extent in comparison of full-length twisted tapes. However, the rate of heat transfer and thermal performance factor reduced with the decrease of length ratio (LR). Some correlations regarding length ratio were reported as below:

$$Nu = 0.0664 Re^{0.693} Pr^{0.4} LR^{0.122} \quad (5-1)$$

$$f = 2.8 Re^{-0.398} LR^{0.19} \quad (5-2)$$

$$\eta = 1.82 Re^{-0.068} LR^{0.067} \quad (5-3)$$







A new type of twisted tapes fabricated with different length in turbulence flow from 10000-28000 was introduced and studied by Man et al. [14]. They found that the decrease in this twisted tapes length could significantly reduce the friction factor. Full-length twisted tapes were found to perform the highest thermal performance in terms of Nusselt number and thermal performance factor. Some correlations associated with length ratio (L/l) have been derived as followings:







$$Nu = 0.2247 Re^{0.6285} Pr^{0.3} (L/l)^{0.19} \quad (5-4)$$

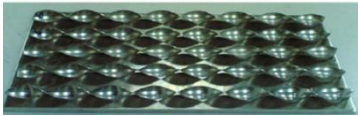


$$f = 286.3 Re^{-0.7886} (L/l) \quad (5-5)$$

Similarly, short-length fabrication also has been utilized to helical tapes [15] and separated multiple twisted tapes [109] for purpose of reducing friction factor. According to Chapter 3, the rotational speed of rotating behavior can smoothen heat transfer surface to reduce the pressure drop. By adopting short-length fabrication and SRTTs, short-length pressure drop and friction factor could be further reduced. Therefore, this chapter aims to study the heat transfer and friction factor characteristics of short-length SRTTs with length ratio of LR=1, 0.6, 0.45 and 0.3 in turbulence flow. Some correlations varying with length ratio are established accordingly for prediction of the Nusselt number and friction factor.

Table 5.1: Previous research on application of various twisted tape

Twisted tapes type	Configurations	Operation condition	Thermal performance improvement	Reference
Double counter twisted tape		Reynolds number: 6950-50050	<i>Comparison of plain tube:</i> Increase in Nusselt number: 60-240% Increase in friction factor: 91-286%	[56]
Center-cleared twisted tape		Reynolds number: 400-1800	<i>Comparison of conventional twisted tapes</i> Increase in thermal performance factor: 7-20%	[5]
Cross hollow twisted tape		Reynolds number: 5600-18000	<i>Comparison of plain tube:</i> Increase in Nusselt number: 93-120% Increase in friction factor: 883-1042%	[3]
Twisted tapes inserts with teflon rings		Reynolds number: 5132-24989	<i>Comparison of plain tube:</i> Increase in Nusselt number: 39-175% Increase in friction factor: 36-168%	[108]
New twisted tapes		Reynolds number: 10000-28000	<i>Comparison of plain tube:</i> Increase in Nusselt number: 1.4-1.9 times Increase in friction factor: 3.69-5.75 times	[14]
Broken twisted tapes		Reynolds number: 1000-40000	<i>Comparison of smooth twisted tape:</i> Increase in Nusselt number: 1.28-2.4 times Increase in friction factor: 2-4.7 times Thermal performance factor: 0.99-1.8 times	[49]

Delta-winglet twisted tape		Reynolds number: 3000–27000	<i>Comparison of typical twisted tapes:</i> Increase in Nusselt number: 1.04-1.64 times Increase in friction factor: 1.09-1.95 times Thermal performance factor: 1.05-1.13 times	[1]
Triple twisted tape		Reynolds number: 7200-50200	<i>Comparison of plain tube:</i> Increase in Nusselt number: 1.73-3.85 times Increase in friction factor: 1.91-4.2 times	[57]
Multiple twisted-tape		Reynolds number: 5300-24000	<i>Comparison of plain tube:</i> Increase in Nusselt number: 1.15-2.12 times Increase in friction factor: 1.9-4.1 times	[55]
Perforated double counter twisted tape		Reynolds number: 7200-50000	<i>Comparison of plain tube:</i> Increase in Nusselt number: 80-290% Increase in friction factor: 111-335%	[58]
Perforated twisted tapes with alternate axis		Reynolds number: 3000-16000	<i>Comparison of plain tube:</i> Increase in Nusselt number: 48.12% Increase in friction factor: 19.1% Maximum thermal performance factor: 1.433	[102]
Twisted tapes consisting of centre wings and alternate-axes		Reynolds number: 5200-22000	<i>Comparison of typical twisted tape:</i> Increase in Nusselt number: 62% Increase in friction factor: 123% Increase in thermal performance factor: 24%	[106]

Multiple twisted tape		Reynolds number: 7200-50000	<i>Comparison of typical twisted tape:</i> Increase in Nusselt number: 80-290% Increase in friction factor: 111-335%	[58]
Twin counter twisted tapes		Reynolds number: 3700-21000	<i>Comparison of twin co-twisted tapes</i> Increase in Nusselt number: 12.5-44.5% Increase in friction factor: 26.5-45.5%	[96]
Trapezoidal-Cut twisted tapes		Reynolds number: 2000-12000	<i>Comparison of plain twisted tapes</i> Increase in Nusselt number: 12.5-44.5% Increase in friction factor: 26.5-45.5%	[60]

5.2 Experimental strategy

A sketch map of the test bed is presented in Figure 5.1. The test bed primarily contained a test section, an electrical heater, a heat sink, and measurement devices. Two circular tubes with a 20000 mm length were implemented as the test section in which the inner tube allows working fluid to flow through and the outer tube permits the delivery of cold water. The inner tube is made of copper material with an inner diameter of 20 mm and an outer diameter of 25 mm. In addition, the inner tube has an observational section to monitor the rotating behavior of SRTTs, as displayed in Figure 5.2 (a). The outer tube is made of stainless steel with an inner diameter of 65 mm and an outer diameter of 70 mm. An electrical heater can be utilized to offer a constant heat flux. The heat sink functions in releasing heat to the ambient environment by controlling the fan speed. For measurement devices, two water pumps were installed to deliver working fluids to the inner and outer tubes, respectively. Two rotameters were used to record the water flow rate in the inner and outer tubes. Some thermocouples were attached on the external surface of the inner tube to record the tube wall temperature. Two RTDs at the inlet and outlet of the inner tube measure the hot water temperature before and after the heat transfer process. Another two RTDs were assembled at the inlet and outlet of the outer tube to record the temperature of the cold water. Additionally, pressure tapes were assembled at the inlet and outlet of the inner tube to calculate the pressure drop of the water across the inner tube.

Prior to conducting the experiment, the thermocouples and rotameters were calibrated to guarantee the accuracy of the measurements. During the experiment, hot water with a controlled temperature of 40 °C was distributed to the inner tube, and cold water with a controlled temperature of 21 °C was pumped to the outer tube. The water flow rate was

regulated by adjusting the output power of the water pump. In this experiment, the Reynolds number varied from 12000 to 45000 in the turbulence range. Approximately, 1 h is needed for the water temperature and flow rate to be stabilized. All the experimental data of the water temperature, pressure drop, and volume flow rate were recorded at steady state for 20 min. These data were delivered to the data logger for the following calculation. Moreover, a Digital Tachometer RPM meter with a contactless mode, as shown in Figure 5.2 (b), could record the rotational speed of the different short-length SRTTs through the observational section.

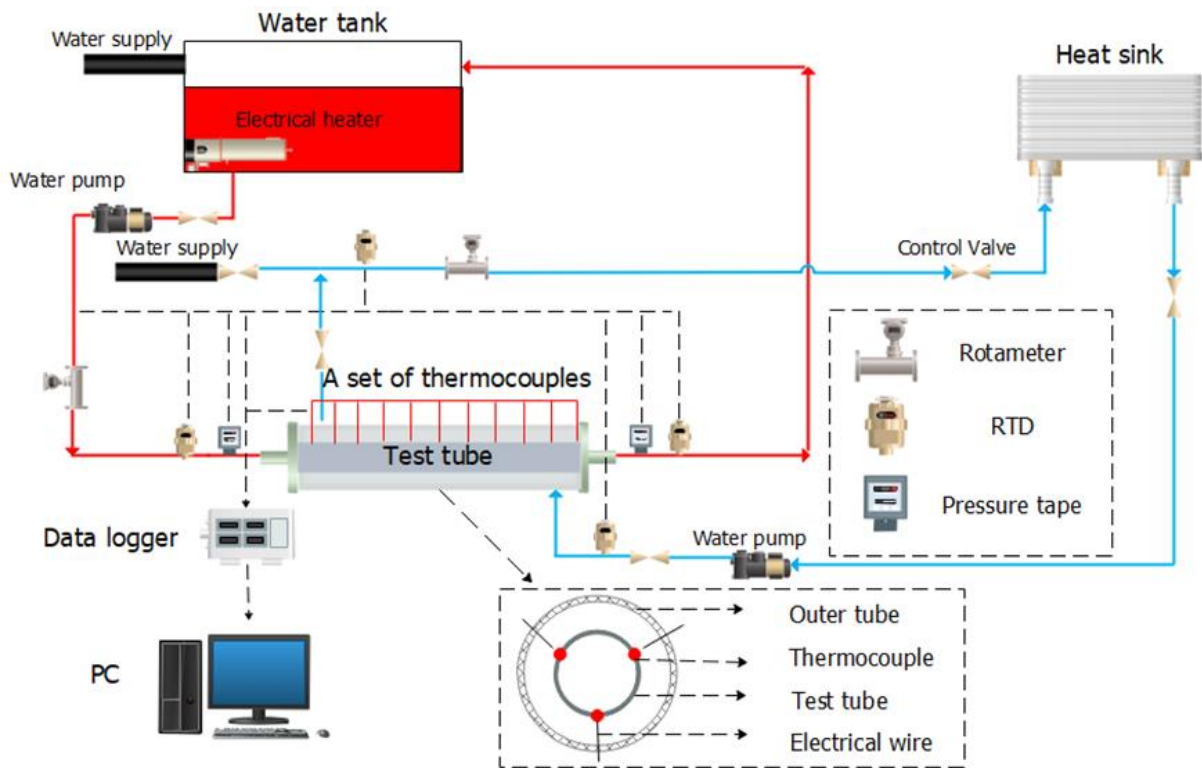


Figure 5.1 Schematic diagram of the test bed



Figure 5.2 (a) The circular tube designed with observational section; (b) Rotational speed measurement: Digital tachometer RPM meter with contactless mode

The SRTTs consist of the twisted tapes, a bearing, and support structure, as shown in Figure 5.3 (a). The support structure fixes the twisted tapes firmly at the test tube inlet. The bearing is made of ceramic materials that can help the twisted tapes rotate flexibly. The twisted tapes are manufactured of a polymer material with a thickness of 1 mm, a length of 2000 mm, and a width of 14 mm. As shown in Figure 5.3 (b), the short-length SRTTs were fabricated with different length ratios (LR=0.3, 0.45, 0.6, and 1). The length ratio is defined as the ratio of length of the SRTT to the tube length. All short-length SRTTs used in this experiment had the same twist ratio of 4.

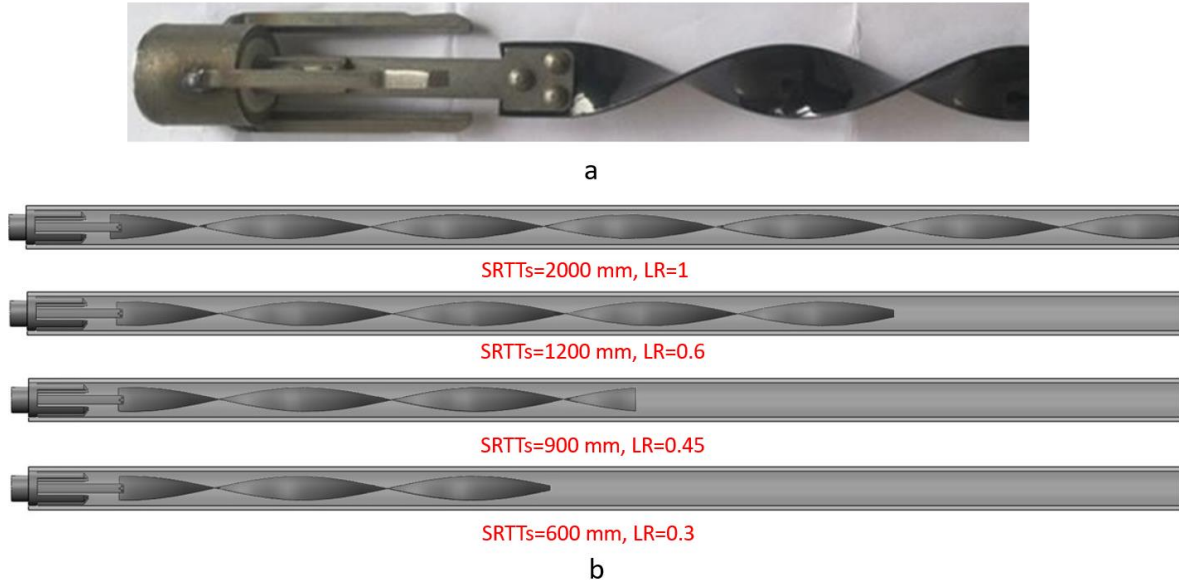


Figure 5.3 (a) The structures of the SRTTs; (b) short-length SRTTs with different length ratios

5.3 Data processing

In this present study, hot water as tested fluid moved through the inner tube under a constant heat flux condition. Cold water flowed through the outer tube with a constant volume flow rate for convective heat transfer. In addition, the Reynolds number varied from 12000 to 45000 in the turbulence flow. The heat absorbed by cold water and the heat discharged by hot water should have excellent agreement of thermal equilibrium:

$$Q = (Q_h + Q_c) / 2 \quad (5-6)$$

$$Q_h = m_i C_p (T_{h,in} - T_{h,out}) \quad (5-7)$$

$$Q_c = m_o C_p (T_{c,out} - T_{h,in}) \quad (5-8)$$

$$\left| \frac{Q_h - Q_c}{Q} * 100\% \right| \leq 5\% \quad (5-9)$$

The amount of heat from hot water to cold water is hypothesized to be the same as the convective heat transfer rate as expressed below.

$$Q = Q_{conv} = h_i A_i (T_b - T_s) \quad (5-10)$$

where

$$T_b = (T_{out} + T_{in}) / 2 \quad (5-11)$$

$$\bar{T}_s = \sum T_s / 10 \quad (5-12)$$

The local heat transfer coefficient of the inner tube and local Nusselt number are estimated from

$$h_i = Q / A_i (\bar{T}_s - T_b) \quad (5-13)$$

$$Nu = \frac{h D_i}{\lambda} \quad (5-14)$$

The friction factor and Reynolds number are given below.

$$f = \frac{\Delta P}{\left(\frac{L}{D_i}\right) \left(\rho \frac{v^2}{2}\right)} \quad (5-15)$$

$$Re = \frac{\rho v D_i}{\mu} \quad (5-16)$$

Although the Nusselt number can be improved by the insertion of twisted tapes, more pumping energy will be consumed owing to the increase in the pressure drop. Hence, the thermal performance factor is an important indicator to appraise the thermal performance efficiency, as proposed by previous research [1]. It can be obtained from the below equations:

$$(\overline{V\Delta P})_p = (\overline{V\Delta P})_t \quad (5-17)$$

By combining Equation (9) and (10), then

$$(f \text{Re}^3)_p = (f \text{Re}^3)_t \quad (5-18)$$

$$\text{Re}_p = \text{Re}_t \left(\frac{f_t}{f_p} \right)^{1/3} \quad (5-19)$$

The thermal performance factor (η) is the ratio of heat transfer performance of the augmented tube to the plain tube at a constant pumping power, which is indicated below as:

$$\eta = \frac{h_t}{h_p} \Big|_{pp} = \frac{(Nu_t / Nu_p)}{(f_t / f_p)^{1/3}} \quad (5-20)$$

The estimation of uncertainty in the non-dimensional parameters is calculated according to the ANSI/ASME standard [103]. The chosen data for the physical properties are depended on the bulk temperature of the water. The combined uncertainties of the non-dimensional parameters were estimated based on the measured experimental quantities with given uncertainties, as presented in Table 2. The uncertain analysis revealed that the

maximum uncertainties in these non-dimensional parameters were found to be within $\pm 8.8\%$ for the Nusselt number, $\pm 3.4\%$ for the Reynolds number, and $\pm 9.2\%$ for the friction factor.

Table 5.2: Uncertainties of experimental parameters

Parameter	Uncertainty (%)	Parameter	Uncertainty (%)
Fluid temperature	1.6	Pressure drop	4.2
Inner diameter	2.2	Test tube length	1.4
Fluid velocity	3.1	Heat quantity	4.6

5.4 Results and Discussion

5.4.1 Verification results for the plain tube

Before conducting the experiments, experimental data of the Nusselt number friction factor needed to be measured to test the reliability of the experimental facilities and measurement devices. The present data for the plain tube were compared with some standard correlations [8]. As presented in Figures 5.4 and 5.5, the measured experimental data agreed well with Dittus–Boelter (Eq. (5-21)) with an 8.2% deviation and with the Gnielinski correlation (Eq. (5-22)) with a 6.8% deviation. The friction factor data were also validated by the Blasius (Eq. (5-23)) and first Petukhov (Eq. (5-24)) equations with agreements of 7.4% and 8.8%, respectively. These standard correlations used to calculate the Nu and f are listed below:

Dittus–Boelter equation:

$$Nu = 0.023 Re^{0.8} Pr^{0.3} \quad (5-21)$$

Gnielinski equation:

$$Nu = \frac{(f/8)(Re-1000)Pr}{1+12.7(f/8)^{0.5}(Pr^{2/3}-1)} \quad (5-22)$$

Blasius equation:

$$f = 0.316 Re^{-0.25} \quad (5-23)$$

First Petukhov equation:

$$f = (0.79 \ln Re - 1.64)^{-2} \quad (5-24)$$

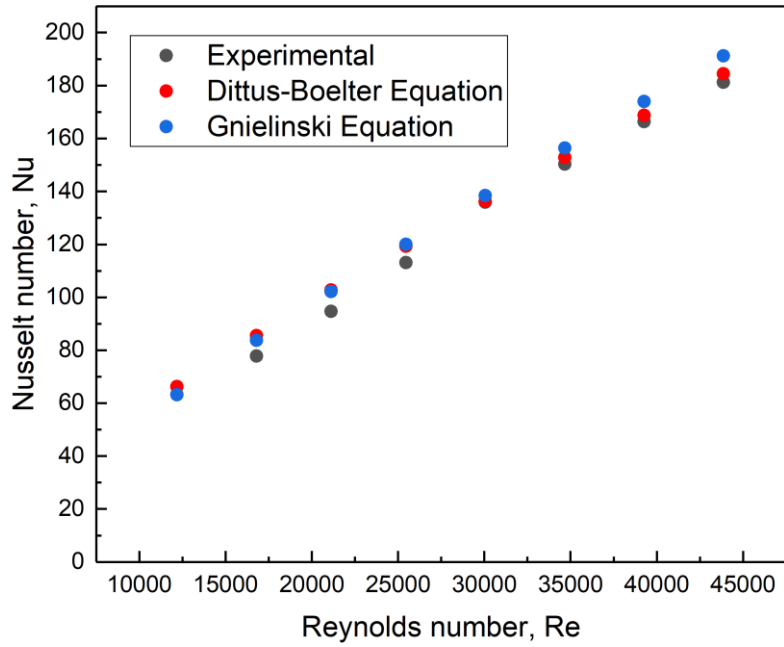


Figure 5.4 Validation test for the plain tube: Nu

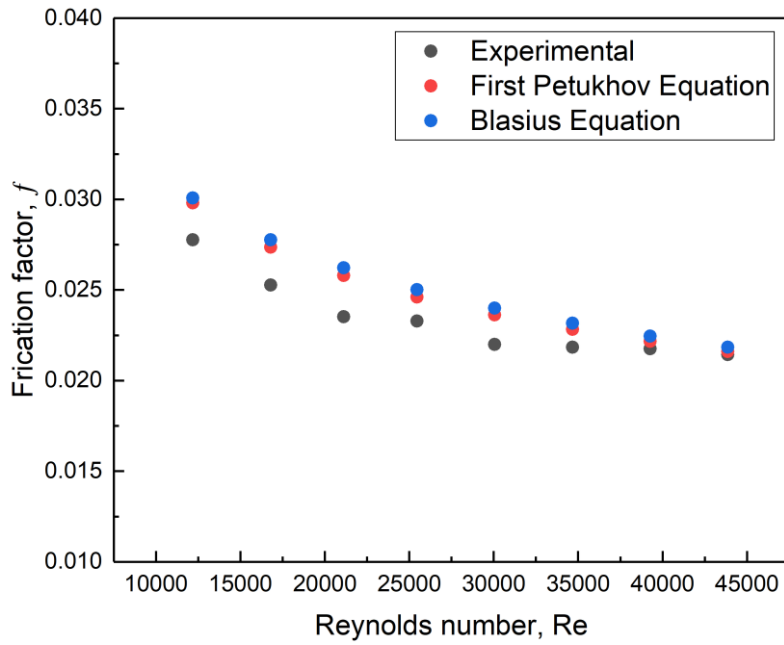


Figure 5.5 Validation test for the plain tube: f

5.4.2 Influences of length ratio on the rotational speed

Figure 5.6 illustrates the variation in the rotational speed with variation of Reynolds number for the SRTTs as a function of different length ratios. When the water velocity or Reynolds number is relatively low, SRTTs do not rotate until the water velocity reaches a certain value. The experimental results indicated that the length ratio performs a vital effects on the initial stage of rotating behavior. SRTTs with a larger length ratio (LR=1) can begin to rotate at lower Reynolds numbers compared to those with a larger length ratios (LR=0.3, 0.45 and 0.6). Moreover, the decrease in length ratio has a positive effect on increasing the rotational speed of SRTTs. This may be because of the larger contact area due to the increase in the length ratio, which can more easily drive SRTTs to rotate.

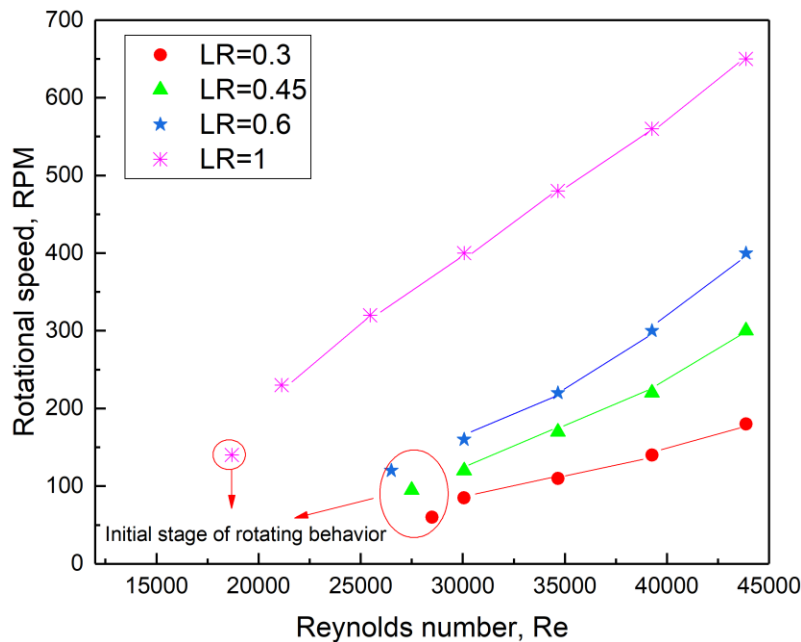
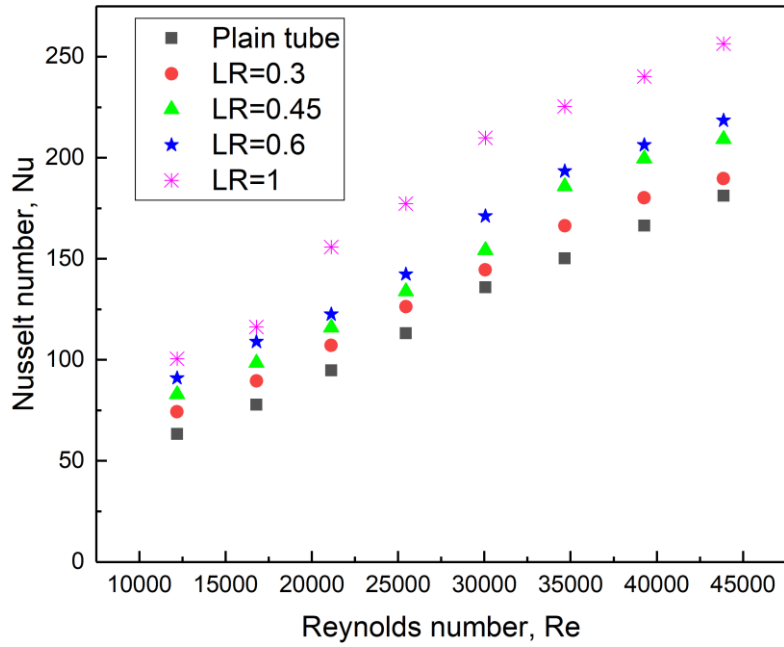


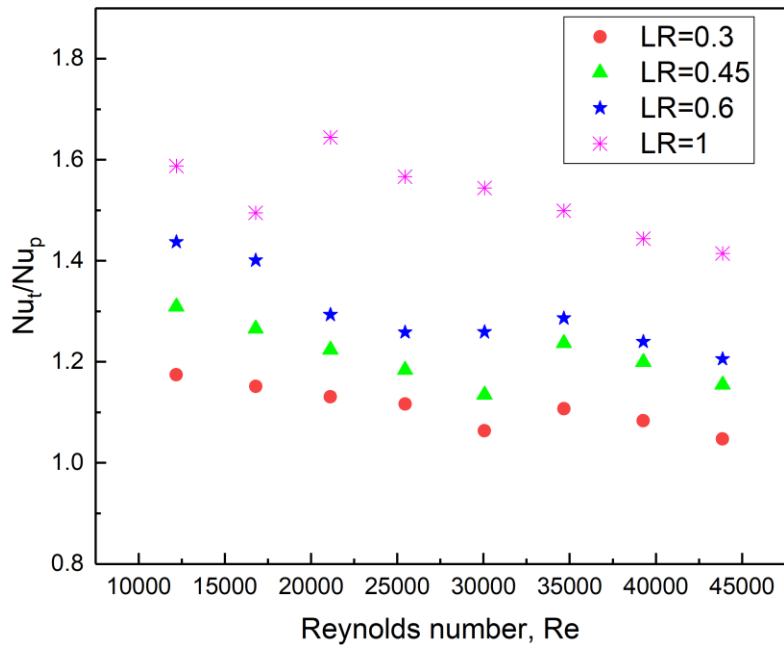
Figure 5.6 Variation in the rotational speed (RPM) as a function of the Re number

5.4.3 Effect of the length ratio on the thermal characteristics

The impact of the length ratio on the heat transfer coefficient in the form of Nu and Nu_t/Nu_p is depicted in Figure 5.7. We observed that the heat transfer performance considerably raises with increasing Reynolds number for all short-length SRTTs. This can be attributed to the higher turbulence intensity existing between the centric and near wall region, which is induced by increasing the Reynolds number [22]. Consistent with previous results [13], the experimental results also demonstrated that SRTTs with a full length (LR=1) can achieve a higher Nu number than SRTTs with lower length ratios (LR=0.3, 0.45 and 0.6). Due to the flow impingement between fluids and the contact surface, a stronger swirl flow along twisted tapes can be induced by full-length SRTTs compared with SRTTs with lower length ratios. As stated by previous research [110], rotating behavior with high rotational speed also contributes to enhanced intensity of swirl flow along tangential direction. Hence, extra swirl flow produces high intensity turbulences, which allows a decrease in the hydrodynamic thickness. Additionally, the overall trend of the Nusselt number ratio (Nu_t/Nu_p) tends to decline as the Reynolds number increases. The results confirm that the effects of the Reynolds number on the Nusselt number is more dominant than the insertion of SRTTs. Interestingly, Nu_t/Nu_p increased considerably from 1.06 to 1.1, 1.13 to 1.23, 1.25 to 1.28, and 1.49 to 1.64 for LR=0.3, 0.45, 0.6, and 1, respectively, when the SRTTs changed from a stationary to rotation condition. It is likely that the existence of rotation behavior also enables the delivery of fluids from the core region to the marginal region, which also contributes to the excellent fluids mixture.



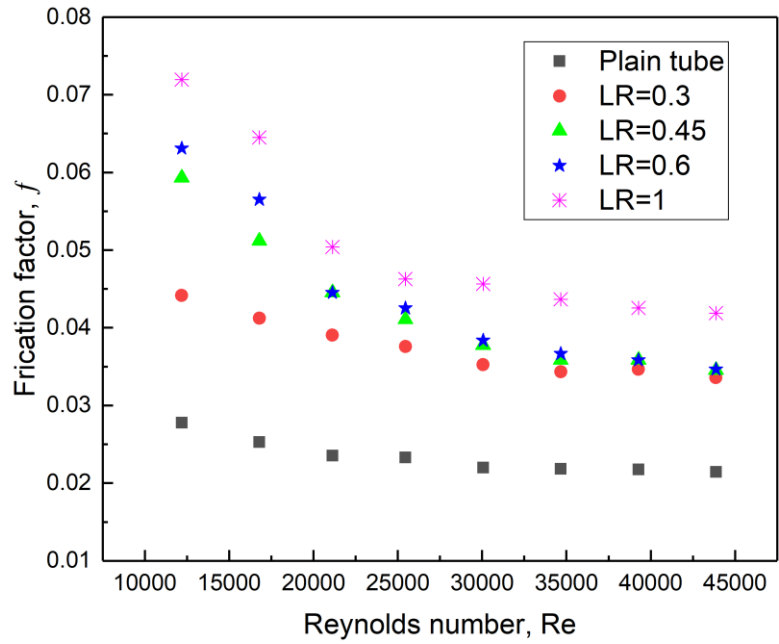
(a)



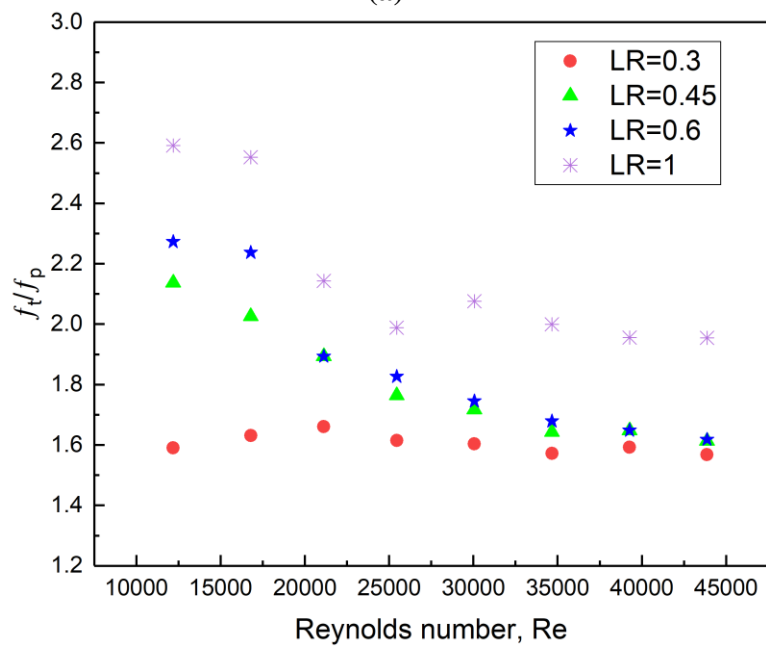
(b)

Figure 5.7 Variation of heat transfer performance with Reynolds number: (a) Nu and (b) Nu_t/Nu_p

The impact of the length ratio on the friction factor in the form of Reynolds numbers is depicted in Figure 5.8. We observed that the friction factor considerably increases with the length ratio and decreases with Reynolds number. From Figure 5.8 (a), for the inner tube fitted with SRTTs, the friction factor with LR=0.3, 0.45, 0.6, and 1 can increase by 57–66%, 61–114%, 62–127%, and 95–160%, respectively, as compared with a plain tube. In addition, the SRTTs with shorter length ratios (LR=0.3, 0.45, and 0.6) yield lower friction factors than those that are full length (LR=1). Thus, the full-length SRTTs are expected to cause flow blockage and a longer residence time, which induces a larger pressure drop across the entire test tube compared with full-length twisted tapes. As expected from Figure 5.8 (b), the friction factor ratio (f_t/f_p) slightly decreased with an increase in the Reynolds number for all SRTTs. This can be ascribed to the fact that working fluids produce relatively lower friction forces at higher Reynolds numbers or flow rates.



(a)



(b)

Figure 5.8 Variation of friction factor with Reynolds number: (a) f ; (b) f_t/f_p

As shown in Figure 5.9, the variation of the thermal performance factor with Reynolds number for the SRTTs at different length ratios (LR=0.3, 0.45, 0.6, and 1) is presented. We observed that the thermal performance factor raises significantly from 0.91 to 0.95, 0.95 to 1.05, 1.04 to 1.08 and 1.09 to 1.27 for the four SRTTs after switching from the stationary to rotation condition. These relationships may be partly explained by the contribution of the rotation behavior to increasing the Nusselt number and reducing the increase in the pressure drop. Additionally, the SRTTs that were full length (LR=1) were found to provide a much higher thermal performance factor in comparison of the SRTTs with the smaller length ratios (LR=0.3, 0.45, and 0.6), which was in great agreement with previous research [13].

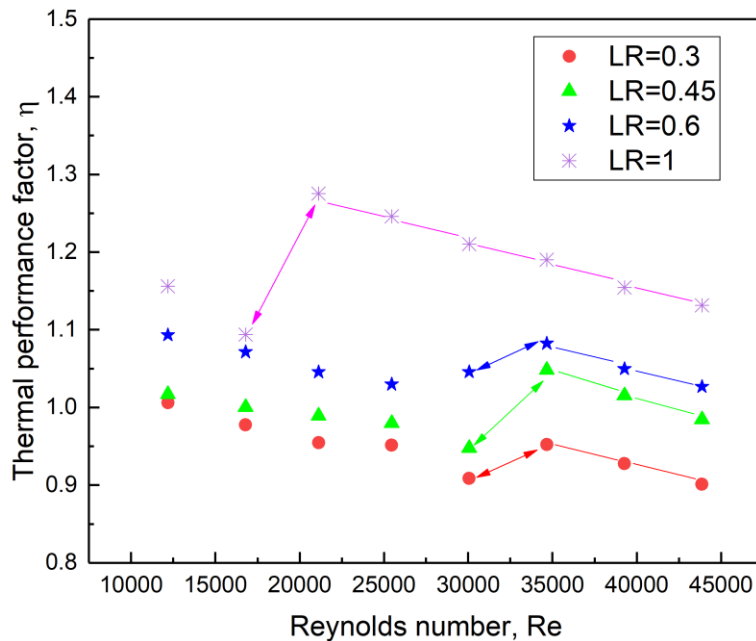


Figure 5.9 η vs Re for SRTTs at different length ratios

(Colored arrow means that SRTTs changed from stationary to rotating conditions)

5.4.4 Proposed correlations

This study proposes two correlations for the function of the length ratio to predict thermal performance in the form of the Nusselt number and friction factor. These correlations are developed from Equations (5-25) and (5-26) and can be applicable to Reynolds numbers of 12000–45000 in a turbulence flow. As presented in Figures 5.10 and 5.11, the prediction results of the Nusselt number and friction factor calculated from Equations (5-25) and (5-26) match the experimental values well with 10% and 15% deviations, respectively.

$$Nu_{SRTTs} = 0.02785 Re^{0.7748} Pr^{0.3} (1 + LR)^{0.6139} \quad (5-25)$$

$$f_{SRTTs} = 3.4143 Re^{-0.4168} (0.06517 + LR)^{0.2867} \quad (5-26)$$

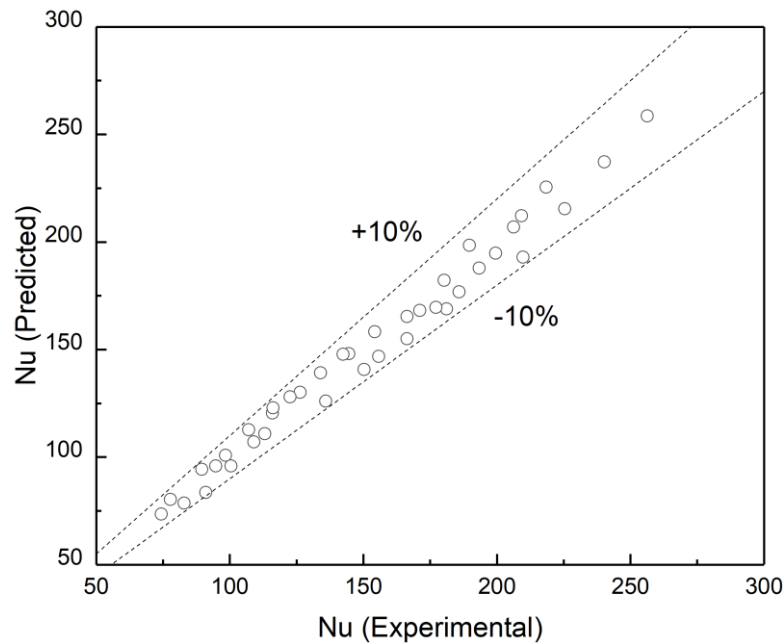


Figure 5.10 Experimental results versus predicted results for the SRTTs with different length ratios: Nu

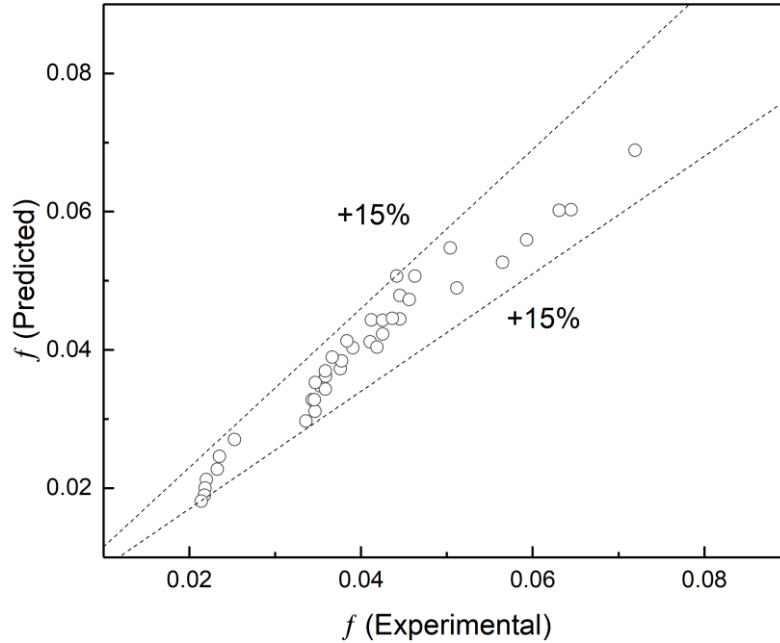


Figure 5.11 Experimental results vs predicted results for the SRTTs with different length ratios: f

5.4.5 Comparison of short-length SRTTs and previous work

Based on the thermal performance factor, short-length SRTTs at LR=0.3, 0.45, 0.6, and 1 were compared with the short-length twisted tapes at the same length ratio and operating conditions. The thermal performance factor of short-length twisted tapes was estimated from Equation (5-27) proposed by previous research as follows [13]:

$$\eta = 1.82 \text{Re}^{-0.068} LR^{0.067} \quad (5-27)$$

Note from Figure 12 that the SRTTs achieved a higher thermal performance factor in comparison of the twisted tapes at the same length ratio. The differences in the thermal performance factor (η) between the SRTTs and short-length twisted tapes may be

associated with the existence of rotating behavior SRTTs. The existence of a rotating behavior enhances the water velocity or secondary motion along the tangential direction and smooths the heat transfer surface, which can contribute to a remarkable reinforce in the thermal performance factor.

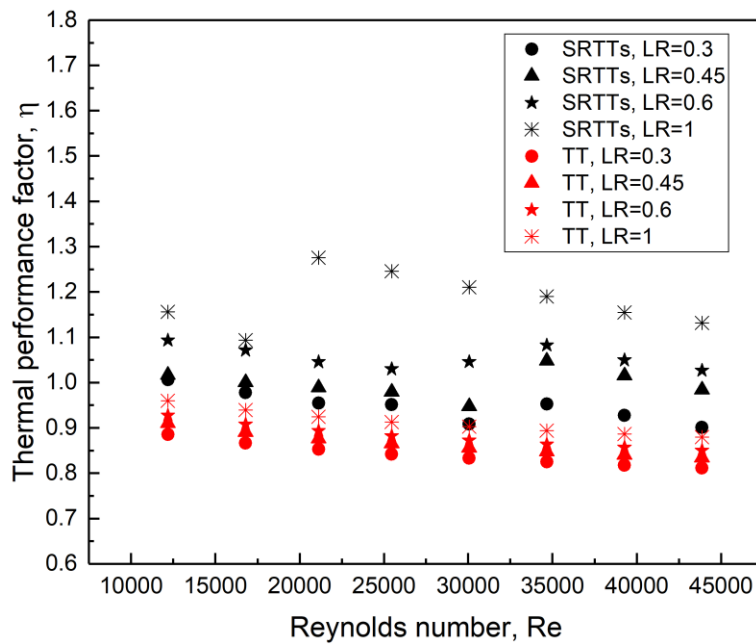


Figure 5.12 Comparisons of the thermal performance factor between short-length SRTTs and short-length twisted tapes (TT)

5.5 Summary

The present research experimentally explored the thermal behavior of SRTTs with different length ratios in the range of Reynolds numbers from 12000–45000. Some major outcomes from this chapter are summarized as below:

- Full-length SRTTs (LR=1) were confirmed to start to rotate at relatively lower Reynolds numbers compared with SRTTs with lower length ratios (LR=0.3, 0.45, 0.6). In addition, SRTTs with larger length ratios appeared to rotate much faster than those with smaller length ratios.
- At similar Reynolds numbers, the tubes fitted with full-length SRTTs had a higher thermal performance in terms of Nusselt number, thermal performance factor and friction factor. The increase in the thermal performance factor from 0.91 to 0.95, 0.95 to 1.05, 1.04 to 1.08, and 1.09 to 1.27 was accompanied by the start of rotating behavior for SRTTs with LR=0.3, 0.45, 0.6, and 1, respectively. All short-length SRTTs were demonstrated to have a better thermal efficiency than short-length twisted tapes at the same length ratio.
- Finally, some empirical correlations varying with length ratio were established to predict the thermal performance as for Nusselt number and friction factor. The predicted results agreed excellently with the experimental results with 10 and 15% deviation for the Nusselt number and friction factor, respectively.

CHAPTER 6

CONCLUSION AND FUTURE WORK

The present study investigates the significance of a new type of twisted tapes, namely self-rotating twisted tapes (SRTTs), in heat transfer enhancement by analyzing experimental results of Nusselt number, friction factor and thermal performance factor. Due to existence of rotating behavior, SRTTs in theory can induce stronger turbulence for excellent convective heat transfer. Hence, SRTTs and STTs with the same geometry are prepared to be comprehensively compared for exploring significance of rotating behavior. Then, the effects of design parameters of twist ratio (e.g. twist ratios, perforation ratio and length ratio) on rotational speed and initial stage of rotating behavior are observed. Besides, influences of twist ratio, perforation ratio and length ratio on heat transfer and pressure drop characteristic. Some correlations associated with twist ratio, perforation ratio and length ratio are established respectively to calculate Nusselt number and friction factor. Main conclusions from this study are drawn as followings.

6.1 Conclusion

Twisted tapes as a swirl flow promoter is an alternative choice to be utilized in heat exchanger system for enhancement of thermal performance. In order to study the novelty of SRTTs, SRTTs and STTs with the same twist ratio of 2, thickness of 1 mm and length of 2000 mm were adopted to be examined in a double-pipe heat exchanger experimentally. Under the stationary condition with lower Reynolds number, there are less discrepancies of thermal performance between the heat exchanger with SRTTs and with STTs. However, under rotating condition, it is observed that the heat transfer rate of heat exchanger with SRTTs is consistently higher by 8-18.8% than that of heat exchanger with STTs, and the friction factor of heat exchanger with SRTTs increases less than that of the one with STTs. Therefore, the thermal performance factor in the tube fitted with SRTTs seems to be much higher than that fitted with STTs. Especially at the initial stage of rotating behavior, the maximum thermal performance factor of 1.03 could be achieved.

As twist ratios is often used as a design parameter of twisted tapes in previous studies, SRTTs are fabricated with four twist ratios ($Y=2.2, 3, 4$ and 6). According to the findings in Chapter 3, SRTTs with lower twist ratio ($Y=2.2$) performed larger heat transfer rate, higher pressure drop and higher thermal performance factor for all investigated cases. In addition, smaller twist ratio ($Y=2.2$) appears to have more influences on the initial stage of rotating behavior and enhancing rotational speed compared with larger twist ratios ($Y=3, 4$ and 6). Hence, it is found that not only twist ratio but also rotational speed of rotating behavior can both contribute to strengthening the heat transfer performance of the heat exchanger. Some empirical correlations with the variable of twist ratio are derived and proposed within 10% deviation to estimate the Nusselt number and the friction factor.

Perforated fabrication is another feasible solution to have combined effects on heat transfer enhancement in heat exchanger system. In this thesis, five SRTTs are perforated with five perforation ratios (PR= 0%, 1.16%, 3.63%, 6.46%, and 10.1%). The experimental results show that larger perforation ratio or larger perforated area has negative influences on the initial stage of rotating behavior, increasing the rotational speed. In addition, this study reports that the tube equipped with SRTTs with perforated SRTTs can increase the Nusselt number and friction factor significantly by 13.8% to 57.5%, and by 116% to 163%, respectively as compared with the empty tube. Larger perforation ratio (PR=10.1%) is suggested to be prior choice due to their stronger effects on enhancing heat transfer rate and thermal performance factor in comparison of smaller perforation ratio (PR=0%, 1.16%, 3.63%, 6.46%). Afterwards, some correlations varying with perforation ratios for evaluating the tube thermal performance are established, and validated by experiment results with 10% deviation.

In addition, to increase the heat transfer rate within allowable pressure drop, short-length fabrication is considered to be adopted for various twisted tapes. In Chapter 5, full-length SRTTs (LR=1) and short-length SRTTs (LR=0.6, 0.45 and 0.3) are manufactured before conducting experiments. It is observed that all short-length SRTTs can improve the rate of heat transfer by 6-10%, 13-23%, 25-28% and 49-64% for LR=0.3, 0.45, 0.6 and 1, respectively. Although short-length SRTTs can reduce pressure drop to some extent, but they seem to be impossible to provide higher thermal performance factor in comparison of full-length SRTT (LR=1). Therefore, the length of SRTTs has to be optimized based on both their thermal behavior but also their hydraulic property. The measured experimental data are used to formulate some correlations associated with length ratio within 10% and

15% discrepancies for prediction of heat transfer and friction factor characteristics, respectively.

This thesis demonstrates the novelty of SRTTs in heat transfer enhancement based on the experimental results of thermal performance. The empirical correlations and the valuable findings from this study can be adopted for application of SRTTs in heat transfer devices, such as heat exchanger system, solar collector and waste heat recovery system.

6.2 Limitations and recommendation for future work

Although some investigations on SRTTs are reported in this thesis, but there are still some limitations existed that can be further solved in the future. The thesis only adopted experiment-based method to investigate the thermal performance of the tube fitted with SRTTs. Lack of numerical study constrained the application of SRTTs at operation conditions that experiment cannot achieve. In addition, the effects of rotational speed of rotating behavior on tangential velocity have not been studied, which cannot offer in-depth explanations about the relationship between rotating behavior and thermal performance.

Therefore, some recommendations for future work are listed out. The mechanism of rotating behavior on generating swirl flow still is not clear. Some numerical investigations can be conducted to study the effects of tangential velocity of working fluids caused by rotating behavior on heat transfer enhancement. The influences of rotational speed on tangential velocity also need to be further investigated.

In addition to twisted tapes, nanofluids perform function in strengthening heat transfer rate due to higher thermal conductivity. Hence, combination of SRTTs and nanofluids appear to have compound effects on heat transfer enhancement. Some experimental and numerical studies are recommended to further explore thermal characteristic of heat exchanger tube fitted with SRTTs in different nanofluids.

Since experimental results of thermal performance can be used to assess design of SRTTs, economic analysis have not been carried out to optimize design and geometry of SRTTs. Hence, genetic algorithm is recommended to find the most optimal solution of combined parameters (e.g. twist ratio, perforation ratio and length ratio) according to results of case study.

References

- [1] S. Eiamsa-ard, K. Wongcharee, P. Eiamsa-ard, and C. Thianpong, "Heat transfer enhancement in a tube using delta-winglet twisted tape inserts," *Appl. Therm. Eng.*, vol. 30, no. 4, pp. 310–318, 2010.
- [2] Y. Hong, J. Du, and S. Wang, "Turbulent thermal , fluid flow and thermodynamic characteristics in a plain tube fitted with overlapped multiple twisted tapes," *Int. J. Heat Mass Transf.*, vol. 115, pp. 551–565, 2017.
- [3] Y. He, L. Liu, P. Li, and L. Ma, "Experimental study on heat transfer enhancement characteristics of tube with cross hollow twisted tape inserts," *Appl. Therm. Eng.*, vol. 131, pp. 743–749, 2018.
- [4] N. Piriyarungrod, M. Kumar, C. Thianpong, M. Pimsarn, and V. Chuwattanakul, "Intensification of thermo-hydraulic performance in heat exchanger tube inserted with multiple twisted-tapes," *Appl. Therm. Eng.*, vol. 136, pp. 516–530, 2018.
- [5] J. Guo, A. Fan, X. Zhang, and W. Liu, "A numerical study on heat transfer and friction factor characteristics of laminar flow in a circular tube fitted with center-cleared twisted tape," *Int. J. Therm. Sci.*, vol. 50, no. 7, pp. 1263–1270, 2011.
- [6] P. Murugesan, K. Mayilsamy, S. Suresh, and P. S. S. Srinivasan, "Heat transfer and pressure drop characteristics in a circular tube fitted with and without V-cut twisted tape insert," *Int. Commun. Heat Mass Transf.*, vol. 38, no. 3, pp. 329–334, 2011.

- [7] A. Hasanpour, M. Farhadi, and K. Sedighi, "Experimental heat transfer and pressure drop study on typical, perforated, V-cut and U-cut twisted tapes in a helically corrugated heat exchanger," *Int. Commun. Heat Mass Transf.*, vol. 71, pp. 126–136, 2016.
- [8] P. Murugesan, K. Mayilsamy, and S. Suresh, "Turbulent heat transfer and pressure drop in tube fitted with square-cut twisted tape," *Chinese J. Chem. Eng.*, vol. 18, no. 4, pp. 609–617, 2010.
- [9] S. Eiamsa-ard, P. Seemawute, and K. Wongcharee, "Influences of peripherally-cut twisted tape insert on heat transfer and thermal performance characteristics in laminar and turbulent tube flows," *Exp. Therm. Fluid Sci.*, vol. 34, no. 6, pp. 711–719, 2010.
- [10] M. M. K. Bhuiya, M. S. U. Chowdhury, M. Saha, and M. T. Islam, "Heat transfer and friction factor characteristics in turbulent flow through a tube fitted with perforated twisted tape inserts," *Int. Commun. Heat Mass Transf.*, vol. 46, pp. 49–57, 2013.
- [11] K. Nanan, C. Tianpong, P. Promvong, and S. Eiamsa-ard, "Investigation of heat transfer enhancement by perforated helical twisted-tapes," *Int. Commun. Heat Mass Transf.*, vol. 52, pp. 106–112, 2014.
- [12] C. Tianpong, P. Eiamsa-ard, and S. Eiamsa-ard, "Heat transfer and thermal performance characteristics of heat exchanger tube fitted with perforated twisted-tapes," *Heat Mass Transf.*, vol. 48, no. 6, pp. 881–892, 2012.
- [13] S. Eiamsa-ard, C. Tianpong, P. Eiamsa-ard, and P. Promvong, "Convective heat transfer in a circular tube with short-length twisted tape insert," *Int. Commun. Heat Mass Transf.*, vol. 36, no. 4, pp. 365–371, 2009.

- [14] C. Man, J. Yao, and C. Wang, “The experimental study on the heat transfer and friction factor characteristics in tube with a new kind of twisted tape insert,” *Int. Commun. Heat Mass Transf.*, vol. 75, pp. 124–129, 2016.
- [15] Y. Hong, J. Du, S. Wang, S. Huang, and W. Ye, “Chemical Engineering Research and Design Effect of decaying swirl flow on tubular turbulent heat transfer enhancement by using short length helical tapes,” *Chem. Eng. Res. Des.*, vol. 138, pp. 1–12, 2018.
- [16] L. Zheng, Y. Xie, and D. Zhang, “Numerical investigation on heat transfer performance and flow characteristics in circular tubes with dimpled twisted tapes using Al_2O_3 -water nanofluid,” *Int. J. Heat Mass Transf.*, vol. 111, pp. 962–981, 2017.
- [17] E. Esmailzadeh, H. Almohammadi, A. Nokhosteen, A. Motezaker, and A. N. Omrani, “Study on heat transfer and friction factor characteristics of $\gamma\text{-Al}_2\text{O}_3$ /water through circular tube with twisted tape inserts with different thicknesses,” *Int. J. Therm. Sci.*, vol. 82, no. 1, pp. 72–83, 2014.
- [18] M. Khoshvaght-aliabadi and M. Eskandari, “Influence of twist length variations on thermal–hydraulic specifications of twisted-tape inserts in presence of Cu–water nanofluid,” *Exp. Therm. Fluid Sci.*, vol. 61, pp. 230–240, 2015.
- [19] V. Mokkaapati and C. Sen Lin, “Numerical study of an exhaust heat recovery system using corrugated tube heat exchanger with twisted tape inserts,” *Int. Commun. Heat Mass Transf.*, vol. 57, pp. 53–64, 2014.
- [20] S. K. Saha, S. Bhattacharyya, and P. K. Pal, “Thermohydraulics of laminar flow of viscous oil through a circular tube having integral axial rib roughness and fitted with center-cleared twisted-tape,” *Exp. Therm. Fluid Sci.*, vol. 41, pp. 121–129, 2012.

- [21] P. Bharadwaj, A. D. Khondge, and A. W. Date, "Heat transfer and pressure drop in a spirally grooved tube with twisted tape insert," *Int. J. Heat Mass Transf.*, vol. 52, no. 7–8, pp. 1938–1944, 2009.
- [22] P. Li, Z. Liu, W. Liu, and G. Chen, "Numerical study on heat transfer enhancement characteristics of tube inserted with centrally hollow narrow twisted tapes," *Int. J. Heat Mass Transf.*, vol. 88, pp. 481–491, 2015.
- [23] A. Karami, E. Rezaei, M. Shahhosseini, and M. Aghakhani, "Optimization of heat transfer in an air cooler equipped with classic twisted tape inserts using imperialist competitive algorithm," *Exp. Therm. Fluid Sci.*, vol. 38, pp. 195–200, 2012.
- [24] S. R. Shabanian, S. Iashgari, and T. Hatami, "Application of intelligent methods for the prediction and optimization of thermal characteristics in a tube equipped with perforated twisted tape," *Numer. Heat Transf. Part A Appl.*, vol. 70, no. 1, pp. 30–47, 2016.
- [25] Department of Energy Statistics, National Bureau of Statistics, Peoples' of China. *China Energy Statistical Yearbook 2016[M]*, China Statistics Press, Beijing, 2011.
- [26] M. R. Salimpour, "Heat transfer coefficients of shell and coiled tube heat exchangers," *Exp. Therm. Fluid Sci.*, vol. 33, no. 2, pp. 203–207, 2009.
- [27] X.B. Zhao, G.H. Tang, X.W. Ma, Y. Jin, W.Q. Tao, "Numerical investigation of heat transfer and erosion characteristics for H-type finned oval tube with longitudinal vortex generators and dimples," *Appl. Energy.*, vol. 127, pp. 93–104, 2014.

- [28] N. Ghorbani, H. Taherian, M. Gorji, and H. Mirgolbabaei, "Experimental study of mixed convection heat transfer in vertical helically coiled tube heat exchangers," *Exp. Therm. Fluid Sci.*, vol. 34, no. 7, pp. 900–905, 2010.
- [29] Y. Dong, L. Huixiong, and C. Tingkuan, "Pressure drop, heat transfer and performance of single-phase turbulent flow in spirally corrugated tubes," *Exp. Therm. Fluid Sci.*, vol. 24, pp. 131–138, 2001.
- [30] S. Pethkool, S. Eiamsa-ard, S. Kwankaomeng, and P. Promvonge, "Turbulent heat transfer enhancement in a heat exchanger using helically corrugated tube," *Int. Commun. Heat Mass Transf.*, vol. 38, no. 3, pp. 340–347, 2011.
- [31] S. Rozzi, R. Massini, G. Paciello, G. Pagliarini, S. Rainieri, and A. Trifiro, "Heat treatment of fluid foods in a shell and tube heat exchanger : Comparison between smooth and helically corrugated wall tubes," *Int. J. Heat Mass Transf.*, vol. 79, pp. 249–254, 2007.
- [32] S. Laohalertdecha and S. Wongwises, "The effects of corrugation pitch on the condensation heat transfer coefficient and pressure drop of R-134a inside horizontal corrugated tube," *Int. J. Heat Mass Transf.*, vol. 53, no. 13–14, pp. 2924–2931, 2010.
- [33] S. Sanaye and H. Hajabdollahi, "Thermal-economic multi-objective optimization of plate fin heat exchanger using genetic algorithm," *Appl. Energy*, vol. 87, no. 6, pp. 1893–1902, 2010.
- [34] Y. Peles, A. Kos, C. Mishra, C. Kuo, and B. Schneider, "Forced convective heat transfer across a pin fin micro heat sink," *Int. J. Heat Mass Transf.*, vol. 48, pp. 3615–3627, 2005.

- [35] A. E. Bergles, "Heat Transfer and Pressure Drop Correlations for the Rectangular Offset Strip Fin Compact Heat Exchanger," *Exp. Therm. Fluid Sci.*, vol. 1777, no. 94, pp. 171–180, 1995.
- [36] J. Jang and C. Chen, "Optimization of louvered- fin heat exchanger with variable louver angles," *Appl. Therm. Eng.*, vol. 91, pp. 138–150, 2015.
- [37] J. C. Han and J. S. Park, "Developing heat transfer in rectangular with rib turbulators," *Int. J. Heat Mass Transf.*, vol. 31, no. 1, pp. 183–195, 1988.
- [38] J. C. Han, "High performance heat transfer ducts with parallel broken and V-shaped broken ribs," *Int. J. Heat Mass Transf.*, vol. 35, no. 2, pp. 513–523, 1992.
- [39] I. Ali, N. Kamaruzaman, N. Azwadi, and C. Sidik, "Transfer Heat transfer augmentation in a microchannel heat sink with sinusoidal cavities and rectangular ribs," *Int. J. Heat Mass Transf.*, vol. 108, pp. 1969–1981, 2017.
- [40] N. Zheng, P. Liu, F. Shan, Z. Liu, and W. Liu, "Effects of rib arrangements on the flow pattern and heat transfer in an internally ribbed heat exchanger tube," *Int. J. Therm. Sci.*, vol. 101, pp. 93–105, 2016.
- [41] Y. Xuan and Q. Li, "Heat transfer enhancement of nanofluids," *Int. J. Heat and Fluid Flow.*, vol. 21, pp. 58–64, 2000.
- [42] J. Albadr, S. Tayal, and M. Alasadi, "Case Studies in Thermal Engineering Heat transfer through heat exchanger using Al_2O_3 nanofluid at different concentrations," *Case Stud. Therm. Eng.*, vol. 1, no. 1, pp. 38–44, 2013.

- [43] W. Duangthongsuk and S. Wongwises, "Heat transfer enhancement and pressure drop characteristics of TiO₂ – water nanofluid in a double-tube counter flow heat exchanger," *Int. J. Heat Mass Transf.*, vol. 52, no. 7–8, pp. 2059–2067, 2009.
- [44] B. Sun, W. Lei, and D. Yang, "Flow and convective heat transfer characteristics of Fe₂O₃ – water nanofluids inside copper tubes," *Int. Commun. Heat Mass Transf.*, vol. 64, pp. 21–28, 2015.
- [45] S. Eiamsa-Ard, P. Somkleang, C. Nuntadusit, and C. Thianpong, "Heat transfer enhancement in tube by inserting uniform/non-uniform twisted-tapes with alternate axes: Effect of rotated-axis length," *Appl. Therm. Eng.*, vol. 54, no. 1, pp. 289–309, 2013.
- [46] A. E. B. R. M. Manglik, "Heat Transfer and Pressure Drop Correlations for Twisted-Tape Inserts in Isothermal Tubes : Part II — Transition and Turbulent Flows," *J. Heat Transf.*, ASME, vol. 115, no. November 1993, pp. 890–896, 1993.
- [47] A. E. Bergles, "Heat Transfer and Pressure Drop Correlations for Twisted-Tape Inserts in Isothermal Tubes : Part I — Laminar Flows," vol. 115, pp. 881–889, 1993.
- [48] S. N. Sarada, A. V. S. R. Raju, K. K. Radha, and L. S. Sunder, "Enhancement of heat transfer using varying width twisted tape inserts," *Int. J. Eng. Sci. Technol.*, vol. 2, no. 6, pp. 107–118, 2010.
- [49] S. W. Chang, T. L. Yang, and J. S. Liou, "Heat transfer and pressure drop in tube with broken twisted tape insert," *Exp. Therm. Fluid Sci.*, vol. 32, no. 2, pp. 489–501, 2007.
- [50] S. Eiamsa-ard and P. Promvong, "Thermal characteristics in round tube fitted with serrated twisted tape," *Appl. Therm. Eng.*, vol. 30, no. 13, pp. 1673–1682, 2010.

- [51] S. Eiamsa-ard and P. Promvonge, "Performance assessment in a heat exchanger tube with alternate clockwise and counter-clockwise twisted-tape inserts," *Int. J. Heat Mass Transf.*, vol. 53, no. 7–8, pp. 1364–1372, 2010.
- [52] N. Piriyaungrod, S. Eiamsa-ard, C. Thianpong, M. Pimsarn, and K. Nanan, "Intensification Heat transfer enhancement by tapered twisted tape inserts," *Chem. Eng. Process. Process Intensif.*, vol. 96, pp. 62–71, 2015.
- [53] S. Eiamsa-ard, C. Thianpong, and P. Promvonge, "Experimental investigation of heat transfer and flow friction in a circular tube fitted with regularly spaced twisted tape elements," vol. 33, pp. 1225–1233, 2006.
- [54] M. Rahimi, S. Reza, and A. Abdulaziz, "Chemical Engineering and Processing : Process Intensification Experimental and CFD studies on heat transfer and friction factor characteristics of a tube equipped with modified twisted tape inserts," vol. 48, pp. 762–770, 2009.
- [55] S. Chokphoemphun, M. Pimsarn, C. Thianpong, and P. Promvonge, "Thermal performance of tubular heat exchanger with multiple twisted-tape inserts," *Chin. J. Chem. Eng.*, vol. 23, no. 5, pp. 755–762, 2015.
- [56] M. M. K. Bhuiya, A. S. M. Sayem, M. Islam, M. S. U. Chowdhury, and M. Shahabuddin, "Performance assessment in a heat exchanger tube fitted with double counter twisted tape inserts," *Int. Commun. Heat Mass Transf.*, vol. 50, pp. 25–33, 2014.
- [57] M. M. K. Bhuiya, M. S. U. Chowdhury, M. Shahabuddin, M. Saha, and L. A. Memon, "Thermal characteristics in a heat exchanger tube fitted with triple twisted tape inserts," *Int. Commun. Heat Mass Transf.*, vol. 48, pp. 124–132, 2013.

- [58] M. M. K. Bhuiya, A. K. Azad, M. S. U. Chowdhury, and M. Saha, "Heat transfer augmentation in a circular tube with perforated double counter twisted tape inserts," *Int. Commun. Heat Mass Transf.*, vol. 74, pp. 18–26, 2016.
- [59] M. E. Nakhchi and J. A. Esfahani, "Numerical investigation of rectangular-cut twisted tape insert on performance improvement of heat exchangers," *Int. J. Therm. Sci.*, vol. 138, no. September 2018, pp. 75–83, 2019.
- [60] P. Murugesan, K. Mayilsamy, and S. Suresh, "Heat transfer in tubes fitted with trapezoidal-cut and plain twisted tape inserts," *Chem. Eng. Commun.*, vol. 198, no. 7, pp. 886–904, 2011.
- [61] E. I. Eid, R. A. Khalaf-allah, A. M. Soliman, and A. S. Easa, "Performance of a beta Stirling refrigerator with tubular evaporator and condenser having inserted twisted tapes and driven by a solar energy heat engine," *Renew. Energy*, vol. 135, pp. 1314–1326, 2019.
- [62] S. Jaisankar, T. K. Radhakrishnan, and K. N. Sheeba, "Experimental studies on heat transfer and friction factor characteristics of thermosyphon solar water heater system fitted with spacer at the trailing edge of twisted tapes," *Appl. Therm. Eng.*, vol. 29, no. 5–6, pp. 1224–1231, 2009.
- [63] S. Jaisankar, T. K. Radhakrishnan, and K. N. Sheeba, "Experimental studies on heat transfer and friction factor characteristics of forced circulation solar water heater system fitted with helical twisted tapes," *Sol. Energy*, vol. 83, no. 11, pp. 1943–1952, 2009.
- [64] S. Jaisankar, T. K. Radhakrishnan, K. N. Sheeba, and S. Suresh, "Experimental investigation of heat transfer and friction factor characteristics of thermosyphon solar water

heater system fitted with spacer at the trailing edge of Left – Right twisted tapes,” *Energy Convers. Manag.*, vol. 50, no. 10, pp. 2638–2649, 2009.

[65] A. Saravanan and S. Jaisankar, “Heat transfer augmentation techniques in forced flow V-trough solar collector equipped with V-cut and square cut twisted tape,” *Int. J. Therm. Sci.*, vol. 140, pp. 59–70, 2019.

[66] R. Garduno-ramirez and O. A. Jaramillo, “Optimal operation of a parabolic solar collector with twisted-tape insert by multi-objective genetic algorithms,” *Renew. Energy*, vol. 143, pp. 540–550, 2019.

[67] O. A. Jaramillo, M. Borunda, K. M. Velazquez-Lucho, and M. Robles, “Parabolic trough solar collector for low enthalpy processes: An analysis of the efficiency enhancement by using twisted tape inserts,” *Renew. Energy*, vol. 93, pp. 125–141, 2016.

[68] A. Mwesigye, T. Bello-ochende, and J. P. Meyer, “Heat transfer and entropy generation in a parabolic trough receiver with wall-detached twisted tape inserts,” *Int. J. Therm. Sci.*, vol. 99, pp. 238–257, 2016.

[69] V. Zimparov, “Prediction of friction factors and heat transfer coefficients for turbulent flow in corrugated tubes combined with twisted tape inserts . Part 2 : heat transfer coefficients,” *Int. J. Heat Mass Transf.*, vol. 47, pp. 385–393, 2004.

[70] V. Zimparov, “Prediction of friction factors and heat transfer coefficients for turbulent flow in corrugated tubes combined with twisted tape inserts . Part 1 : friction factors,” *Int. J. Heat Mass Transf.*, vol. 47, pp. 589–599, 2004.

- [71] S. Bhattacharyya, A. C. Benim, and H. Chattopadhyay, “Experimental investigation of heat transfer performance of corrugated tube with spring tape inserts,” *Exp. Heat Transf.*, 2018.
- [72] P. Promvong, S. Pethkool, M. Pimsarn, and C. Thianpong, “Heat transfer augmentation in a helical-ribbed tube with double twisted tape inserts ,” *Int. Commun. Heat Mass Transf.*, vol. 39, no. 7, pp. 953–959, 2012.
- [73] Y. Hong, J. Du, and S. Wang, “Experimental heat transfer and flow characteristics in a spiral grooved tube with overlapped large / small twin twisted tapes,” *Int. J. Heat Mass Transf.*, vol. 106, pp. 1178–1190, 2017.
- [74] S. K. Saha, “Thermohydraulics of laminar flow of viscous oil through a circular tube having axial corrugations and fitted with centre-cleared twisted-tape,” *Exp. Therm. Fluid Sci.*, vol. 38, pp. 201–209, 2012.
- [75] S. Bhattacharyya and S. K. Saha, “Thermohydraulics of laminar flow through a circular tube having integral helical rib roughness and fitted with centre-cleared twisted-tape,” *Exp. Therm. Fluid Sci.*, vol. 42, pp. 154–162, 2012.
- [76] S. Al-fahed, L. M. Chamra, and W. Chakroun, “Pressure drop and heat transfer comparison for both microfin tube and twisted-tape inserts in laminar flow,” *Exp. Therm. Fluid Sci.*, vol. 18, pp. 323–333, 1999.
- [77] K. Wongcharee, “Heat transfer characteristics in micro-fin tube equipped with double twisted tapes : Effect of twisted tape and micro-fin tube arrangements ,” *J. Hydrodyn.*, vol. 25, no. 2, pp. 205–214, 2013.

- [78] S. Eiamsa-ard and K. Wongcharee, “Convective heat transfer enhancement using Ag-water nanofluid in a micro-fin tube combined with non-uniform twisted tape,” *Int. J. Mech. Sci.*, vol. 146–147, pp. 337–354, 2018.
- [79] P. K. Nagarajan, Y. Mukkamala, and P. Sivashanmugam, “Studies on heat transfer and friction factor characteristics of turbulent flow through a micro- finned tube fitted with left e right inserts,” *Appl. Therm. Eng.*, vol. 30, no. 13, pp. 1666–1672, 2010.
- [80] K. V Sharma, L. S. Sundar, and P. K. Sarma, “Estimation of heat transfer coefficient and friction factor in the transition flow with low volume concentration of Al_2O_3 nanofluid flowing in a circular tube and with twisted tape insert ,” *Int. Commun. Heat Mass Transf.*, vol. 36, no. 5, pp. 503–507, 2009.
- [81] L. S. Sundar and K. V Sharma, “International Journal of Heat and Mass Transfer Turbulent heat transfer and friction factor of Al_2O_3 Nanofluid in circular tube with twisted tape inserts,” *Int. J. Heat Mass Transf.*, vol. 53, no. 7–8, pp. 1409–1416, 2010.
- [82] H. Maddah, M. Alizadeh, N. Ghasemi, S. Rafidah, and W. Alwi, “Experimental study of Al_2O_3 /water nanofluid turbulent heat transfer enhancement in the horizontal double pipes fitted with modified twisted tapes,” *Int. J. Heat Mass Transf.*, vol. 78, pp. 1042–1054, 2014.
- [83] K. Wongcharee and S. Eiamsa-ard, “Enhancement of heat transfer using CuO / water nanofluid and twisted tape with alternate axis ,” *Int. Commun. Heat Mass Transf.*, vol. 38, no. 6, pp. 742–748, 2011.
- [84] L. S. Sundar, N. T. R. Kumar, M. T. Naik, and K. V Sharma, “Transfer Effect of full length twisted tape inserts on heat transfer and friction factor enhancement with Fe_3O_4

magnetic nanofluid inside a plain tube : An experimental study,” *Int. J. Heat Mass Transf.*, vol. 55, pp. 2761–2768, 2012.

[85] W. H. Azmi, K. V Sharma, P. K. Sarma, R. Mamat, S. Anuar, and L. S. Sundar, “Numerical validation of experimental heat transfer coefficient with SiO₂ nanofluid flowing in a tube with twisted tape inserts,” *Appl. Therm. Eng.*, vol. 73, pp. 296–306, 2014.

[86] S. Eiamsa-ard and K. Kiatkittipong, “Heat transfer enhancement by multiple twisted tape inserts and TiO₂ / water nanofluid,” *Appl. Therm. Eng.*, vol. 70, pp. 896–924, 2014.

[87] W. H. Azmi, K. V Sharma, P. K. Sarma, R. Mamat, and S. Anuar, “Comparison of convective heat transfer coefficient and friction factor of TiO₂ nanofluid flow in a tube with twisted tape inserts,” *Int. J. Therm. Sci.*, vol. 81, pp. 84–93, 2014.

[88] S. Eiamsa-ard, K. Wongcharee, P. Eiamsa-ard, and C. Thianpong, “Thermohydraulic investigation of turbulent flow through a round tube equipped with twisted tapes consisting of centre wings and alternate-axes,” *Exp. Therm. Fluid Sci.*, vol. 34, no. 8, pp. 1151–1161, 2010.

[89] S. Eiamsa-ard, K. Wongcharee, and S. Sripattanapipat, “3-D Numerical simulation of swirling flow and convective heat transfer in a circular tube induced by means of loose-fit twisted tapes,” *Int. Commun. Heat Mass Transf.*, vol. 36, no. 9, pp. 947–955, 2009.

[90] Y. Wang et al., “Configuration optimization of regularly spaced short-length twisted tape in a circular tube to enhance turbulent heat transfer using CFD modeling,” *Appl. Therm. Eng.*, vol. 31, pp. 1141–1149, 2011.

- [91] X. Zhang, Z. Liu, and W. Liu, "Numerical studies on heat transfer and flow characteristics for laminar flow in a tube with multiple regularly spaced twisted tapes," *Int. J. Therm. Sci.*, vol. 58, pp. 157–167, 2012.
- [92] H. Han, R. Yu, B. Li, Y. Zhang, W. Wang, and X. Chen, "Multi-objective optimization of corrugated tube with loose-fit twisted tape using RSM and NSGA-II Design of Experiments," *Int. J. Heat Mass Transf.*, vol. 131, pp. 781–794, 2019.
- [93] M. Reza, J. Nasr, and A. H. Khalaj, "Heat Transfer Coefficient and Friction Factor Prediction of Corrugated Tubes Combined With Twisted Tape Inserts Using Artificial Neural Network," *Heat Transfer Eng.*, vol. 31, pp. 59-69, 2010.
- [94] H. Maddah, N. Ghasemi, B. Keyvani, and R. Cheraghali, "Experimental and numerical study of nanofluid in heat exchanger fitted by modified twisted tape : exergy analysis and ANN prediction model," *Heat Mass Transf.*, vol. 53, no. 4, pp. 1413–1423, 2017.
- [95] C. Zhang et al., "A comparative review of self-rotating and stationary twisted tape inserts in heat exchanger," *Renew. Sustain. Energy Rev.*, vol. 53, pp. 433–449, 2016.
- [96] S. Eiamsa-ard, C. Thianpong, and P. Eiamsa-ard, "Turbulent heat transfer enhancement by counter / co-swirling flow in a tube fitted with twin twisted tapes," *Exp. Therm. Fluid Sci.*, vol. 34, no. 1, pp. 53–62, 2010.
- [97] S. W. Chang, Y. J. Jan, and J. S. Liou, "Turbulent heat transfer and pressure drop in tube fitted with serrated twisted tape," *Int. J. Therm. Sci.*, vol. 46, no. 5, pp. 506–518, 2007.

- [98] S. S. Chougule and S. K. Sahu, "Heat transfer and friction characteristics of Al_2O_3 /water and CNT/water nanofluids in transition flow using helical screw tape inserts - a comparative study," *Chem. Eng. Process. Process Intensif.*, vol. 88, pp. 78–88, 2015.
- [99] S. Suresh, K. P. Venkitaraj, P. Selvakumar, and M. Chandrasekar, "A comparison of thermal characteristics of Al_2O_3 /water and CuO/water nanofluids in transition flow through a straight circular duct fitted with helical screw tape inserts," *Exp. Therm. Fluid Sci.*, vol. 39, pp. 37–44, 2012.
- [100] A. Saysroy and S. Eiamsa-ard, "Periodically fully-developed heat and fluid flow behaviors in a turbulent tube flow with square-cut twisted tape inserts," *Appl. Therm. Eng.*, vol. 112, pp. 895–910, 2017.
- [101] S. D. Salman, A. A. H. Kadhum, M. S. Takriff, and A. B. Mohamad, "CFD Simulation of Heat Transfer Augmentation in a Circular Tube Fitted with Alternative Axis Twisted Tape in Laminar Flow under a Constant Heat Flux," *Heat Transfer—Asian Research* vol. 43, pp. 384–396, 2014.
- [102] S. Ponnada, T. Subrahmanyam, and S. V Naidu, "A comparative study on the thermal performance of water in a circular tube with twisted tapes , perforated twisted tapes and perforated twisted tapes with alternate axis," *Int. J. Therm. Sci.*, vol. 136, pp. 530–538, 2019.
- [103] R. B. Abernethy, R. P. Benedict, and R. B. Dowdell, "ASME Measurement Uncertainty," *J. Fluids Eng.*, vol. 107, pp. 161–164, 1985.

[104] S. Eiamsa-ard, C. Thianpong, P. Eiamsa-ard, and P. Promvonge, “Thermal characteristics in a heat exchanger tube fitted with dual twisted tape elements in tandem ,” *Int. Commun. Heat Mass Transf.*, vol. 37, no. 1, pp. 39–46, 2010.

[105] “Study on thermal and fluid flow characteristics in turbulent channel flows with multiple twisted tape vortex generators,” *Int. Commun. Heat Mass Transf.*, vol. 31, pp. 644–651, 2010.

[106] S. Eiamsa-ard, K. Wongcharee, P. Eiamsa-ard, and C. Thianpong, “Thermohydraulic investigation of turbulent flow through a round tube equipped with twisted tapes consisting of centre wings and alternate-axes,” *Exp. Therm. Fluid Sci.*, vol. 34, no. 8, pp. 1151–1161, 2010.

[107] S. Eiamsa-ard, K. Yongsiri, K. Nanan, and C. Thianpong, “Heat transfer augmentation by helically twisted tapes as swirl and turbulence promoters,” *Chem. Eng. Process. Process Intensif.*, vol. 60, pp. 42–48, 2012.

[108] H. Bas and V. Ozceyhan, “Heat transfer enhancement in a tube with twisted tape inserts placed separately from the tube wall,” *Exp. Therm. Fluid Sci.*, vol. 41, pp. 51–58, 2012.

[109] P. Ferroni, R. E. Block, N. E. Todreas, and A. E. Bergles, “Experimental evaluation of pressure drop in round tubes provided with physically separated , multiple , short-length twisted tapes,” *Exp. Therm. Fluid Sci.*, vol. 35, no. 7, pp. 1357–1369, 2011.

[110] S. Zhang, L. Lu, C. Dong, and S. Hyun, “Performance evaluation of a double-pipe heat exchanger fitted with self- rotating twisted tapes,” *Appl. Therm. Eng.*, vol. 158, pp. 113770, 2019.